

**Katholieke Universiteit Leuven
Group Biomedical Sciences
Faculty of Medicine
Department of Dentistry, Oral
Pathology & Maxillofacial Surgery
Oral Imaging Center**



Validation of 2D and 3D Imaging Modalities for Periodontal Diagnosis

Bart VANDENBERGHE

Doctoral thesis in Medical Sciences

Leuven, 2010

**Katholieke Universiteit Leuven
Group Biomedical Sciences
Department of Dentistry, Oral
Pathology & Maxillofacial Surgery
Oral Imaging Center**



Validation of 2D and 3D Imaging Modalities for Periodontal Diagnosis

Bart VANDENBERGHE

Jury:

Promoter: Professor Dr. Reinhilde Jacobs, KULeuven, Belgium

Co-promoter: Professor Dr. Jie Yang, Temple University, USA

Chair: Professor Dr. Frans Vinckier, KULeuven, Belgium

Secretary: Professor Dr. Ignace Naert, KULeuven, Belgium

Jury members: Professor Dr. Hilde Bosmans, KULeuven, Belgium

Professor Dr. Kostas Tsiklakis, University of Athens, Greece

Dr. Jan Casselman, AZ Sint Jan, Brugge, Belgium

Professor Dr. Herve Reyckler, UCLouvain, Belgium

Leuven, 26.04.2010

Doctoral thesis in Medical Sciences

Acknowledgments

X-rays at midnight in a deserted hospital and nothing but cadaver jaws... Sounds like a scary movie and believe me it was. To have these experiences lying at the origin of my PhD project, demonstrates that this work was not possible without the personal and professional support of numerous people.

First of all, I would like to thank the authorities at the Katholieke Universiteit Leuven (M. Waer, Rector; B. Himpens, Decaan; F. Vinckier, Department Chair) for allowing me to undertake this research project and the authorities at Temple University, Tufts University and University of Maryland for accepting me as an exchange scholar.

To my promoter, Reinhilde Jacobs, I am forever grateful for the opportunities she has given me. Even as a young dental student, she already believed in my capabilities as a researcher and easily stimulated me to explore this field. I will never forget how she helped me pursuing my dreams abroad, allowing me to spend the three best years of my life in the United States of America. She has always been there to motivate me and let me grow to be the person I am today. Reinhilde, thanks a lot, you will always be able to count on me.

To my co-promotor, Jie Yang, I would like to express my deep and sincere gratitude for accepting me overseas as a visiting scholar at Temple University. It has been a unique experience for me in Philadelphia and you have taught me so many skills for my academic training.

I kindly thank all the members of the thesis committee: Professor Tsiklakis, Professor Naert, Professor Bosmans, Professor Reychler and Dr Casselman. The good advice you have given me after your thorough reviewing of my manuscript has been of great help!

Starting from the beginning of this project, I would like to thank all the wonderful colleagues I have met along the way and who have helped me to accomplish my professional endeavors. Professor van Steenberghe, thank you for helping and guiding me from the very start to make the jump from Biomedical Sciences to Dentistry. I would also like to thank you, together with Professor Naert and Professor De Laat, for the recommendations to your colleagues abroad. A special acknowledgement must go to Professor Wierinck who has tolerated me many times as a special case and who has always provided me with good advice and the equipment I needed. The same thanks must go to Roland and Paul, for providing me with supplies and tolerating the cadaver smell.

To my dear colleague Olivia, you have been my example and my sunshine in the rain. It feels really good to have gained so much experience from you and to be now "tuned" towards each other. Nele, we should make a song about these x-rays at midnight. :-) Lily, Livia and Bassam, thanks for all your support and friendship, and the joy you brought to the lab. My amazing team of observers, Fang Fang, Livia, Bo, Lily, Limin, Fan and Zhenzhen, but also Drs Gyaw and Saleem, thanks for all the hard work!

A sincere and very warm thank you goes to Roslyn Gorin, statistical application manager at Temple University: you have introduced me to statistic analysis in the first place and have given me a very insightful view into this difficult matter. Furthermore, I would like to express my gratitude to Steffen Fieuws at L-Biostat, who has been able to further help me when I was lost in the more advanced analysis of the tremendous amount of data collected for this project.

Professors Ramesh and Pabla, although my stay was quite short in Boston, it has been a pleasure: thank you for the opportunity you gave me. Dr Liene Molly and Dr Armellini, thanks for believing in me and opening the doors in Maryland for me. I am

indebted to you guys. Adidi, I think I have found myself in you... you are amazing and I need to write a book about our friendship. Endless thanks to the warmest and most generous person I have ever met. I will always be there for you too.

Thanks to all my other new colleagues at the Oral Imaging Center, Ali, Ruben, Pisha, Maryam, Paulo, Christiano, Sam, Yan, Guozhi, Carine, Deborah and Asti, but also all other colleagues from the different departments, including the hospital nurses and the administrative staff. Furthermore, I want to acknowledge the people who are helping me in my continued research projects, especially the ones at the Medical Imaging Center, Joris, Jurgen, Annelies, Maarten and Professors Maes and Bosmans.

Last but definitely not last; I would like to thank my family and friends for all their love and support. Mom, dad, you have been so patient with me! Of course, you were the ones who have made everything possible, including my time abroad and the new projects I have planned in the future. I will always be thankful for everything you have done and taught me, this project is dedicated to you guys! But also all my other (new) family members, including Nikos: thanks for always being there and listening...To all my US friends (Andrew, when are you moving to Brussels??) and especially my Belgian friends (25R, Plazalalala, Biomedische, Starcreek, Sapin...-crews), thanks for your support, love and patience... and now: CHEERS!

Table of Contents

Preface	7
List of abbreviations	8
Chapter 1 – General introduction and aims	9
PART 1: 2D imaging modalities for periodontal diagnosis	31
Chapter 2 – The influence of x-ray generator on periodontal measurements	33
Chapter 3 – The influence of image receptor on periodontal measurements	53
Chapter 4 – The influence of tube potential periodontal measurements	71
PART 2: 3D imaging modalities for periodontal diagnosis	81
Chapter 5 – Bone loss measurements on 2D and 3D panoramic reconstructions	83
Chapter 6 – 3D topographic assessment of crater and furcation involvements	93
Chapter 7 – Bone loss measurements on 3D orthogonal slices	107
Chapter 8 – General discussion and conclusions	123
APPENDIX A – Dose savings for two kV settings	137
Summary - Samenvatting	139
References	145
Curriculum Vitae	158

Preface

This thesis is based on the following papers and book chapters:

- **Chapter 1**

Vandenberghé B, Nackaerts O. Imaging in Periodontology: 2D versus 3D Visualization Techniques. In: Informatics in Oral Medicine: Advanced Techniques in Clinical and Diagnostic Technologies. IGI global, Hershey, pp 204-236.

- **Chapter 2**

Vandenberghé B, Corpas L, Bosmans H, Yang J, Jacobs R. A comprehensive in-vitro study of image accuracy and quality for periodontal diagnosis. PART 1: The influence of x-ray generator on periodontal measurements using conventional and digital receptors. Clin Oral Invest 2010 (Submitted, 1st revision)

- **Chapter 3**

Vandenberghé B, Bosmans H, Yang J, Jacobs R. A comprehensive in-vitro study of image accuracy and quality for periodontal diagnosis. PART 2: The influence of intraoral image receptor on periodontal measurements. Clin Oral Invest 2010 (Submitted, 1st revision)

- **Chapter 4**

Vandenberghé B, Jacobs R. The influence of tube potential on periodontal bone level measurements and subjective image quality using a digital PSP sensor. J Oral Maxillofac Res 2010;1:e5

- **Chapter 5**

Vandenberghé B, Jacobs R, Yang J. Diagnostic validity (or acuity) of 2D CCD versus 3D CBCT-images for assessing periodontal breakdown. Oral Surg Oral Med Oral Pathol Oral Radiol Endod 2007;104:395-401

- **Chapter 6**

Vandenberghé B, Jacobs R, Yang J. Detection of periodontal bone loss using digital intra-oral and CBCT images: an in-vitro assessment of bony and/or infrabony defects. Dentomaxillofac Radiol 2008;37:252-60

- **Chapter 7**

Vandenberghé B, Jacobs R, Yang J. Topographic assessment of periodontal craters and furcation involvements by using 2D digital images versus 3D cone beam CT: an in-vitro study. Chin J Dent Res 2007;10:21-29

List of abbreviations

AC	Alternating Current
ALARA	As Low As Reasonably Achievable
ANOVA	ANalysis Of VAriance
CBCT	Cone Beam Computed Tomography
CCD	Charged Coupled Device
CEJ	CementoEnamel Junction
CI	Confidence Interval
CMOS	Complementary MetalOxide Semi-conductor
CT	Computed Tomography
DC	Direct Current
DSR	Digital Subtraction Radiography
FOV	Field Of View
FMX	Full Mouth X-rays, radiographic series
Gy	Gray
HF	High Frequence
ICC	Intraclass Correlation Coefficient
kV(p)	kilovoltage (peak)
LCD	Liquid Crystal Display
lp/mm	linepairs per millimeter
mA	milliampere
mAs	product of mA x s
MDCT	Multi Detector Computed Tomography (=MSCT)
MPR	Multi Planar Reformatting
ms	milliseconds
MSCT	Multi Slice Computed Tomography (=MDCT)
μ	micro-(n)
PDL	PerioDontal Ligament
PSP	Photostimulable Storage Phosphor
Sv	Sievert
TACT	Tuned Aperture Computed Tomography
TIFF	Tagged Image File Format
TFT	Thin Film Transistor

Chapter 1:

General Introduction and Aims

Parts of this chapter have been published as:

Vandenberghe B, Nackaerts O. Imaging in Periodontology: 2D versus 3D Visualization Techniques. In: Informatics in Oral Medicine: Advanced Techniques in Clinical and Diagnostic Technologies. Medical Information Science Reference, IGI Global, Hershey, pp 204-236.

1.1. PERIODONTAL DISEASE

Periodontal diseases are inflammatory processes causing loss of tooth support. Clinical attachment and alveolar bone loss lead to tooth exfoliation, generally over a long period of time. These chronic infectious diseases consist of several disorders of the periodontium, including gingivitis and periodontitis (Lindhe et al 2004). Bacterial metabolism in dental supra- and/or subgingival plaque will affect soft tissues surrounding the teeth and cause inflammation. This gingivitis associated with bleeding of the gums, can progress to periodontitis when soft tissue attachment loss and/or supporting bone loss is seen, resulting in pocket formation between the teeth and remaining soft tissues or alveolar bone. It may affect one to all teeth and eventually, when left untreated, lead to tooth loss. Periodontal disease is one of the leading causes of tooth loss and shows an increasing incidence with age (Lindhe et al 2004, Burt et al 2005, Müller & Ulbrich 2005). Although most epidemiological studies cannot be compared because of different methodologies and investigated populations, periodontal disease prevalence is most likely not decreasing due to improved oral hygiene and decreasing edentulousness (Papapanou 1999, Lindhe et al 2004). In addition, there is strong evidence that periodontal diseases are associated to certain systemic diseases such as cardiovascular disorders (Khader et al 2004). Many studies have shown the importance of early detection of periodontal disease, in relation to the prevention of tooth loss and/or the patient's general health (Slots 2003, Oliveira Costa et al 2007, Seymour et al 2007). Diagnostic tools are therefore crucial for accurate assessment of the periodontal status. Unfortunately, attachment loss patterns are unpredictable and may vary in frequency, location and severity (Papapanou & Wennström 1991, Brown & Löe 1993, Oliver et al 1998, Müller & Ulbrich 2005), often resulting in complex surface topology. The two main bone loss manifestations are horizontal and vertical or angular bone loss (Figure 1.1).

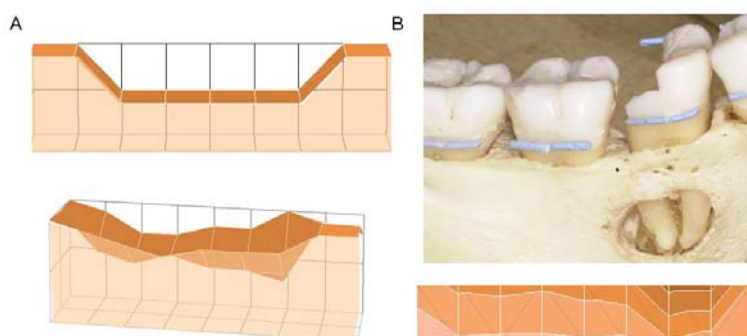


Figure 1.1: a) Schematic view of horizontal (top) and angular (bottom) bone loss; b) Local angular bone loss of a dry skull mandibular first molar: the schematic view depicts depth measurements seen from above.

This architecture is important to depict for diagnostic and treatment purposes. Especially angular defects vary tremendously and many different architectural patterns have been described (Hamp et al 1975, Karn et al 1984, Tarnow & Fletcher 1984). These infrabony defects (crater-like lesions) are a perfect habitat for pathogenic bacteria which may invade the space between roots of multi-rooted teeth causing furcation problems. Angular lesion types are thus more likely to progress and are associated with poor prognosis (Loos et al 1989). Similarly, treatment approaches may vary with bone morphology: periodontal surgical techniques such as osteoplasty with or without ostectomy as well as bone regeneration are highly dependent upon the convoluted topology resulting from disease progression (Müller et al 1995, Svärdröm & Wennström 2000). Examination of the bony architecture is therefore a crucial aspect in periodontal diagnosis and treatment planning (Mol 2004, Brägger 2005). Interestingly, the most commonly used diagnostic tools in this field have barely changed over the years (Armitage 2003, Brägger 2005). Traditional screening methods consist of a thorough clinical examination complemented with two-dimensional panoramic and/or intraoral radiographs. However, digital radiographic imaging and the recently introduced low dose cone beam computed tomography for three-dimensional radiographic analysis may bring new potential in the diagnosis and treatment of periodontal diseases.

1.2. CLINICAL MEASUREMENTS

Clinical signs of gingivitis are discoloration and texture change of the marginal soft tissues surrounding the teeth and are associated with the presence of dental plaque and (supra-) gingival calculus. Using a periodontal probe, the bleeding tendency can be assessed –which is increased when inflammation is present- and clinical attachment loss and pocket depths around each individual tooth can be measured. Tooth mobility may indicate a more severe stage of bone loss causing instability in the alveolar socket because of insufficient bony support. Several indices have been proposed for these diagnostic markers and these methods are well established, simple and cost effective. Much information can thus be derived from the clinical examination alone, although this only pertains to establishing disease extent and predicting its progression (Tugnait et al 2000, Armitage 2003, Nyman & Lindhe 2003).

Probing attachment levels or pockets depths are aiming to measure a distance from respectively the cemento-enamel junction (CEJ) or gingival margin to the base of the pocket or in other words the most apical cells of the dentogingival epithelium. Especially pocket depths (Figure 1.2A) can rapidly be recorded and are the most common in dental practice since the CEJ is often found poorly visible or hindered by local factors such as dental restorations.

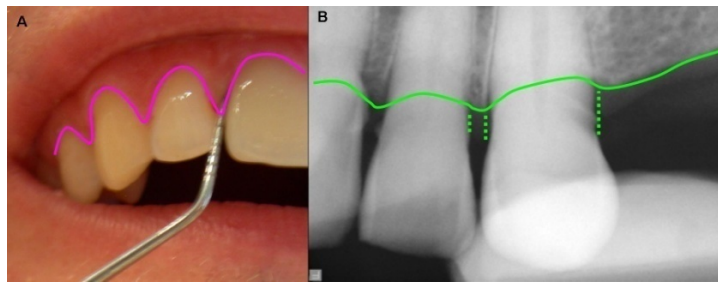


Figure 1.2: A) Pocket depths assess the distance between gingival margin (line) and pocket-base. B) Intraoral radiographs visualize the bony structures and allow measuring the distance from the CEJ to the alveolar bone (line) (in relation to the tooth root)

However, these measurements may overestimate the depth when tissues are locally inflamed or underestimate destruction when gingival recession has occurred. In addition, both types of measurements are prone to inter- and intra-observer errors (Goodson, 1992). In a review paper by Hefti (1997) errors due to probing force, angle, positioning, diameter of the tip and read-out are described and research on methods to reduce these errors are discussed. Clinical measurement errors of 2-3 mm are acceptable, resulting in limited ability to detect disease progression. In fact, examiners involved in clinical research, requiring more accurate measurements to study disease or treatment modalities, must undergo training and calibration sessions in the hope measurements can be standardized. Yet, even in such controlled environment, 1-2 mm errors are common (Polson 1997). More advanced measurement tools such as semi-automated probes have provided only limited additional benefits with similar precision, and are therefore rarely utilized (Quirynen et al 1993, Armitage 2003). Furthermore, traditional clinical tools lack accuracy for the exact determination of disease activity and progression. For instance, at this moment, it does not seem to be possible to know exactly when gingivitis progresses to periodontitis. Therefore, many studies are being conducted investigating potential markers of disease activity. Eley & Cox (1998) have published a series of articles describing these advanced research areas and categorize potential biomarkers in bacterial flora and their products, inflammatory and immune products, enzymes released from inflammatory or dead cells and connective tissue degraded products.

Although some of these tests seem very promising, they still need further research and clinical validation and are beyond the scope of this thesis. Furthermore, the exact extent as well as osseous morphology –needed for adequate treatment choice- cannot be determined using these various tests. The use of a radiographic method to assess damage to the bony tissues will continue to play a central role in diagnosis (Eley & Cox 1998, Armitage 2003, Brägger 2005).

1.3. 2D RADIOGRAPHIC MEASUREMENTS

The most important purpose of the radiographic examination for periodontal diagnosis is to measure the clinical attachment loss or the level of the alveolar bone relative to the roots (Figure 1.2B) and determine the pattern and extent of this bone loss (Jeffcoat & Reddy 2000, Tugnait et al 2000, Armitage 2003, Mol 2004, Brägger 2005). This does not only impact treatment decisions but also allows visualizing small bony changes over time. In addition, the periodontal ligament space (PDL), lamina dura (LD), periapical regions and other related factor like subgingival calculus can be depicted on radiographs (Lindhe et al 2003). Given the limitations of clinical tools, it is often desirable to complement the examination with imaging tools, especially when complex topography of alveolar bone loss is at stake (Tugnait et al 1999, Jeffcoat & Reddy 2000, Armitage 2003, Mol 2004, Brägger 2005).

1.3.1 Methods

There are two types of radiographic methods frequently used in dentistry: panoramic radiography and intraoral bitewing or periapical radiographs.

Panoramic radiography

Panoramic radiographs provide an overall picture of the periodontium but are susceptible to image distortion. They are a curvilinear variant of conventional tomography (see section 1.4.1) having a curvilinear focal trough following the jaw's contours rather than a cross-sectional region of interest. This allows projecting most of the upper and lower jaws on one 2D image, but with associated magnification and distortion. Besides the many overlapping anatomical structures, the thin image layer makes patient positioning critical (Figure 1.3). Their diagnostic value in the assessment of periodontal osseous destruction is therefore more limited than

periapical radiographs (Rohlin et al 1989, Pepelassi & Diamanti-Kipiotti 1997) and is not further considered in this thesis.

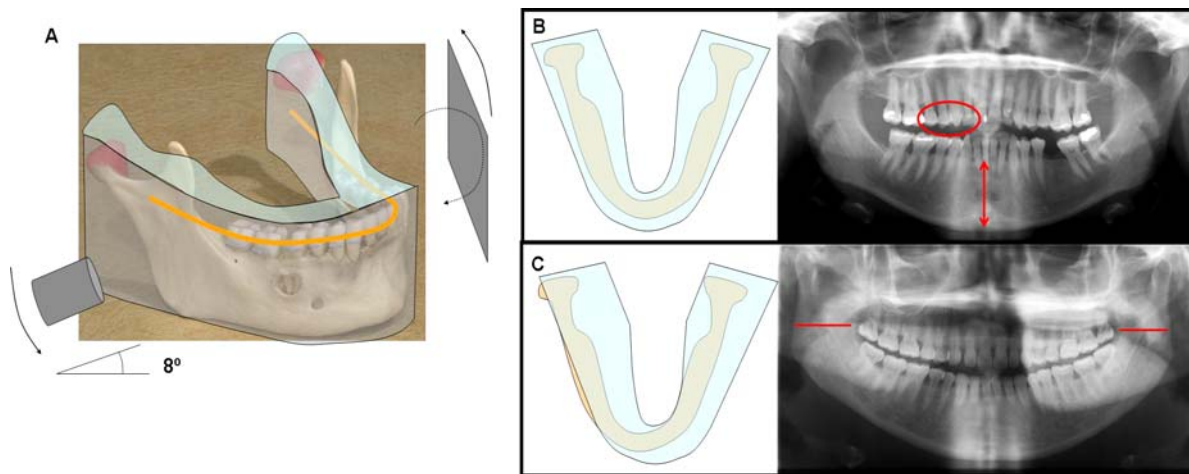


Figure 1.3: (A) Panoramic imaging: a variant of the tomographic technique with a curvilinear focal trough. The narrow image layer makes patient positioning critical. (B) Normal positioning reveals a (distorted) overview of both jaws, but with overlapping anatomical structures such as overlapping interproximal contacts (circle) or magnification (enlarged frontal mandibular height, double arrow). (C) A sideways tilting of the head leads to unequal magnification between left and right side (unequal mandibular rami).

Intraoral radiography

Periapical and bitewing radiographs are projection images which present a more detailed picture of the alveolar crest and other periodontal landmarks or pathologic conditions not visible during clinical examination. Compared to panoramic radiographs, intraoral radiographs have the advantage of high spatial resolution and, with the optimal exposure settings, a vast amount of contrast information. Using a steady x-ray source and an image receptor (film or digital), the periodontal structures are displayed without any magnification or distortion, but only when properly using the paralleling technique. Unfortunately, even when using aiming devices and correct positioning, the inherent property of intraoral radiographs is a two-dimensional (2D) projection. Buccal and oral structures are superimposed on each other and it is therefore difficult to distinguish buccal from oral alveolar bone (Figure 1.4).

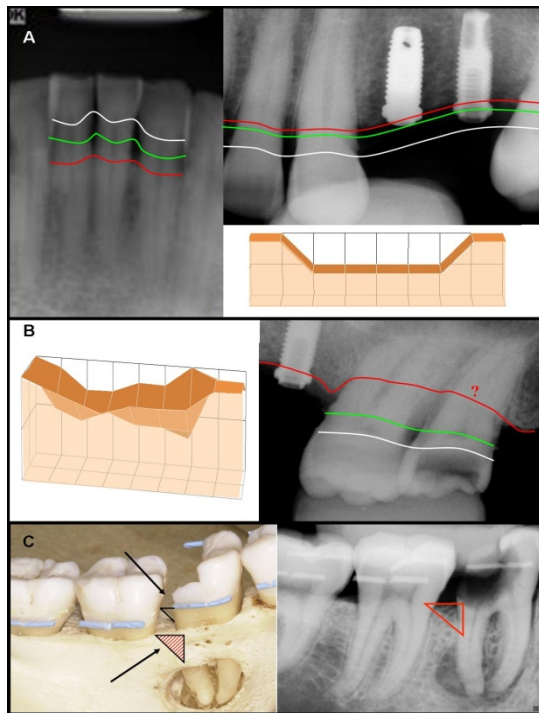


Figure 1.4: (A) Incisor and premolar radiographs revealing an overall horizontal breakdown of bone. The distance from the CEJ (white line) to the actual bony crest (red line) is larger than 1.5mm (the green line should be the healthy bone level) and appears similar for all teeth. (B) The radiograph of the maxillary molars reveals a non-uniform pattern of bone loss. Note that actual bone levels (?) are difficult to assess because of the complex bony topography. (C) A lingual infrabony defect is hard to visualize on the radiograph of the mandibular molars due to supraprojection of the buccal bony plate.

The projective nature of the technique also exposes intraoral radiographs to the risk of projection errors. This can lead –together with observer variation in the identification of anatomical landmarks- to over- or under- estimations of alveolar bone levels (Figure 1.5) (Zulqarnain & Almas 1998). Precise parallel geometry using positioning instruments help to counteract possible projection errors, increasing the sensitivity when high quality images are utilized.



Figure 1.5: Mesio-distal (A) and cranio-caudal (B) projection errors can cause overlapping interproximal tooth contacts (*, A) or incorrect radiographic projection of bone levels (*, B: bone normally lies more than 1 mm from the CEJ, in this case the bony crest is projected at the same level). Note the two carious lesions in A indicated by the arrows.

For the measurements of periodontal bone levels, inter-observer agreement is strong with observer differences within 1mm, if standardized conditions and proper positioning are used (Pecoraro et al 2005). Clinically, this standardization may often be more difficult. Still, clinical studies from Borg et al (1997) reported overall measurement deviations between 0.4mm and 1.4 mm from the surgical

standard. Eickholz and Hausmann (2000) report a mean deviation of 1.4 mm and Pepelassi and Diamanti-Kipiotti (1997) report 80% of their measurements within 1mm, 91% within 2 mm and 96% within 3 mm. Measurement deviations are also dependent of the severity of the alveolar destruction and the tooth type. In general, assessments on radiographs tend to underestimate the amount of bone loss, although in severe osseous defects overestimations are typical. Larger measurement deviations are typically seen in the molar regions. This is due to the usually more complex nature of the alveolar loss.

For the detection of infrabony defects, Rees et al (1971) confirmed that periodontal buccal or lingual defects are difficult to diagnose using radiographs only. In addition, Ramadan and Mitchell (1962) confirmed that most funnel-shaped defects or lingually located defects cannot be detected. Later studies supported these claims: Eickholz and Hausmann (2000) compared radiographs and per-surgical measurements, concluding that angular infrabony defects from vertical bone loss were underestimated with great variation (± 2.6 mm).

1.3.2 Radiographic parameters

Digitalization of intraoral imaging has brought several advantages in patient treatment and disease diagnosis: the required radiation dose for dental imaging may be reduced (Brettel et al 1996, Scarfe et al 1997, Paurazas et al 2000, Pfeiffer et al 2000, Kaeppler et al 2007), image enhancement can be applied (Mol 2000, Analoui 2001^{a,b}, van der Stelt 2004) and an overall easier and faster work-flow can be accomplished (van der Stelt 2000, Farman 2008). Unfortunately, this rapid technological advancement has overwhelmed dental professionals with a multitude of diagnostic options but no related research on the outcome of these possibilities. As a matter of fact, over the last few years there have been many publications concerning the applicabilities of digital intraoral radiography, but hardly any of them has examined its validity to monitor periodontal bone lesions (Borg et al 1997, Kaeppler et al 2000, Wolf et al 2001, Pecoraro et al 2005, Deas et al 2006, Jorgenson et al 2007, Li et al 2007). This is surprising since radiography is one of the most powerful diagnostic tools to assess the bone surrounding a tooth or dental implant. Besides, studies on digital imaging only investigate the digital sensor but do not consider the x-ray generator type. Nevertheless, the latter and its exposure parameters also

influence radiographic contrast and may therefore affect periodontal diagnosis (Chapter 2 & 3).

1.3.2.1 Intraoral digital detectors

Direct systems: CCD (Charged Coupled Device) and CMOS (Complementary Metal Oxide Semi-conductor) solid-state sensors contain silicon crystals converting photons to electrons. For CCDs, pixel charges are transferred to a common output source, while for CMOS conversion takes place at each pixel (Litwiller 2001). Although CCD chips have generally been found to produce lower noise, both have proven reliability for intraoral radiography (Paurazas et al 2000, Kitagawa et al 2003, Farman & Farman 2005). They can be fabricated into intraoral formats (except occlusal sizes), but their active areas are somewhat smaller than film. In addition, read-out technology and cable connection for electrical supply make them much thicker. CMOS technology can provide slightly larger areas and its lower power consumption enables manufacturing of wireless devices (Tsuchida et al 2005), but at the cost of a thicker sensor due to battery integration. The signal transfer curve of solid-state detectors depicts their higher sensitivity compared to conventional films (Figure 1.6), allowing lower exposure times (Borg 1999, Borg et al 2000, Pfeiffer et al 2000, Berkhout et al 2004). One considerable drawback is the occurrence of blooming artefacts (Figure 1.7) (Borg 1999, Borg et al 2000, Litwiller 2001, Berkhout et al 2004). CMOS technology is said to be more resistant to these artefacts by correcting small areas of overexposure (Litwiller 2001). These limitations are gradually overcome.

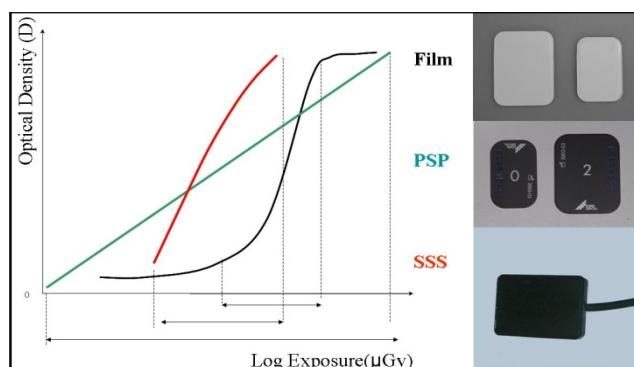


Figure 1.6: Sensitometric curves of conventional film, PSP and solid-state sensors (SSS). Exposure latitude is the widest for PSP and comparable for Film and SSS. However, the latter do not have the S-shaped shoulders (zones of unuseful contrast), and allow latitude extension using contrast enhancement.

Indirect systems: Photostimulable Storage Phosphor (PSP) plates for dental imaging (Kashima 1995) strongly resemble the small and especially thin intraoral

films. These plates can be designed into similar formats, including occlusal sizes, and are thus often better tolerated by patients. The major difference with film is the absence of saturation (Kashima 1995, Borg 1999, Araki et al 2000, Berkhout et al 2004, Bhaskaran et al 2005, Farman & Farman 2005). PSP detectors have a much larger dynamic range than solid-state detectors, decreasing risk of radiographic retakes. Still, optimized exposure levels for PSP should carefully be established since high doses may still generate adequate radiographic contrast (Figure 1.7).

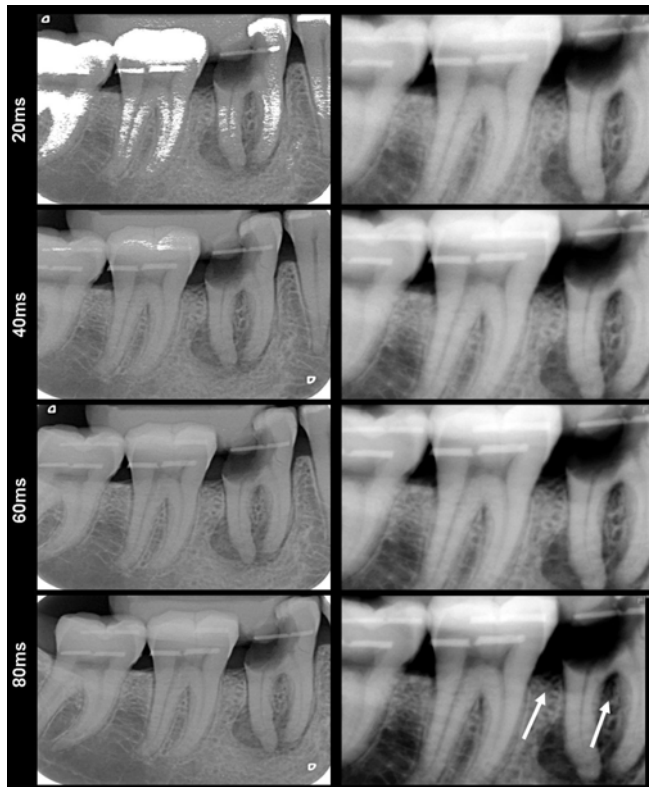


Figure 1.7: PSP (left column) and CCD (right column) radiographs of a dry skull's mandibular molar region at different exposure times. PSP plates are less sensitive than the CCD system and produce artefacts at low exposure times. However, because of their wide dynamic range, the images appear alike when rising exposure time. Using the CCD, the distal and intra-radicular furcation defects of the 1st molar (arrows) are darkening at rising exposure time, simulating larger osseous destruction.

Since both PSP and CCD/CMOS sensor have a different dynamic range, it is important to relate the latter to the specific diagnostic task. PSP plates have a wide dynamic range which allows correction for under- or overexposure of the radiograph: the periodontal structures will appear similar over a wide range of exposures (Figure 1.7). For CCD/CMOS sensors, this is not the case. They are more sensitive than PSP plates and produce adequate image quality at very low exposure times, but they only have a small dynamic range: when rising exposure time, the image will therefore darken (Figure 1.7). This darkening phenomenon produces so called blooming artefacts when exposure time is too high. This may give appearance of larger destruction or bone loss of the alveolar crest, infrabony defects and furcation involvements (*see Chapters 2 & 3*).

1.3.2.2 Radiographic exposure

Another important factor that may hinder a correct periodontal diagnosis is the exposure condition. The x-ray generator has a tube potential (kilo-Voltage or kV), a tube current (milliamperere or mA) and an exposure time (milliseconds or ms) which all influence radiographic contrast and may affect periodontal diagnosis. However, none of these variables have been investigated for digital receptors in the diagnosis of periodontal diseases (*see Chapters 2, 3 & 4*). In addition, the influence of the specific x-ray generator itself has never been researched for dental applications (*see Chapter 2*). Traditional x-ray units using alternating current (AC) deliver sinusoidal potentials between a positive and negative voltage peak, which only generates x-rays in a fraction of the time (positive wave-peak), while the rest of the wave only contributes to scatter radiation (Figure 1.8A). Improvement was accomplished by using high frequency (HF) units, which rectify the negative backflow of electrons, oscillate between higher voltages and therefore produce more useful x-rays during one cycle and less unnecessary low-energy photons (Figure 1.8B). Finally, the constant potential generators (direct current or DC) produce for a given nominal tube voltage and a given filtration of the tube a harder beam spectrum with few low-energy photons. This may result in up to 20% lower skin dose and therefore allow shorter exposure times and/or greater filtration (Helmrot et al 1994) (Figure 1.8C).

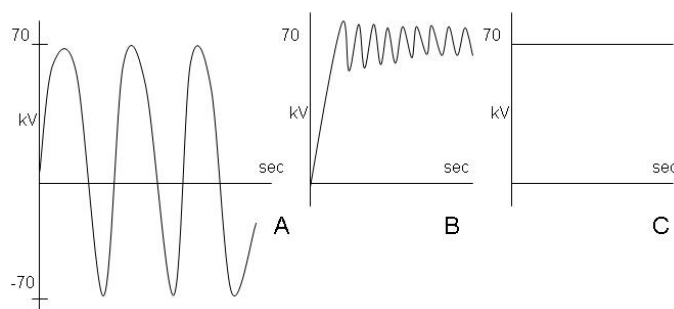


Figure 1.8: Waveforms of three generations of x-ray generators. A) Alternating Current (AC) generator. B) High Frequency (HF) generator. C) Direct Current (DC) generator.

1.3.2.3 Digital image enhancement

One of the most important properties of digital imaging is the ability to manipulate the digital image. Image enhancement can be accomplished by optimizing contrast and/or brightness, or increasing sharpness and decreasing noise using specific filters.

Contrast resolution indicates the amount of grey values that can be imaged. For digital receptors, contrast resolution is expressed in bit depth, where bits represent the amount of grey values. Computer language is written in a binary

language with 0 and 1 bits and therefore 8 bit-language systems can only represent 2^8 or 256 bytes. The pixel from an 8 bit image receptor can thus only provide 256 shades of grey. The use of these grey values in an image can easily be seen in the histogram. In this histogram, the number of grey values is represented on the x-axis (for 8 bit: 0 to 255) and the number of pixels having a specific grey value is presented on the y-axis. By dynamically choosing the grey values from the histogram, the image can be darkened or brightened (Analoui 2001^a) (Figure 1.9).

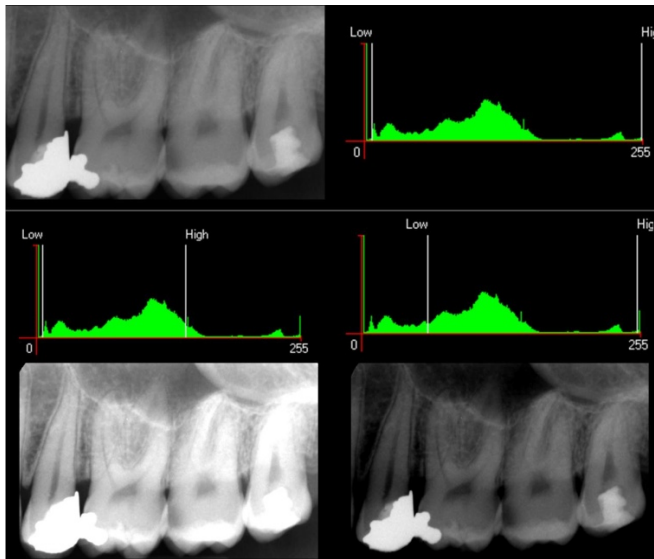


Figure 1.9: Digital periapical radiograph and its histogram of a left upper molar region after image acquisition (top). When choosing different upper and lower limits of the grey values to be displayed, the image is brightened (left) or darkened (right).

Although conventional films show excellent contrast since the image can display any shade of grey possible, a higher and fixed dose to the detector is required and only illumination and a magnification glass are at hand for analysis. The human eye can namely only distinguish approximately 60 shades of grey at once without any aids (Künzel et al 2003). This is of course also true for digital images and in addition, the resolution of the display screen can limit the display of many grey values at once. On the other hand, digital enhancement may thus help in visualizing the whole dynamic range and even adjust for small over- or underexposures. New digital systems reach now even higher bit depths (12 bit= 2^{12} or 4096 grey shades, 16 bit= 2^{16} or 65.536 grey shades) which may influence the diagnostic image quality of intraoral radiographs (Wenzel et al 2007, Heo et al 2009). For periodontal diagnosis, the ability of newer systems to depict more grey values may thus cause a better visualization of the alveolar crest (*see Chapter 3*). However, image enhancement is the ability to change an image in order to make it more visually appealing. In other words, this does not mean that this manipulation will lead to a better diagnosis. Therefore, given the limited literature on the use of these contrast

resolutions for periodontal diagnosis, more research needs to be done to investigate its influence on diagnosis.

Another form of image enhancement is the use of image filters (Analoui 2001^{a,b}). Filters are simple mathematical operations that are applied to the image pixels with as result a visually more appealing image (Figure 1.10).

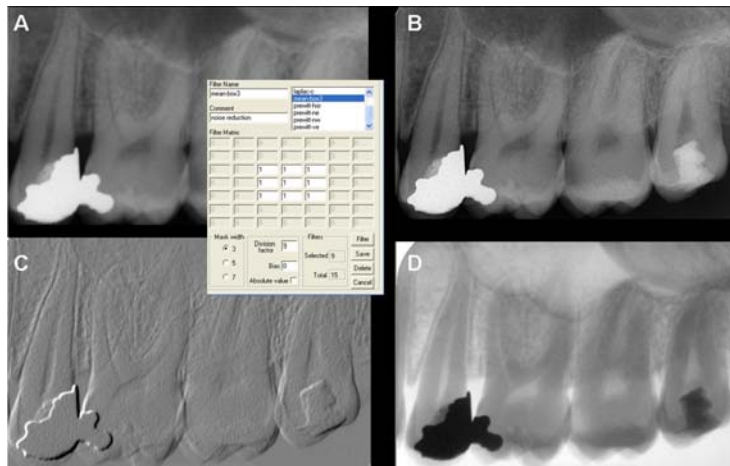


Figure 1.10: (A) Original image with filter window: a filter matrix and mask width can be chosen for the mathematical operation to be applied on the image. (B) Sharpened image. (C) Edge enhancement. (D) Inverse function.

The description of these operators is beyond the scope of this thesis, but it is important to note that much research is ongoing to investigate the value of these operations. Most studies in different dental fields seem to report contradictory results when using enhanced versus unenhanced digital images. This may be due to several factors like the use of newer image receptors with higher contrast and/or spatial resolution, the use of different computer displays or viewing conditions. Because of the many variables in the image process, it is important to fully standardize the research set-up for adequate assessments. Then only can the influence of filtering be investigated. For periodontal diagnosis, research is limited. Eickholz et al (1999) and Wolf et al (2001) did not find any significant differences when using digital enhancement, although they used digitized conventional films with a 10 bit flatbed scanner. Li et al (2007) also did not find any differences for bone level measurements using enhanced images but no information is provided on the exposure set-up. More research in this field is needed, not only for the value of filters when assessing bone loss, but also for detection and measurements of crater depths and furcation involvements (*see Chapter 3*).

1.4. 3D RADIOGRAPHIC MEASUREMENTS

1.4.1 Methods

Because two-dimensional radiographs are often of limited diagnostic value, and a 3-dimensional imaging method is necessary to describe irregular bony defects, advanced imaging techniques have been explored for periodontal diseases. Conventional tomography (Figure 1.11) produces a 2-dimensional cross-section but presents an inherent magnification and is of poor diagnostic quality: identification of major structures such as the mandibular canal is as low as 20% of cases (Kassebaum et al 1990).

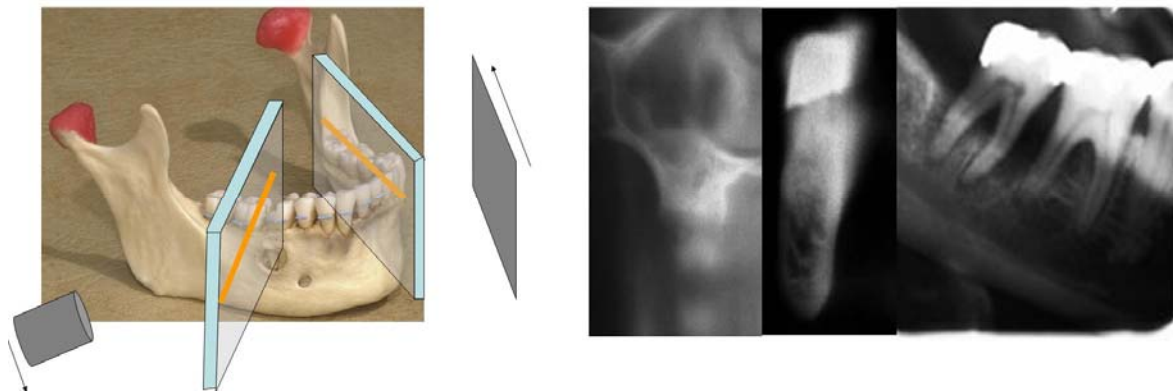


Figure 1.11: With conventional tomography, x-ray beam and receptor move in opposite direction and image a section of interest while the remaining anatomical structures are blurred out. The section can be chosen in many directions, but magnification, distortion and blur may negatively influence diagnosis.

This is primarily due to the unavoidable blur inherent to the method. Another disadvantage is the necessary subsequent acquisition of multiple slices to ensure the region of diagnostic interest is sampled adequately, but making the process time-consuming, expensive, and exposing patients to a relatively high radiation dose (Tyndall & Brooks 2000). To address the need of three-dimensional imaging, tuned aperture computed tomography (TACT™) was developed (Ruttimann et al 1989), which is based on principles of tomosynthesis. This method utilizes traditional radiography and has shown its potential for detection of peri-implant defects (Webber et al 1997, Ramesh et al 2002). However, a complex multiradiographic method must be performed for each site, making this approach appropriate for research but unpractical for clinical practice. Finally, TACT is not readily available commercially.

Computed Tomography

A more promising technique for 3D imaging was the development of axial or incremental computed tomography (CT) which uses a narrow fan-shaped beam rotating around the patient. This generates axial slices without distortion or magnification. The sequential scanning for multiple slices was quickly followed by the continuous x-ray beam rotation in spiral CT, where the patient (table) is moved into the gantry of the unit and a helical or spiral path is described. This generates multiple slices that can be stacked into a volume (Figure 1.12A). Furthermore, modern (third generation) CT units are capable of imaging multiple slices per rotation (multi-slice (MS) or multi-detector (MD) CT), thereby reducing examination and exposure time (Goldman 2008). This stack of slices can be reformatted into the sagittal or coronal direction which is called multiplanar reformatting (MPR).

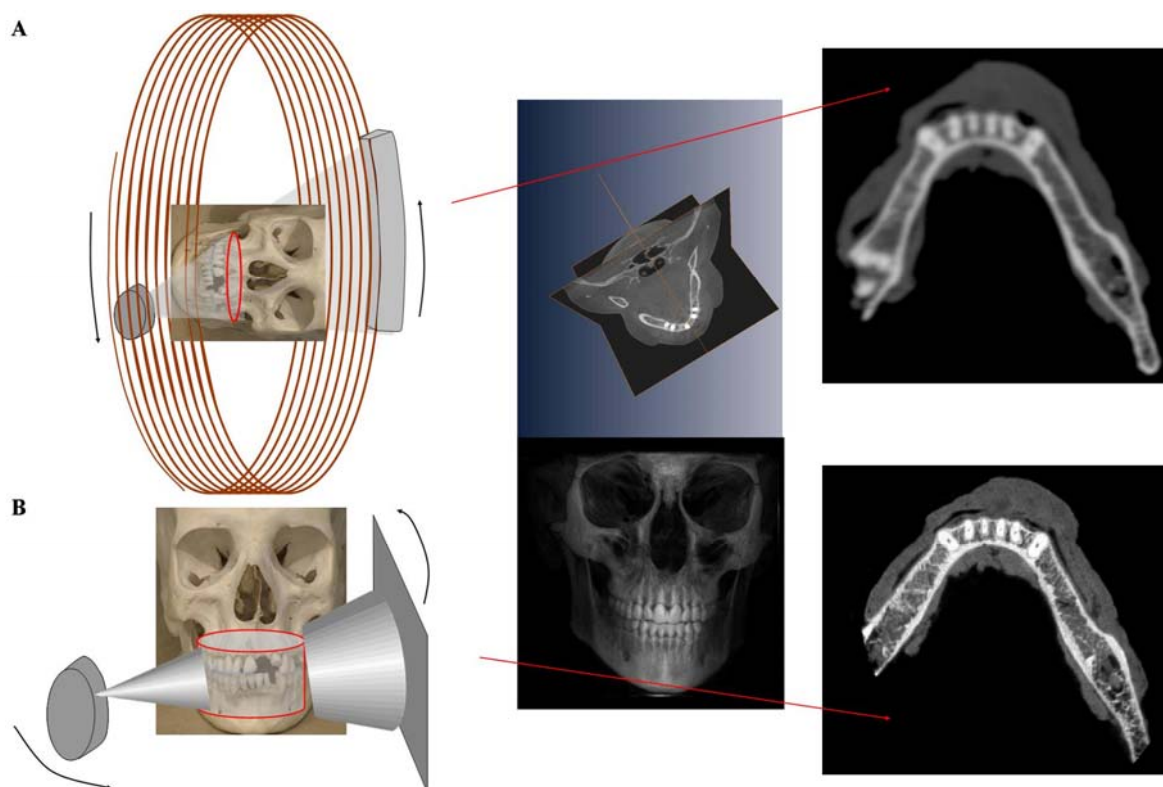


Figure 1.12: Principles of (spiral) computed tomography (A) and cone beam computed tomography (B). While CT generates consecutive axial slices that can be stacked into a volume, CBCT generates an entire volume which can be recalculated to consecutive slices.

Primarily, CT is being used in medicine for imaging the whole body, but because of these excellent 3D capabilities, its use in dentistry has been researched and validated for many years (Gahleitner et al 2003). The third dimension namely allows locating important anatomical structures like the inferior alveolar canal and maxillary sinusses, or allows assessing the width and height of the alveolar process,

thus aiding in precise planning of implant surgery (Klinge et al 1989, Preda et al 1997, Yang et al 1999). For the detection of periodontal defects causing furcation problems, Fuhrmann et al (1997) performed a comparison between intraoral radiographs and CT scanning and found that only 21% of the furcation defects were visible using radiography compared to 100% for CT. The same encouraging results were found in other studies investigating the utility of CT for imaging alveolar bone levels (Langen et al 1995, Schliephake et al 2003).

Despite its excellent contrast resolution, the major drawbacks of this technology are high cost, limited spatial resolution, high radiation dose and limited availability in the dental practice. Further improvements have already been made for the latter two since modern MSCT units have reached sub-millimeter accuracy at lower radiation doses which expand applications for dental imaging (Gahleitner et al 2003).

Cone Beam Computed Tomography

In contrary to medical computed tomography, cone beam computed tomography (CBCT) distinguishes itself by a different scan procedure. In stead of obtaining the region of interest (ROI) or volume slice-by-slice using a fan-shaped beam, it utilizes a conical beam which only makes one convolution around the patient's head: the dentomaxillofacial complex is scanned entirely in one rotation (Figure 1.12B) (Mozzo et al 1998, Arai et al 1999, Miracle & Mukherji 2009). The detector row used in spiral CT is replaced by a flat panel detector which allows acquiring radiographic projections of the jaws from all angles in a 360° rotation. From the scanned volume, axial slices are reconstructed and MPR can follow. The different method to obtain these axial cross-sections makes that both CT and CBCT have some different intrinsic properties. Since only one rotation is needed with a lower power configuration, and given the different detector technology and geometric configuration, the associated high radiation dose of medical CT has greatly been decreased. Furthermore, the CBCT detectors have an excellent spatial resolution and the isotropic voxel acquisition reaches sizes as small as 75 µm (compared to 0.5-1mm for medical CT). This allows for an excellent and detailed visualization of the bony structures in the maxillofacial complex. Furthermore, CBCT units are compact-sized and the cost is drastically less than medical CT. A drawback of CBCT

is the lower contrast resolution and increased noise due to the lower power configuration. The advantage of CT over CBCT is the high contrast resolution for soft tissues which allows distinguishing tissues with very small differences in physical density.

1.4.2 Requirements for periodontal assessments

A drastic change has occurred in dental imaging since the introduction of modern CBCT technology. But, when making the cost-benefit analysis for decision making of a patient's examination type, the clinician should always justify the use of ionization radiation and follow the ALARA (as low as reasonably achievable), and this for each patient individually (Horner et al 2009). When the added value of 3D information is required -for instance in the planning of dental implants- CBCT is thus the imaging modality of choice (compared to MSCT) given the relatively low radiation dose (Guerrero et al 2006, Dreiseidler et al 2009, SedentexCT 2009). This obvious justification is less evident for other dental applications such as periodontal diagnosis, even though the dose of CBCT examinations lies within the range of an intraoral full mouth radiographic x-ray series (FMX) which is often used to complement clinical periodontal diagnosis (Ludlow et al 2006, Scarfe et al 2006). When using the latest intraoral imaging protocols for adequate dose savings (with fast films or digital systems), the dose of an FMX may be around 34.5 μSv , but may run up to 100 μSv when following incorrect guidelines (Gibbs 2000, Ludlow et al 2008). This range is also found for CBCT examinations although it depends on the specific type of CBCT unit and its settings like the field-of-view (FOV), kV and mAs (Palomo et al 2008). Unfortunately, the use of CBCT for periodontal diagnosis seems to be a controversial topic considering the limited research published. Much information can indeed be derived from the clinical examination alone (Tugnait et al 2000), but for more complex patterns of bone destruction and the multitude of modern regenerative treatment techniques, the 3-dimensional examination seems inevitable.

Adding a third dimension to the radiographic image of the periodontium, requires a thorough understanding of periodontal anatomy in 3D. While only two interproximal mesial and distal measurements on intraoral radiographs are used to estimate alveolar bone loss, many more measurements are possible in 3D. Furthermore, not only buccal and oral measurements are possible, but the exact

topography of infrabony craters can be derived by scrolling through the data (**see Chapter 6**). In Figure 1.13, the same molar region of the dry skull in Figure 1.1 (or 1.4C) is imaged using CBCT, revealing the lingually located defect and the exact involvement of the furcation defect.

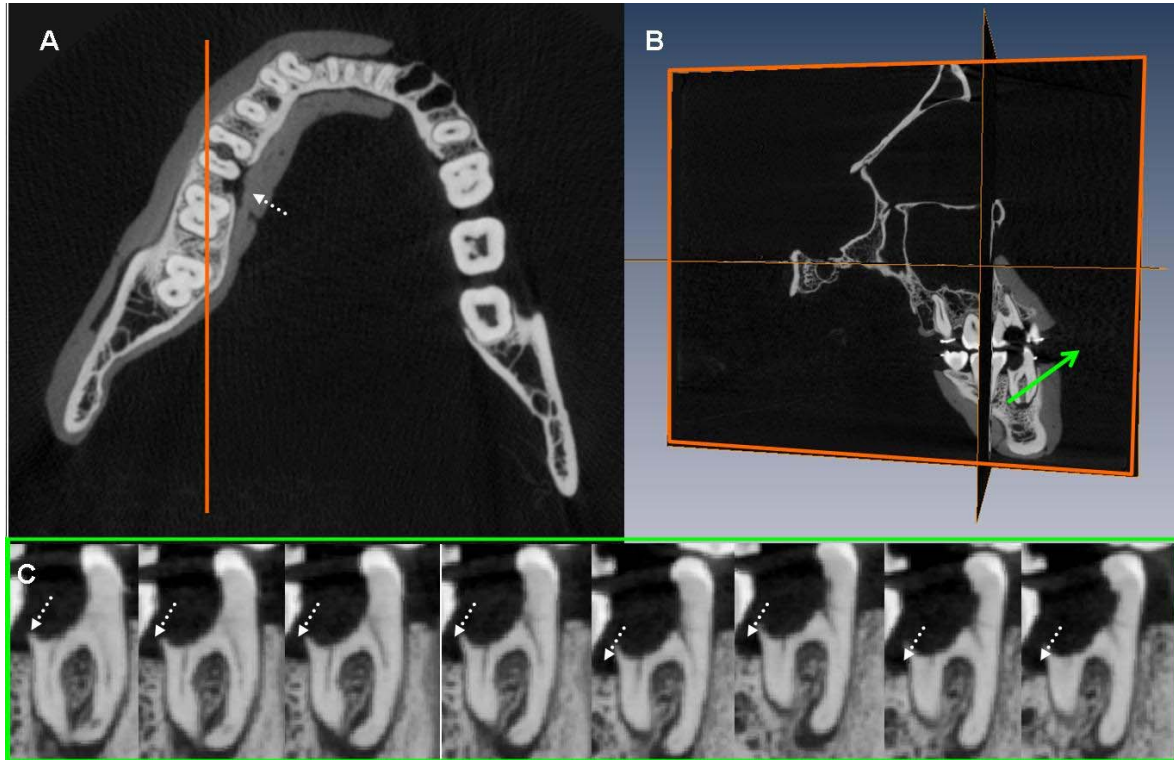


Figure 1.13: (A) Axial slice through the dry skull at the level of the furcation of the right mandibular first molar. A disto-lingual defect (dotted arrow) of the first right molar is already visible (Note that this is a view from below). The orange line is the sagittal slice in the multiplanar view of the skull (B). When moving the slice from buccal to oral (green arrow), the clinician can scroll through the region of interest. It can be noticed that the distal bone (dotted arrows) of the first molar is present buccally, but is slowly breaking down towards the lingual side, confirming the lingual localization of the defect. (C).

Besides orthogonal reslicing of the axial data, oblique reslicing in all directions is also possible. One useful example of this is the simulation of a panoramic overview. By drawing an oblique line that follows the jaw's arch, an overview of the periodontal bone is possible at sub-millimeter slice thickness (Figure 1.14A) (**see Chapter 5**). By raising the slice thickness -or in other words stacking several slices on top of each other- a high resolution panoramic reconstruction is simulated without all the image artefacts of the panoramic technique (Figure 1.14B).

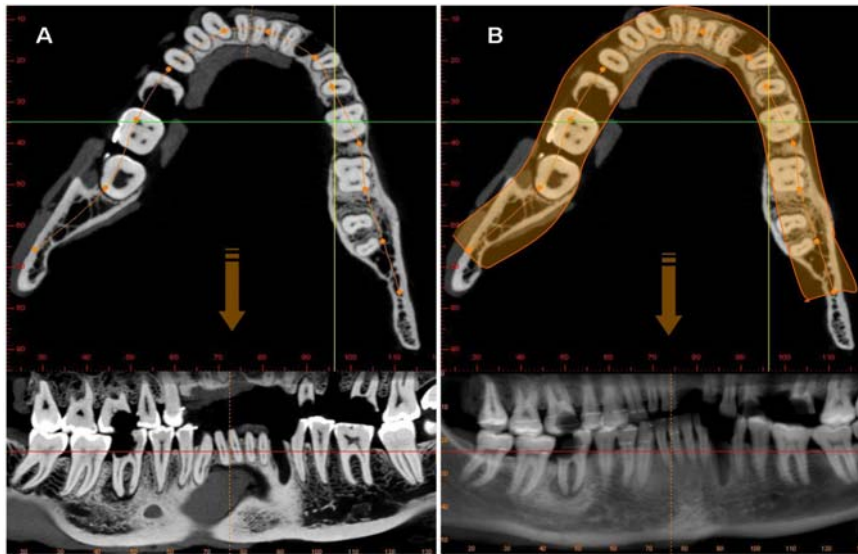


Figure 1.14: (A) The oblique line drawn onto the axial slice through the mandible is reconstructed as an oblique reformatting of the CBCT data. (B) By raising the slice thickness, the oblique reformat is widened to include more structures and simulate a high resolution panoramic overview.

Furthermore, true 3-dimensional evaluation is made possible by software which allows rendering of the CBCT data into a volume (Figure 1.15). Just like any digital image, CBCT data has a histogram showing the grey values attributed to each pixel or voxel. By choosing a threshold value, all grey values below or above this threshold are included in the rendered volume. This allows for 3-dimensional display of different structures, like the bony contours with or without the overlying soft tissues (in vivo soft tissue visualization is mostly limited to facial contours). A careful interpretation of the CBCT data is thus a prerequisite, and a diagnosis should never only be based on such display tools. For instance, bony particles can have many different grey values depending on their density (calcification). Thus, a certain threshold may exclude some bony particles in the rendered volume. Therefore, the histogram should be used to see which structures are displayed in 3D.

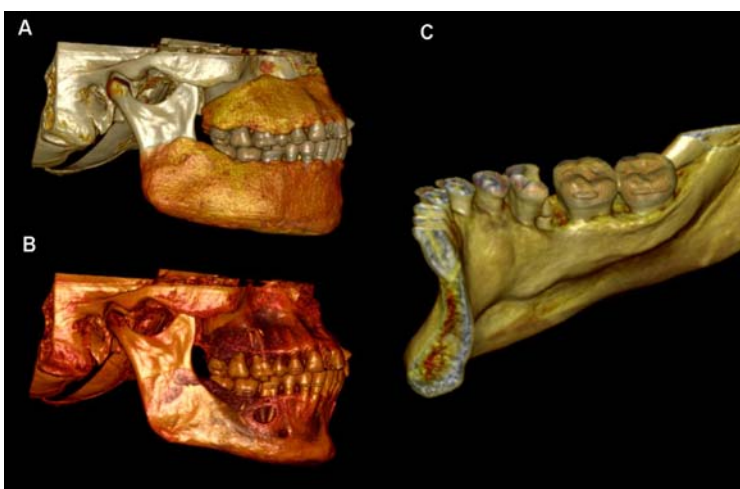


Figure 1.15: (A) Rendered volumes of the dry bony skull (from Figures 1.1, 1.13 & 1.14) with soft tissue simulation modelled over the upper and lower jaws. (B) Rendered volume without the soft tissues revealing alveolar bone. (C) The right mandibular side cropped out of the volume and seen from lingual to inspect the lingual bone loss of the first mandibular molar.

Alveolar bone loss measurements

Only few in-vitro studies have compared the accuracy of alveolar bone loss measurements on intraoral radiographs and CBCT cross-sectional images. In addition, these studies use in vitro standardization methods which cannot be used in clinical practice. Mengel et al (2005) and Misch et al (2006) both explored artificially created defects and included gutta percha markers along the defects for the measurements. Furthermore, both studies assessed bone defects on 1mm cross-sections which only partially represent the available spatial information from CBCT. Nevertheless, the results showed that CBCT reaches an excellent sub-millimeter measurement accuracy which indicated that no magnification of the images was present. However, more studies needed to be conducted –especially with naturally occurring bone loss sites- to determine the accuracy on CBCT sub-millimeter cross-sections (*see Chapter 7*) or even on oblique reformatted slices (panoramic reconstructions) when keeping in mind the many periodontal measurements needed in clinical practice (*see Chapter 5*).

Infrabony defects and furcation involvement diagnosis

In addition to bone level measurements, it is as important to be able to detect and classify the periodontal infrabony defects, since their exact topography will affect periodontal treatment (Müller et al 1995, Svärdröm & Wennström 2000). Surprisingly, literature is sparse even though the limitations of current 2D techniques. Fuhrmann et al (1995, 1997) studied the detection of artificially created defects in human cadavers on high resolution CT and periapical radiographs and found 21% of furcation involvements and 67% of infrabony defects detected on intraoral images compared to 100% for CBCT. However, even though classification of the topographic involvement was conducted and promising results were found, studies using new low dose imaging techniques like CBCT need to be conducted (*see Chapter 6*). Misch et al (2006) similarly described that all artificially created defects in their study were detectable using CBCT, but no classifications were made and limited information on these detections was given. They conclude though that CBCT may be a suitable imaging modality to make adequate treatment decisions of periodontally affected maxillary molars. These encouraging results indicate that CBCT may be a desirable method in selected cases where complex periodontal defects cannot be adequately assessed clinically and radiographically.

Other periodontal landmarks

Other radiographic parameters often utilized in the diagnosis of periodontal diseases are the integrity of the lamina dura or the width of the periodontal ligament space but also the bony trabecularization for bone quality determination prior to implant placement (Lindh et al 1996). However, no studies have been performed to compare these intraoral radiographic findings to CBCT. Liang et al (2009) compared the subjective image quality of five different CBCT units to MSCT and found that lamina dura delineation, PDL space and trabecular pattern of bone scored the least of all image quality criteria and ratings vary depending on the CBCT unit. More research needs to be performed to determine CBCT's accuracy in these more subjective ratings of periodontal markers (*see Chapters 5 & 7*), especially since modern CBCT units are showing improved contrast and spatial resolution.

1.5. AIMS

Given the rather limited research for periodontal diagnosis using digital 2D or the more recently introduced 3D techniques, general recommendations are often not followed in clinical practice, revealing the need for more evidence-based research to ensure high standards of radiographic practice (Tugnait et al 2004).

The overall aim of this thesis was to compare the accuracy of current 2D and 3D imaging techniques for periodontal diagnosis. Therefore, the first aim was to investigate the diagnostic yield of digital intraoral radiography for periodontal diagnosis and demonstrate an associated improvement in imaging accuracy and quality at reduced radiation exposure compared to conventional film imaging. The second aim was to determine the accuracy of periodontal diagnosis using the recently introduced low-dose 3D CBCT imaging technique.

To reach the two main objectives of this research, the following specific aims were addressed:

2D DIGITAL IMAGING MODALITIES

- **Chapter 2:** To determine the influence of the x-ray generator type in periodontal measurements

Hypothesis: The characteristic x-ray beam of direct current or high frequency x-ray units produces accurate periodontal measurements at lower exposure times than alternating current units

- **Chapter 3:** To determine the influence of the digital image receptor on periodontal measurements

Hypothesis 1: Accuracy of periodontal measurements is accomplished at different exposure times for film, PSP or solid-state sensors

Hypothesis 2: High resolution detectors improve the accuracy of periodontal assessments

Hypothesis 3: Dedicated periodontal filtering improves accuracy of periodontal measurements

- **Chapter 4:** To determine the influence of tube potential (kV) on periodontal measurements

Hypothesis: Small changes in tube potential (kV) do not influence digital measurement accuracy for periodontal diagnosis

3D IMAGING MODALITIES

- **Chapter 5:** To compare the accuracy of 2D and 3D panoramic reconstructions for periodontal diagnosis

Hypothesis: Accuracy of periodontal measurements is at least as reliable on 3D panoramic reslices as on 2D intraoral radiographs

- **Chapter 6:** To compare topographic assessments of infrabony defects on 2D radiographs and 3D CBCT

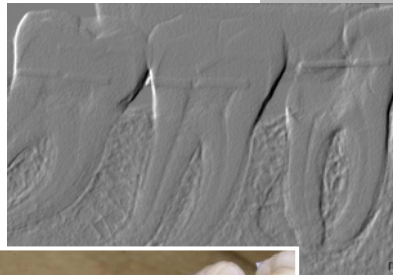
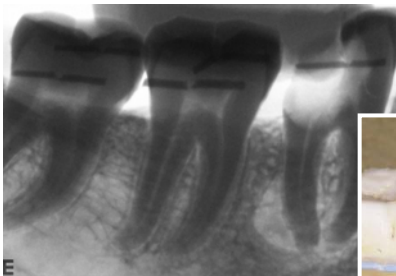
Hypothesis: The detection and topographic classification of local and invasive bony defects is more accurate using 3D CBCT

- **Chapter 7:** To compare the accuracy of 2D and 3D sub-millimeter cross-sectional measurements for periodontal diagnosis

Hypothesis: Accuracy of periodontal measurements on 3D sub-millimeter cross-sections is at least as reliable as on 2D intraoral radiographs

2D Imaging Modalities for Periodontal Diagnosis

PART I



Chapter 2:

The influence of x-ray generator on periodontal measurements

This chapter has been submitted as:

Vandenberghe B, Corpas L, Bosmans H, Yang J, Jacobs R. A comprehensive in-vitro study of image accuracy and quality for periodontal diagnosis. PART 1: The influence of x-ray generator on periodontal measurements using conventional and digital receptors. Clin Oral Invest 2010 (Submitted, 1st revision)

INTRODUCTION

The rapid evolution towards digital imaging has brought several advantages in patient treatment and disease diagnosis. Digitalization has reduced the required radiation dose for dental imaging (Brettler et al 1996, Scarfe et al 1997, Paurazas et al 2000, Pfeiffer et al 2000, Kaeppler et al 2007), allowed the use of image enhancement (Borg et al 1997, Eickholz et al 1999, van der Stelt 2000, Wolf et al 2001, Jorgenson et al 2007, Li et al 2007) and brought an overall easier and faster work-flow (van der Stelt 2000, Farman et al 2008). Furthermore, the amount of quality assurance steps has been down-sized due to elimination of the many processing steps of conventional film development, with the final diagnostic quality of digital images now mostly depending on a specific sensor's sensitivity profile and resolution and the x-ray generator exposure settings. Due to the fast technology turnover, many studies have investigated the constant improvement of film or digital sensor sensitivity and resolution. Reports have demonstrated dose savings of 50% when using E/F-speed films compared to D-speed types (Ludlow et al 2001) and even further savings when using digital sensors (Brettler et al 1996, Kaeppler et al 2007). However, the x-ray generator and its specific settings have often not been explored despite their direct impact on radiographic contrast and image density (Curry et al 1990).

International recommendations on mA (tube current or beam intensity) and kV (tube voltage or penetration level) ranges –usually fixed on dental x-ray units- have been published (European Commission 2004) but actual exposure times (or mAs) for intraoral radiographs still need to be balanced towards receptor- and x-ray generator-type. Traditional x-ray units based on alternating current (AC) delivered sinusoidal potentials between a positive and negative voltage peak, only generating x-rays in a fraction of the time (positive wave-peak), while the rest of the wave only contributed to scatter radiation. Most AC units now have rectified this negative backflow of electrons, but more modern high frequency (HF) units oscillate between higher voltages and therefore produce more useful x-rays during one cycle and less unnecessary low-energy photons (Helmrot et al 1988). Although the latest HF or multipulse waves resemble those of constant potential generators, HF units are marked by a small pre-heating time: kV variation (or ripple) decreases at rising

exposure times. Constant potential generators (direct current or DC) produce a harder beam with smaller ripple and no pre-heating (McDavid et al 1982). For many years now, the impact of these different waveforms has been investigated using experimental phantom tests and indicated possible skin dose savings by maintaining subject contrast. Unfortunately, up to now, no studies have reported the clinical impact on diagnostic image quality. Especially in combination with sensitive digital sensors, a more accurate and predictable x-ray output obtained by DC generation may allow further dose savings (European Commission 2004), while older generators may not be able to cope with the low exposure settings for digital receptors. Surprisingly, most studies on digital imaging have not considered x-ray generator type in the determination of exposure range. Direct solid state sensors (complementary metal-oxide semiconductors or CMOS and charged coupled device or CCD) and indirect imaging plates (photostimulable storage phosphor or PSP) have namely different sensitometric properties which may be influenced by the x-ray generator type.

For general dental diagnosis, Borg et al (2000) compared the subjective image quality ratings (visibility of important structures) for varying exposure times using several digital systems and a DC tube. They found PSP systems to have a wider useful exposure range and CCD the narrowest. In a similar research set-up, Bhaskaran et al (2005) and Berkhout et al (2004) found comparable results although a HF generator was used. Similarly, for periodontal diagnosis, no studies could be found investigating different x-ray generators but in addition, most studies did not explore exposure ranges (Müller & Eger 1999, Kaeppler et al 2000, Wolf et al 2001, Pecoraro et al 2005, Deas et al 2006, Gomes-Filho et al 2007, Jorgenson et al 2007, Li et al 2007). Pecoraro et al (2005) investigated observer reliability in assessing periodontal bone height using conventional E-speed film and a digital CMOS sensor and found no significant difference when using the digital system. However, the x-ray generator used was of the AC type and in addition, the exposure range was halved for the digital system without investigating other exposure times. As a matter of fact, the added value from (digital) radiography for periodontal diagnosis has often been questioned because research in digital imaging is lacking (Hausmann 2000, Tugnait et al 2000, Mol 2004). Only one study explored a range of radiographic exposure times in the detection of periodontal bone loss using two digital systems and a DC

tube, but high exposure times -comparable to film- were used (Borg et al 1997). Therefore, the overall aim of this study was to investigate the effect of x-ray tube generator on image accuracy and quality for assessment of periodontal bone lesions using conventional and digital imaging receptors at a range of increasing exposure times.

MATERIALS AND METHODS

Thirty-one periodontal bone defects of two adult human skulls, a cadaver head and a dry skull, were evaluated using intraoral conventional and digital radiography. The upper and lower jaws of the cadaver head were fixed with 10% formalin and functioned as a clinical subject. The cadavers were obtained with permission and ethical approval from the Department of Anatomy at the Catholic University of Leuven, Belgium. The adult human dry skull was covered with a soft tissue substitute, Mix D and used as a simulation (White 1977). For the intraoral protocol, the paralleling technique was applied in a standardized exposure set-up. A film holding system (XCP, RINN Corporation, Elgin, IL, USA) was used and standardized repositioning and stabilisation was guaranteed by an individually adapted stent material, serving as a rigid occlusal key during exposure. These waxed imprints of the anterior, premolar and molar regions were made on the bite blocks of the radiographic aiming device (see Figure 2.1A).

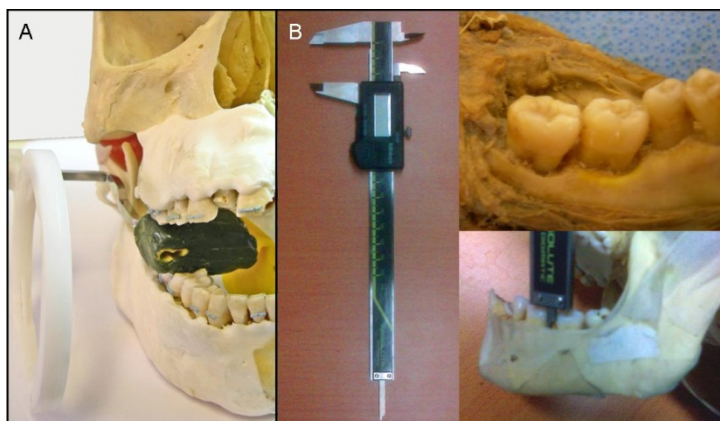


Figure 2.1: (A) Standardized intraoral radiographic exposure set-up: aiming and positioning device with occlusal keys (green stent) (notice the soft tissue simulation on the dry skull). (B) Digital caliper with inside and outside measurements, and depth blade. For the cadaver jaws, measurements were done after flapping. The depth blade allowed measuring infrabony defects to the base of the crater.

Intraoral x-ray units

To investigate the influence of x-ray generation, three x-ray generator types corresponding to AC (IRIX 70, Trophy Radiologie, Marne-La-Vallée, France), HF (Prostyle Intra, Planmeca Oy, Helsinki, Finland) and DC (Minray, Soredex, Tuusula,

Finland) generators were used. Exposure settings were 70 kVp and 7 mA (Minray) or 8 mA (IRIX 70, Prostyle Intra). For comparison of the tubes with different mA values, the different exposure time intervals (ms) were recalculated according to one mA setting by using their linear relationship (mAs). The exposure times used for conventional film and PSP were 0.020, 0.040, 0.060, 0.080, 0.120, 0.160 seconds. For CCD however, the used range was limited to 0.020 or 0.040, 0.060 and 0.080 seconds. A mechanically interlocking rectangular (4cm x 3cm) collimator (Universal Collimator, RINN Corporation, Elgin, IL, USA) was used for the AC and HF unit for comparison to the DC unit, equipped with an integrated 3 by 4 cm beam collimation. The focal-film distance was (set to) 30 cm for all tubes.

Imaging modalities

For the radiographic assessments, peri-apical radiographs were made with conventional film, indirect digital and direct digital systems using the standardized set-up. The conventional films used in this study were Agfa Dentus M2 Comfort E-speed film (Heraeus Kulzer GmbH, Dormagen, Germany) and Kodak Insight F/E-speed film (Carestream Health, Rochester, NY). The indirect digital PSP systems were Digora Optime (Soredex, Tuusula, Finland), Vistascan (12 bit) and Vistascan Perio (16 bit) (Dürr Dental GmbH, Bietigheim-Bissingen, Germany). For the Vistascan 12 bit, both original and images with a dedicated periodontal filter were included for analysis. The direct digital CCD sensors were Sigma (Instrumentarium Dental, Tuusula, Finland) and VistaRay (Dürr Dental GmbH, Bietigheim-Bissingen, Germany). Two examples of the radiographic set-up are given in Figure 2.2 and 2.3: the three x-ray generators are combined with a PSP (Figure 2.2) and a CCD (Figure 2.3) system while exposure time is increased.

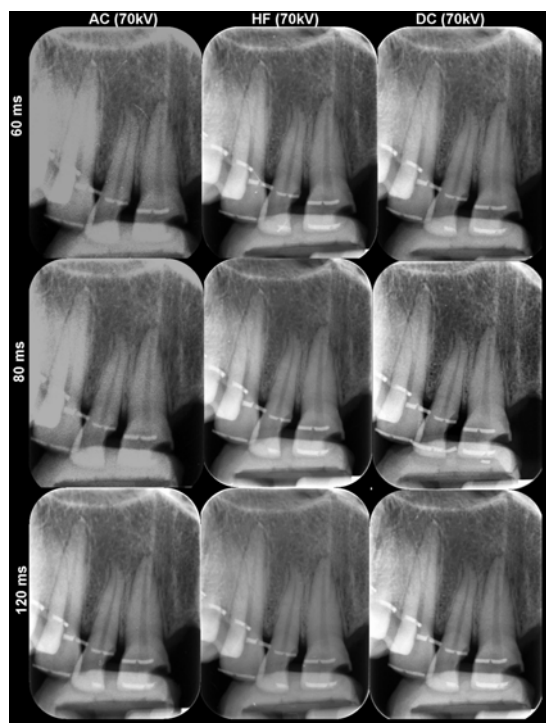


Figure 2.2: PSP radiographs (front region) of the standardized dry skull with three x-ray generator types at rising exposure times. Notice the increase in radiographic contrast from left to right (AC to HF to DC) but mostly at low exposure times. From the top down (60 to 80 to 120 ms) this difference is less apparent except for the AC tube.

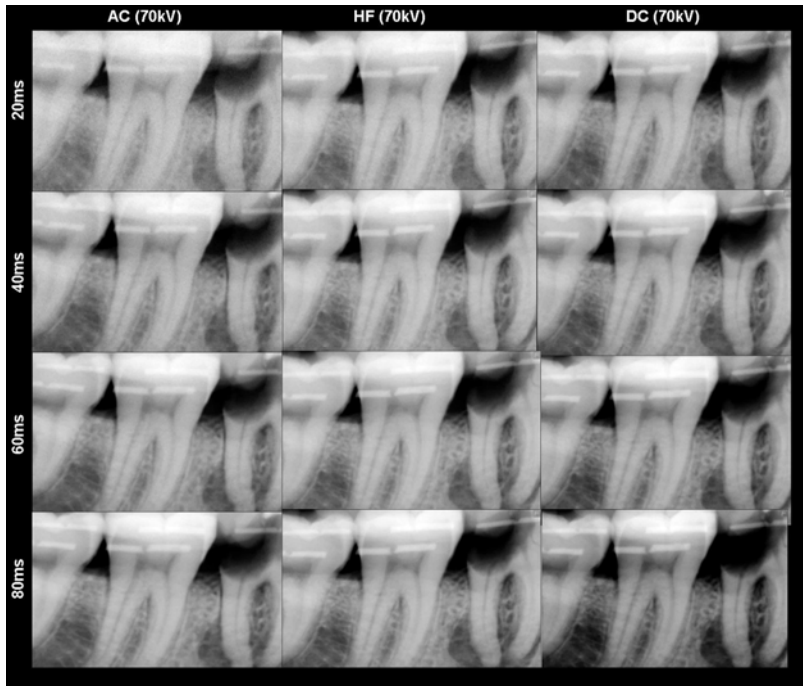


Figure 2.3: CCD radiographs (molar region) of the standardized dry skull with the three x-ray generator types at rising exposure times. Notice the change in radiographic contrast from left to right (AC to HF to DC) especially at low exposure times. From the top down (rising exposure) this change can also be noticed and at high exposure times, blooming effects (darkening of the alveolar crest) become apparent especially when using the DC tube.

Radiographic assessments

The radiographic assessments consisted of objective measurements on one hand and subjective evaluations on the other hand. Images were viewed by three observers (all dentists specialized in oral imaging) in a darkened room on three standardized notebooks with 17 inch TFT based LCD monitors (contrast ratio 750:1) having anti-reflective layers, same screen resolution (1440 x 900 pixels), and contrast and brightness levels. The intraoral peri-apical images from all possible x-ray tube, image receptor and exposure time combinations were exported in Tagged Image File Format (TIFF) and displayed in a random order with the Emago Advanced, V.3.5.2. software (Oral Diagnostic Systems, Amsterdam, The Netherlands) at true size (pixel-size x number of pixels, ratio 1:1). Image processing, including zoom functions, was not allowed for the digital observer assessments. The conventional films were processed with an automatic film processor (XR24 Nova, Dürr Dental, Bietigheim-Bissingen, Germany) with Dürr Chemistry (Röntgen Spezial-Set für Dürr Automat XR24). The films were viewed in a darkened room using a 6"x12" countertop illuminator (Universal Viewer, Dentsply International, York, PA, USA) with magnifier and film mounts to cover surrounding light.

For the objective measurements, thirty-one naturally occurring sites were selected, including linear defects, three-dimensional craters and furcation

involvements, to measure periodontal bone levels. The observers were asked to measure the distance from the cemento-enamel junction to the alveolar bone using the linear measurement tool of the Emago Advanced software or for the conventional films, using a digital sliding calliper (Mitutoyo, Andover, UK) both with an accuracy to the nearest 0.1mm. Physical measurements of the skulls were considered as the gold standards for further accuracy assessment of all imaging combinations. For the cadaver jaws, the gold standard was obtained after image acquisition, by flap surgery to allow physical measurements using a digital sliding caliper (Mitutoyo, Andover, UK) with accuracy to the nearest 0.01 mm. For the dry skull however, gold standards were obtained, prior to adding soft tissue substitute and image acquisition. Mesial, central and distal bone levels and bone crater depths on the oral and vestibular sides of each selected tooth were measured by two observers using the inside measurement arms of the calliper and averaged. For infrabony defects containing several walls, the depth blade was used allowing measurements until the base of the defect (see Figure 2.1B). Because of dehydration of the dry skull, the faded CEJ could not be used as a reference point as in the formalin-fixed cadaver jaws. Therefore, radio-opaque gutta-percha fragments with a small central indentation were glued onto the respective teeth to serve as standardized fiducials.

For the subjective evaluations, important periodontal diagnostic criteria were analysed by the three observers. The delineation of lamina dura, crater visibility, furcation involvement visibility, depiction of trabecular bone and radiographic contrast was evaluated on all images. An ordinal scale was assigned to these variables, ranging from 0 to 3 (1=bad, 2=medium, 3=good), with 0 as a score when it was not possible for an observer to evaluate the criterion properly.

Dose measurements

Using a Barracuda multimeter (RTI Electronics AB, Mölndal, Sweden) with a solid state dose detector (R100 dose probe), the kV, time, pulses, dose, dose rate, dose per pulse, half value layer and filtration were measured for the AC, HF and DC units within a range of 0 to 200 ms. The probe was positioned at the same source-distance for the three tube types. Accuracy of the multimeter was tested indicating a range within 3% inaccuracy for entrance dose and less than 1% for kV measurements.

Statistical methodology

All analyses have been performed using SAS software, version 9.2 of the SAS System for Windows (SAS Institute Inc 2008).

Table 2.1 gives an overview of the number of measurements per combination of x-ray tube- image receptor (group) and exposure time. In the analyses 7 groups are distinguished defined by tube and image receptor combination.

Table 2.1: Number of measurements presented by exposure time and group. A total of 2479 bone level measurements were done by each observer. For example, measurements for the 31 bone defects are obtained with four different PSP systems/configurations at exposure time ≤ 20 ms, resulting in 124 measurements made by each of the three observers. Note that some landmarks can be missing on radiographs with smaller receptor-size, for instance CCD vs PSP size. The exposure time is recalculated from mAs, if mA were equal to 7.

Group	Exposure time							Total
	0<ms≤20	20<ms≤40	40<ms≤60	60<ms≤80	80<ms≤100	100<ms≤140	ms>140	
<i>Film, AC (kV=70)</i>	0	58	58	58	58	58	58	348
<i>PSP, AC (kV=70)</i>	0	62	62	62	62	62	62	372
<i>PSP, HF (kV=70)</i>	0	62	62	62	62	62	62	372
<i>PSP, DC (kV=70)</i>	124	124	124	124	0	124	124	744
<i>CCD, AC (kV=70)</i>	0	27	27	116	116	89	0	375
<i>CCD, HF (kV=70)</i>	0	27	27	27	27	0	0	108
<i>CCD, DC (kV=70)</i>	40	40	40	40	0	0	0	160
Total	164	400	400	489	325	395	306	2479

Accuracy

The accuracy of measurements has been defined as the absolute distance from the gold standard (GS). In some cases, radiographic image quality was too low for the observer to obtain an actual measurement. In respectively 302, 5, 29 and 2143 (86.4%) cases none, only one, only two and all three observers made an actual measurement. Ignoring this rather large set of cases would substantially bias the evaluation of the accuracy. In case no bone level measurement was possible due to lack of image quality, the measurement accuracy was considered to be right-censored at an arbitrarily value of 6, a value which exceeds the lowest observed measurement accuracy (the lower the accuracy, the higher the absolute distance from the GS). As a result, the statistical analysis of accuracy was cast into a survival

analysis framework. The accuracy has been averaged over the three observers. In the 34 cases with a discrepancy between the observers in assigning an actual value, the mean accuracy was also considered right-censored.

Comparisons were made between groups separately within intervals of exposure level (≤ 20 ms, 20-40 ms,...). Kaplan-Meier estimates were used to visualise the cumulative distribution function of the distance from the gold standard. The hazard for an accurate measurement was compared between the groups using a Cox model. Since each combination of bone defect and group was measured repeatedly (by possible multiple products and multiple exposure levels), this clustered structure was accounted for using the COVS option in the PROC PHREG procedure. For each combination of bone defect and group, a Spearman correlation was calculated to quantify the relation between the exposure level and accuracy. A Wilcoxon signed rank test was then used to verify if the distributions of this set of correlations differed from zero.

Subjective Measurements

For illustrative purposes only, the mean of the ordinal scores (giving a zero value in case the quality was too low to make an assessment) has been plotted for each group separately as a function of the exposure time. Note that for each of the skulls only one measurement was present with each device combination (receptor-tube) at a specific exposure level. Interest was in the relation between exposure level and rating (ignoring the device) and the differences between the tubes (ignoring exposure level and image receptor). A proportional odds model was used to model the ratings (0-1-2-3) as a function of exposure level and tube respectively. Generalised estimating equations were used to take into account the aforementioned clustered structure (using PROC GENMOD). These models have been fitted for each observer separately. In all analyses, p-values smaller than 0.05 were considered to be significant.

RESULTS

Measurement accuracy

Figure 2.4 presents the cumulative distribution function (based on Kaplan-Meier estimates) of the absolute distance from the gold standard. This function gives the percentage of measurements (Y-axis) falling within a specific distance (X-axis) from the gold standard. Hence, the faster the curve increases, the higher the accuracy. The groups are compared within intervals of exposure range (≤ 20 ms, $20 \text{ ms} < \text{ms} \leq 40$ ms, ..., $\text{ms} > 140$ ms).

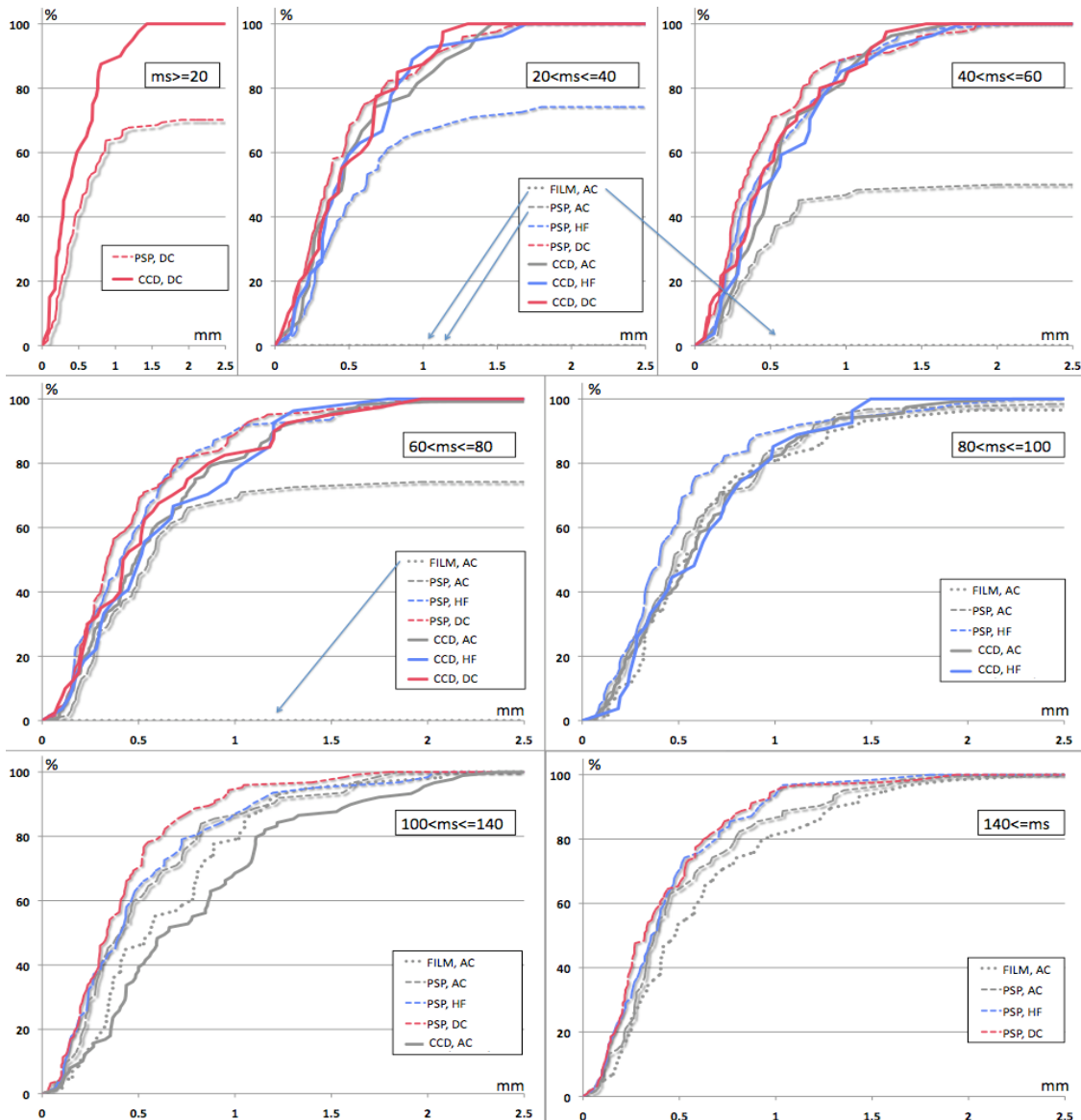


Figure 2.4: Cumulative distribution function (based on Kaplan-Meier estimates) of the absolute distance from the gold standard. This function gives the percentage of measurements (Y-axis) falling within a specific distance (X-axis) from the gold standard. Hence, the faster the curve increases, the higher the accuracy. The graphs are presented at rising exposure intervals: $ms \geq 20$, $20 < ms \leq 40$, ..., $140 \leq ms$.

Chapter 2: the influence of x-ray generator on periodontal measurements

Table 2.2 summarizes some relevant results from the Cox regression models comparing the accuracy between various groups within ranges of exposure level.

Table 2.2: Relevant results from the Cox regression models comparing the accuracy between various groups within ranges of exposure level. The significant differences in bold indicate a greater accuracy for the second group versus the first except for the significant difference marked by [*] which demonstrates greater accuracy for the first one. The [x] represents missing combinations. (R=receptor, T=Tube)

Group	Variable	Exposure Time (at mA=7)						ms >140
		20≤ms	20<ms≤40	40<ms≤60	60<ms≤80	80<ms≤100	100<ms≤140	
R	AC vs HF	x	p<0.0001	p<0.0001	p<0.0001	p>0.05	p>0.05	p>0.05
	AC vs DC	x	p<0.0001	p<0.0001	p<0.0001	p>0.05	p>0.05	p>0.05
	HF vs DC	x	p<0.0001	p>0.05	p>0.05	p>0.05	p>0.05	p>0.05
	AC vs HF	x	p>0.05	p>0.05	p>0.05	x	x	x
	AC vs DC	x	p>0.05	p>0.05	p>0.05	x	x	x
	HF vs DC	x	p>0.05	p>0.05	p>0.05	x	x	x
	CCD vs HF	x	p>0.05	p>0.05	p>0.05	p>0.05	p>0.05	p>0.05
	CCD vs DC	x	p>0.05	p>0.05	p>0.05	p>0.05	p>0.05	p>0.05
	CCD vs HF vs DC	x	p>0.05	p>0.05	p>0.05	p>0.05	p>0.05	p>0.05
T	Film vs PSP	x	p>0.05	p<0.0001	p<0.0001	p>0.05	p>0.05	p>0.05
	Film vs CCD	x	p<0.0001	p<0.0001	p<0.0001	p>0.05	p>0.05	x
	PSP vs CCD	x	p<0.0001	p<0.0001	p<0.0001	p>0.05	p<0.01*	x
	PSP vs HF	x	p<0.01	p>0.05	p>0.05	p>0.05	x	x
	PSP vs DC	x	p<0.001	p>0.05	p>0.05	p>0.05	x	x
	HF vs DC	x	p<0.001	p>0.05	p>0.05	p>0.05	x	x
	CCD vs HF vs DC	x	p<0.001	p>0.05	p>0.05	p>0.05	x	x

When considering the x-ray generator type as a first variable, a lower accuracy was found for AC compared to HF or DC units ($p<0.0001$) at low exposure times ($ms\leq 80ms$), although only for PSP sensors. For the HF versus DC unit, a significant difference was only found at very short exposure times ($20<ms\leq 40$) for PSP ($p<0.0001$) but again not for solid state sensors.

When considering the image receptor as a second variable, differences in accuracy between PSP and CCD are especially seen when using the AC tube type. At shorter exposure times ($ms\leq 80$), measurements using direct sensors were more accurate than PSP but this changed for higher exposure times ($ms>100$). On the other hand, for both HF and DC units, only at very small exposure times (respectively $ms\leq 40$ and $ms\leq 20$) significant differences were found (respectively $p<0.01$ and $p<0.001$). This indicated greater sensitivity of CCD receptors. In comparison to

conventional film (only considered using AC), digital sensors produce more accurate measurements at low exposure times, except for PSP at $ms \leq 40$.

Figure 2.5 is a graphic representation of the median accuracy as function of the mAs. Based on the distribution of the Spearman correlations, the quality (measurement accuracy) was significantly increasing as a function of exposure level for Film and PSP. For CCD, the quality decreased (significantly for CCD-AC) or remained constant. Both for PSP and CCD sensors measurement accuracy was higher when using a DC tube.

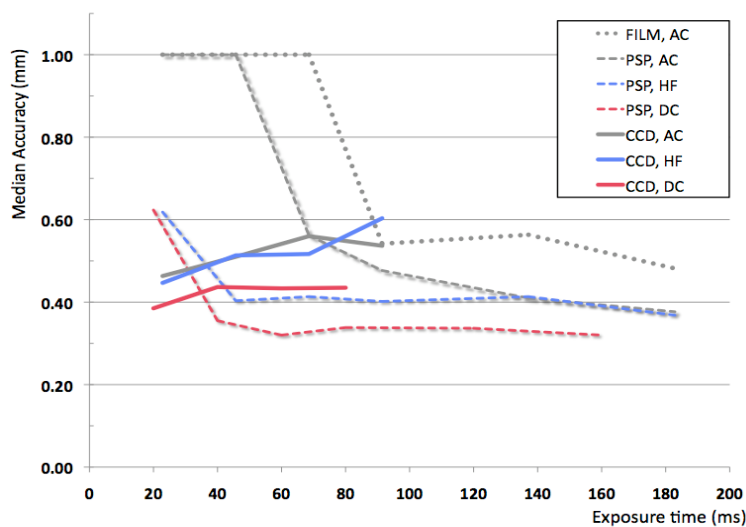


Figure 2.5: Median accuracy (absolute distance from gold standard) as a function of exposure time. The exposure time is recalculated from mAs, if mA were equal to 7. Outlying median accuracies (medians > 1) are depicted in the figure as value 1.

Skin doses (μGy) per x-ray unit and exposure time are presented in Figure 2.6. Furthermore, dose rates ($\mu\text{Gy/s}$) and kV generation are plotted by exposure time for each tube. While the AC tube only reached the desired kV levels at certain peaks, the HF unit gradually increased to reach the desired kV after approximately 20-30 ms and the DC tube almost instant after 4-5 ms. The measured exposure time deviated from the chosen setting by 30 to 75% for the AC unit, with increasing error at lower exposures. For the HF and DC unit, this error was <1%.

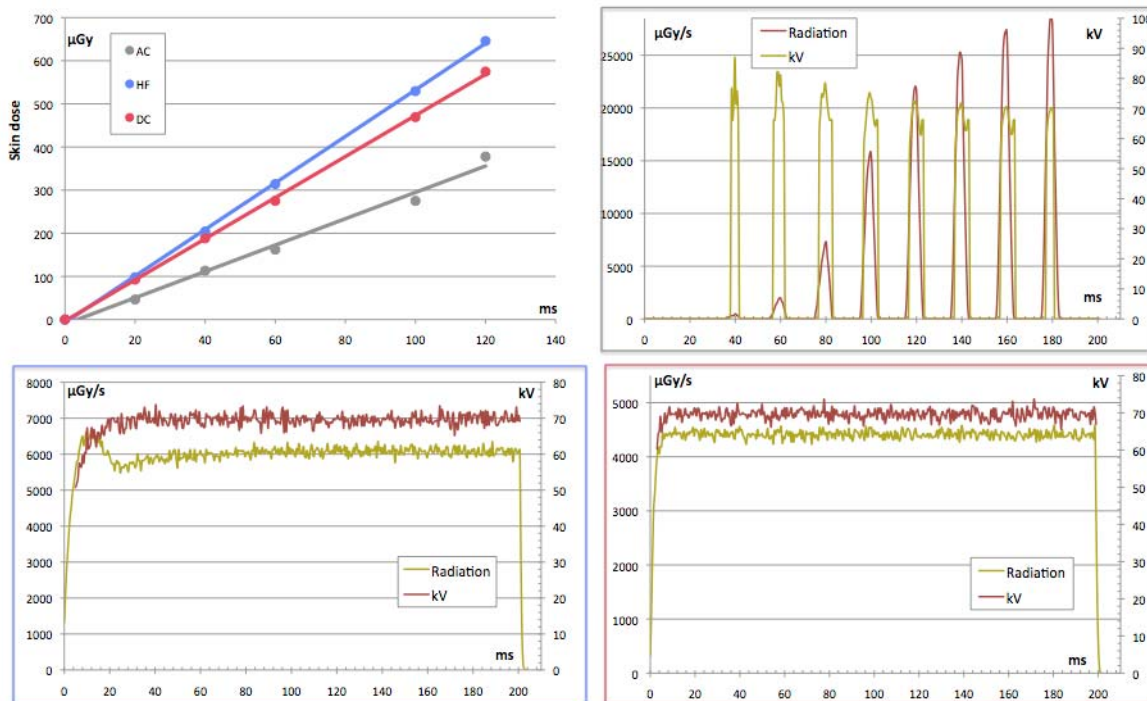


Figure 2.6: A) Skin dose measurements at rising exposure times for the three x-ray tubes: Trophy IRIX 70 AC, Planmeca Prostyle-Intra HF and Soredex Minray DC. The corresponding waveforms ($\mu\text{Gy/s}$) for the three tube types including kV generation are indicated by color-coded borders (upper right=AC, lower left=HF, lower right=DC).

Relative dose savings were calculated by linking these dosimetry results to the measurement accuracy obtained using the different tubes (see Table 2.3). Considering an accuracy level of respectively 0.5 mm and 1 mm, dose savings of 27 to 53% with HF and 32 to 55% with DC were found for PSP compared to AC. For CCD no dose savings were apparent, demonstrating their high sensitivity. For the AC tube (only unit combined with film, serving as a reference), digital PSP systems allowed 15-51% dose saving compared to film, depending on the accuracy level chosen. This is even higher when using CCD sensors (75-90%). The latter allowed 71-79% dose savings compared to PSP, but when using HF or DC these savings are decreased to approximately 50% for 0.5 mm accuracy and no dose savings at 1 mm accuracy.

Table 2.3: Skin dose comparisons for AC, HF and DC units in combination with Film, PSP and CCD at an accuracy of 0,5 and 1 mm. Relative dose savings for PSP were approximately 27-53% when using HF versus AC and 32-55% when using the DC tube. No apparent dose saving were seen for CCD sensors (lowest exposure times for the three tubes seemed to deliver adequate accuracy) showing their high sensitivity. The use of a digital system reduces the skin dose needed for accurate measurements (only AC combination with Film was present), but for all tube types at a 0.5 mm accuracy especially CCD sensors

allowed further dose savings (ca. 50%) compared to PSP. The [x] represents missing combinations.

Accuracy	Receptor	AC		HF		DC		Dose savings
		mAs	microGy	mAs	microGy	mAs	microGy	
0.5mm	Film	1.28	529.2	x	x	x	x	/
	PSP	0.64	257.4	0.32	187.7	0.28	176.3	27-32%
	CCD	0.16	54.5	0.16	90.2	0.14	86.7	none?
			51-90%		52%		51%	
1mm	Film	0.64	224.1	x	x	x	x	/
	PSP	0.48	190.9	0.16	90.2	0.14	86.7	53-55%
	CCD	0.16	54.5	0.16	90.2	0.14	86.7	none?
			15-76%		none		none	

Subjective quality evaluation

Figure 2.7 shows the mean scores for all groups plotted by exposure time for the lamina dura ratings. For the four other subjective ratings, the pattern of results was similar to these ratings. A significant positive relation was observed between exposure level and subjective rating.

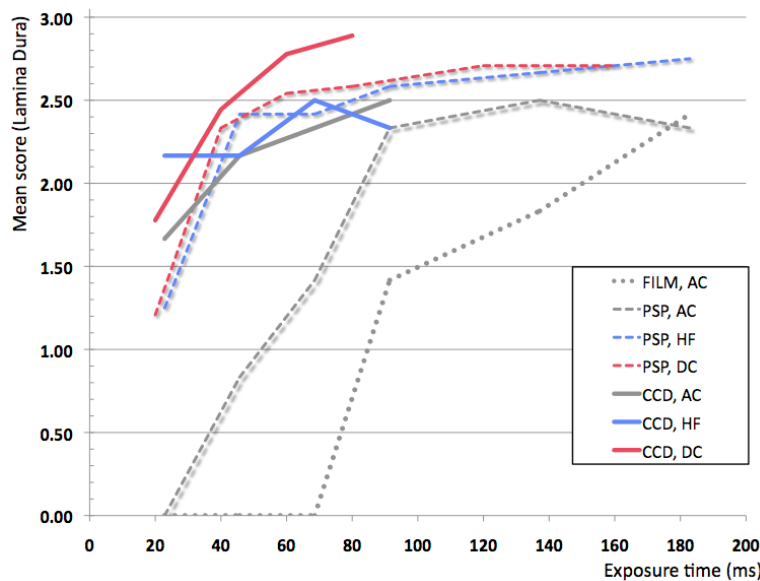


Figure 2.7: For the lamina dura, the means of the ordinal scores of each group are plotted by the exposure time, which is recalculated from mAs, if mAs were equal to 7. The remainder subjective criteria produced similar graphics.

Statistical comparisons between groups are summarized per observer in Table 2.4. Irrespective the type of rating and observer, the observed subjective rating was the highest for DC and the lowest for AC. For all variables, the observed subjective rating was significantly higher for DC compared to AC for all observers. DC was only scored significantly higher than the HF unit for lamina dura delineation and trabecular pattern depiction, and only by observer 1. HF was only scored significantly higher than AC for crater and furcation visibility by two observers.

Chapter 2: the influence of x-ray generator on periodontal measurements

Table 2.4: Comparisons of the subjective quality rating of lamina dura visibility (LD), trabecular depiction (BQ), contrast perception (C), crater (CR) and furcation (FU) visibility. The results are based on the proportional odds model. The significant differences in bold indicate a greater accuracy for the second group versus the first.

		LD	BQ	C	CR	FU
Obs1	AC vs HF	p>0.05	p>0.05	p>0.05	p>0.05	p>0.05
	AC vs DC	p<0.005	p<0.005	p<0.05	p<0.05	p<0.05
	HF vs DC	p<0.05	p<0.05	p>0.05	p>0.05	p>0.05
Obs2	AC vs HF	p>0.05	p<0.05	p>0.05	p<0.05	p<0.005
	AC vs DC	p<0.005	p<0.05	p<0.05	p<0.005	p<0.005
	HF vs DC	p>0.05	p>0.05	p>0.05	p>0.05	p>0.05
Obs3	AC vs HF	p>0.05	p>0.05	p<0.05	p<0.05	p<0.05
	AC vs DC	p<0.05	p<0.005	p<0.0005	p<0.005	p<0.0005
	HF vs DC	p>0.05	p>0.05	p>0.05	p>0.05	p>0.05

When considering a minimum ordinal score of 2 (=medium visibility) for all variables, dose reductions were comparable with those of the bone level measurements (Table 2.5). Lower exposure times were found when using the HF or DC unit compared to AC, but not for contrast perception using CCD sensors. Dose savings (approximately 50%) were demonstrated when using the latter compared to PSP for lamina dura and bone quality ratings but not for crater and furcation visibility, except using the AC tube. For contrast perception however, the opposite was found for HF and DC tubes.

Variable	Receptor	AC		HF		DC		Dose savings
		mAs	μGy	mAs	μGy	mAs	μGy	
LD	Film	1.28	529.2	x	x	x	x	
	PSP	0.64	257.4	0.32	187.7	0.28	176.3	27-32%
	CCD	0.32	133.3	0.16	90.2	0.14	86.7	32-35%
			48-75%		52%		51%	
BQ	Film	0.96	444.6	x	x	x	x	
	PSP	0.64	257.4	0.32	187.7	0.28	176.3	27-32%
	CCD	0.48	190.9	0.16	90.2	0.14	86.7	53-55%
			26-57%		52%		51%	
C	Film	1.28	529.2	x	x	x	x	
	PSP	1.28	529.2	0.32	187.7	0.28	176.3	65-67%
	CCD	0.64	257.4	0.48	288.9	0.42	257.8	none?
			0-51%		-35%*		-32%*	
CR	Film	0.96	444.6	x	x	x	x	
	PSP	0.96	444.6	0.32	187.7	0.28	176.3	58-60%
	CCD	0.64	257.4	0.32	187.7	0.28	176.3	27-32%
			0-42%		none		none	
FU	Film	1.28	529.2	x	x	x	x	
	PSP	0.96	444.6	0.32	187.7	0.28	176.3	58-60%
	CCD	0.64	257.4	0.32	187.7	0.28	176.3	27-32%
			16-51%		none		none	

Table 2.5: Skin dose comparisons for AC, HF and DC units in combination with Film, PSP and CCD at an ordinal score of minimum 2 (=medium visibility). The same trend is seen as with the bone level measurements for most variables. For contrast perception using HF or DC with CCD sensors*, care should be taken since PSP allows lower exposure times for similar radiographic contrast perception. Relative dose reductions are indicated in bold.

DISCUSSION

For the first variable, x-ray generator type, significant differences between measurement accuracy using the AC versus HF or DC tube were found at low exposure times (between 20 and 80 ms). The HF compared to DC tube was found to produce similar accuracy however with a significant difference at very low exposure times (between 20 and 40 ms). However, this is only true for PSP systems. Solid-state sensors allowed accurate measurements of periodontal bone levels using the lowest exposure times for all three tubes (see Table 2.3). This is mainly due to the high sensitivity of these sensors, but may also partially be explained by the inability to investigate lower tube settings. The AC tube namely revealed large deviations in measured exposure time at low settings (<100 ms) which resulted in the lowest measured dose between the tubes at 20ms. This still demonstrated adequate accuracy of periodontal measurements and may thus also be the case when lowering HF or DC tubes to this dose level. The differences between tubes for PSP sensors are directly reflecting the beam quality produced by the different tubes, where low exposure times produced fewer high energy photons for AC (see Figure 2.6). The HF unit only needed a small "heat up" time to obtain the desired potential (and further behave similar to a constant potential or DC unit with small ripple).

In current literature, no clinical research has been conducted to investigate the use of HF or DC tubes. McDavid et al (1982) and Helmrot et al (1994) described dose reductions of respectively 26% and 35-40% when using a DC unit in stead of a conventional AC one, without loss of radiographic contrast. These studies were physical performance tests using phantoms and do not take into account the receptor and its sensitivity profile. In our study, we could see that accuracy and associated dose savings increased from AC to HF and DC, but only for PSP. Accuracy was determined by bone level measurements deviating from a gold standard. The clinically acceptable deviation for bone loss measurements has been reported -when using a correct standardized radiographic set-up to be less than 1 mm or even up to 0.5mm (Mol 2004). Considering respectively 1 mm and 0.5 mm deviation, dose savings of 53-55% and 27-32% were found for PSP receptors when using HF or DC units in stead of AC. These percentages were in the same range or a bit higher than the mentioned laboratory studies, but also considered the effect of digital sensors (in

stead of conventional film). In this way, for solid-state sensors (CCD) no apparent dose savings were found, in contrary to PSP receptors.

This brings us to the second variable, the image receptor type, which by itself helps in further dose reductions. For this variable, some studies –however only one for periodontal diagnosis (Borg et al 1997)- have explored specific exposure ranges (Borg & Gröndahl 1996, Hayakawa et al 1996, Borg et al 2000, de Almeida et al 2003, Berkhout et al 2004, Bhaskaran et al 2005, Vandenberghe et al 2008). Borg & Gröndahl (1996) described the wide exposure latitude of PSP systems compared to solid-state sensors, although the latter demonstrated better resolution and require less radiation dose. Berkhout et al (2004) found 30-70% dose reduction with solid-state sensors and 50% with PSP systems when using an older multi-pulse x-ray generator type. In this report, we found 15-51% dose savings for PSP receptors and 76-90% for solid-state sensors when using the AC unit. Borg et al (2000) used a constant potential or DC unit, and found useful exposure ranges between 515-1800 μGy for solid-state sensors and 180-9110 μGy for PSP systems. These minimal threshold doses for PSP (180 μGy) are similar to the 176.3 μGy found in this study at 0.5 mm accuracy level (see Table 2.3). However, for CCD 515 μGy is considerably higher than our threshold doses with DC, being 86.7 μGy . This difference may be explained by the fast technological advancement over the last few years. The sensors used in Borg's study (2000) are older models (from 1995), while the solid-state sensors in this study were more recently introduced (having higher sensitivity and higher resolution, up to 20 lp/mm). Nevertheless, the difference between PSP and solid-state sensors was confirmed in this study with approximately 50% dose savings when using solid-state versus PSP receptors. At a threshold level of 1 mm, these savings were lost with modern tubes (HF or DC), but not with the conventional AC type. Furthermore, care should be given when using higher exposure times for solid-state sensors. Decreasing accuracy was found for CCD sensors (see Figure 2.4 and 2.5) with even a significant difference ($p < 0.01$) compared to PSP when using the AC tube (see Table 2.2). While PSP receptors showed increasing accuracy at rising exposure times, the contrary was found for solid-state sensors, confirming a more limited useful exposure range of the latter. The reason for this phenomenon may be found in the occurrence of blooming artefacts at high exposure times, which has also been reported in previous studies (Borg et al 2000, de Almeida et al 2003, Berkhout

et al 2004). These blooming artefacts are typically located at the alveolar crest and cause darkening of the bony crest, which may result in overestimation of periodontal bone loss (see Figure 2.3). This was also the reason why most exposure ranges, especially with the DC tube, were kept under 100 ms in this study for solid-state sensors.

For periodontal diagnosis, not only measurement accuracy but also subjective evaluations of periodontal landmarks are important diagnostic criteria (Tugnait et al 2000). For all evaluated subjective variables, the DC unit scored significantly better than AC. At a threshold rating of 2 (=medium visibility), dose savings were similar to the ones considering measurement accuracy when using HF or DC compared to AC, confirming the previous dose reductions. However, for CCD sensors, lower exposure times with HF or DC tubes did result in higher ratings. Although bone level measurements were possible at the previously discussed low settings, subjective ratings may thus prove to be insufficient. Higher settings were for instance required for adequate contrast perception. Nevertheless, image enhancement for contrast and brightness (window-levelling) was not explored in this study and may thus also alter the current findings (also for measurement accuracy) since small under- and overexposure errors might be corrected. The wide dynamic range of PSP receptors was also confirmed here for the contrast variable which scored better at lower exposure times compared to solid-state sensors (see Table 2.5).

It must be noted that no differentiation between the different Film, PSP and CCD image receptors have been made in this report. These might cause small deviations in dose savings for a specific image receptor, but should remain in the same range. This more individual analysis of the current research set-up is explored in the next chapter. However, for every new or particular detector, the semi clinical research should be repeated. Or alternatively, the detectors in the present study could be characterized in terms of fundamental physical parameters and if a new or particular detector is very similar to the types used in this study, their clinical performance will presumably be similar.

Lastly, since the introduction of new low dose imaging modalities in dentistry, like cone beam computed tomography (CBCT), optimization of current intraoral radiographic protocols with digital sensors becomes even more important for periodontal diagnosis. Modern CBCT units can nowadays image both jaws containing

the entire periodontal tissues at very low radiation doses. Vandenberghe et al (2008) found that periodontal bone level measurements were closer to the gold standard when using CBCT 0.4 mm slices compared to digital intraoral radiographic assessment and that crater and furcation depiction was more accurate using CBCT. A recent study from Roberts et al (2009) reported that a CBCT system only required 39.5 μSv for this, which is close to the radiation dose of a full mouth radiographic examination (FMX). Ludlow et al (2008) reported the latter to be around 37 μSv when using F-speed film or a PSP system and Gibbs (2000) described effective doses even around 13-100 μSv when using E-speed film. This comparison may somewhat be overrated given the many other CBCT variables, but it should reflect the importance of the required optimization of intraoral radiographic protocols which should consider the many variables in the radiographic chain, most of which were investigated and discussed in this study.

CONCLUSION

The present study described the influence of x-ray generator type on the specific exposure settings of digital PSP and CCD sensors (in comparison to film) for periodontal diagnosis. Measurement accuracy of periodontal bone levels was the highest for DC and HF compared to the AC unit. Accepting 0.5 to 1 mm deviation, 27-53% and 32-55% dose savings could be accomplished using respectively the HF and DC unit but only for PSP sensors. These results indicated the high sensitivity of solid-state sensors (compared to PSP). For these CCD sensors, care should be given when using higher exposure times, since blooming effects may deteriorate image quality.

The use of a specific image receptor by itself also influenced the dose required for periodontal diagnosis. For each x-ray tube tested, solid-state sensors allowed radiation dose reductions of approximately 50% compared to PSP, This depended not only on tube-type but also on the threshold level used for periodontal accuracy.

For subjective ratings of lamina dura, trabecular pattern, contrast, furcation and crater visibility, similar results were found but the small deviations should be investigated in future studies where image enhancement is allowed.

ACKNOWLEDGMENTS

I would like to thank the observers for the many measurements made, Joris Nens for his help with the dosimetry measurements and Steffen Fieuws for the statistical analyses.

Chapter 3:

The influence of image receptor on periodontal measurements

This chapter has been submitted as:

Vandenberghe B, Bosmans H, Yang J, Jacobs R. A comprehensive in-vitro study of image accuracy and quality for periodontal diagnosis. PART 2: The influence of intraoral image receptor on periodontal measurements. Clin Oral Invest 2010 (Submitted, 1st revision)

INTRODUCTION

Many laboratory studies have investigated the physical properties of digital sensors compared to film and described dose savings when using the digital ones (Brettel et al 1996, Scarfe et al 1997, Kaeppler et al 2007). Although these tests are very adequate for comparing inherent characteristics of a digital receptor (Araki et al 2000, Farman & Farman 2005, Heo et al 2009), they cannot simulate the clinical situation given the diversity in diagnostic tasks of oral diseases. For instance, the spatial resolution of an image receptor may be of importance for the detection of fine endodontic instruments (Vandenberghe et al 2009) while it may not influence the detection of small carious lesions (Wenzel et al 2007). It is therefore important to investigate the properties of digital sensors in a clinical simulation or environment for specific diagnostic tasks. In addition, the radiographic chain has many variables which should also be included in such investigations.

Two main variables in the chain are the x-ray generator and image receptor. In the previous chapter, the influence of x-ray generators (producing different waveforms) on periodontal measurement accuracy has been demonstrated using various receptors (Vandenberghe et al 2010). However, no distinction between the latter was made except for their main categorization: conventional film, photostimulable storage phosphor (PSP) plates and charged-coupled device (CCD) sensors. These three groups have different inherent properties like sensitivity and dynamic range which directly influence image quality and the associated required exposure time (Borg et al 2000, Berkhout et al 2004, Bhaskaran et al 2005, Vandenberghe et al 2010). Nevertheless, besides these major variables, other physical properties of digital receptors and not to forget the opportunity of image enhancement need also to be taken into account when establishing proper clinical protocols. While the receptor's spatial resolution -expressed in line pairs per millimetre (lp/mm)- reflects the ability to discern small details in a radiographic image, its contrast resolution -expressed in bit depth- reflects the amount of gray values that can be imaged (grayscale range), and both are important variables of the final image quality (Suetens 2002). Although most digital sensors have been found to perform well in terms of spatial and contrast resolution (Farman & Farman 2005), there is a discrepancy between older and newer technology where the latter now reach up to

20 lp/mm (pixel sizes as small as 25 μm) or 16 bit ($2^{16}=65.536$ shades of gray) contrast resolution. These differences may influence the diagnostic image quality of intraoral radiographs (Wenzel et al 2007, Heo et al 2008, Heo et al 2009, Vandenberghe et al 2009). For periodontal bone level measurements adequate contrast may thus be crucial for accurate visualization of the alveolar crest which can easily be deteriorated by blooming artefacts (Borg et al 2000, Berkhout et al 2004, Vandenberghe et al 2010). Furthermore, contrast resolution can often be limited by the resolution of the display screen and by ambient light (Hellén-Halme et al 2008) but also by the perception ability of the human eye (Künzel et al 2003).

In the previous chapter (Vandenberghe et al 2010), we demonstrated the differences in exposure time needed when using various receptor types, with up to 50% dose savings when using CCD sensors compared to PSP. Most studies on periodontal diagnosis unfortunately do not take into account the influence on exposure range (Eickholz et al 1999, Paurazas et al 2000, Kaeppler et al 2000, Wolf et al 2001, Gomes-Filho et al 2007, Jorgenson et al 2007, Li et al 2007) or make use of older generators (Pecoraro et al 2005, Jorgenson et al 2007). In addition, only few studies have described the clinical accuracy of different sensor resolutions and their individual influence on exposure time. One in-vitro study from Borg et al (1997) investigated marginal bone loss with a PSP and CCD sensor at a wide exposure range, but it did not describe different sensor resolutions and in addition, a high exposure range was used. Another study from Wenzel et al (2007) described the possible influence of contrast resolution on exposure time but for the detection of small carious lesions. Since for periodontal diagnosis no studies could be found researching this impact, the main aim of this report was to determine the influence of various image receptors on exposure parameters for the visualization of local bone height and for subjective rating of the image quality for periodontal evaluation.

MATERIALS AND METHODS

Periodontal analysis consisted of two main radiographic assessments. Measuring alveolar bone levels of an adult human dry skull and an upper and lower cadaver jaw was the first assessment, while the second one was the subjective evaluation of periodontal landmarks/symptoms including lamina dura delineation,

trabecular pattern depiction, crater and furcation involvement visibility and in addition the evaluation of radiographic contrast.

The maxillary and mandibular bony plates of the dry skull were covered with Mix D (White 1977), a solid synthetic material with similar attenuation and absorption properties as muscle and water, in order to simulate the soft tissues. Mix D, mostly containing paraffin wax and polyethylene, was heated at 180 degrees Celsius for plastic modeling over the jaw bones. Radiopaque gutta percha fragments were glued onto the buccal and oral crown surfaces in order to obtain standardized fiducials for alveolar bone level measurements since the cemento-enamel junctions (CEJs) were faded by dehydration. A central indentation in the fragment allowed not only mesial and distal bone level measurements but also central measurements on both buccal and oral sides. For the cadaver jaws, soft tissues and CEJs were preserved by fixing the specimens in a formalin solution. The cadavers were obtained with permission and ethical approval from the Department of Anatomy at the Catholic University of Leuven, Belgium. Upper and lower incisor, premolar and molar regions were imaged, giving a total of 12 regions. The gold standard (GS) of the measurements was obtained by physical measurements of two observers using a digital caliper (Mitutoyo, Andover, UK) with accuracy to the nearest 0.01 mm, prior to Mix D modeling for the dry skull and after radiographic exposures and flap surgery of the cadavers (a more detailed description can be found in our previous report) . Of the seventy-two gold standard measurements, thirty-one sites including linear bone loss and angular or infrabony defects were selected for the assessments, excluding most missing sites on radiographs.

For the intraoral radiographic protocol, standardized rigid occlusal keys were fabricated by melting green stent over bite-blocks of aiming devices (XCP, RINN Corporation, Elgin, IL, USA), thus obtaining individualized teeth imprints for correct repositioning of the x-ray tube. The paralleling technique was used for radiographic exposure of conventional films and digital image receptors. For this set-up, only two types of x-ray generators were further considered (of the three in our previous report) corresponding to low and high frequency x-ray generation, namely the alternating current (AC) IRIX 70 tube (Trophy Radiologie, Marne-La-Vallée, France) and the direct current (DC) Minray tube (Soredex, Tuusula, Finland), both with 30 cm focal-film distance and rectangular collimation. Exposure settings were 70 kVp, 7 or 8 mA

(DC and AC type respectively) and an exposure time range of 0.020, 0.040, 0.060, 0.080, 0.120, 0.160 seconds for Film or PSP and 0.020 or 0.040, 0.060 and 0.080 seconds for CCD. In addition to the radiographic assessments, the skin doses (in μGy) for all x-ray tubes were also measured using a Barracuda multimeter (RTI Electronics AB, Mölndal, Sweden) with a solid state dose detector (R100 dose probe) to evaluate the threshold levels where diagnostic accuracy might be insufficient (cfr previous report).

Image receptors: conventional film, PSP and CCD

To test the influence of image receptor and its specific properties (contrast resolution), periapical radiographs of the subjects (12) were taken at the various exposure times with 7 different image receptors using the standardized set-up (see Table 3.1). The conventional films used in this study were Agfa Dentus M2 Comfort E-speed film (Heraeus Kulzer GmbH, Dormagen, Germany) and Kodak Insight F/E-speed film (Carestream Health, Rochester, NY). The indirect digital PSP systems were Digora Optime (Soredex, Tuusula, Finland), Vistascan (12 bit) and Vistascan Perio (16 bit) (Dürr Dental GmbH, Bietigheim-Bissingen, Germany). For the Vistascan 12 bit, both original and images with a dedicated periodontal filter were included for analysis. The direct digital CCD sensors were Sigma (Instrumentarium Dental, Tuusula, Finland) and VistaRay (Dürr Dental GmbH, Bietigheim-Bissingen, Germany). Conventional films were processed using an automatic film processor (XR24 Nova, Dürr Dental, Bietigheim-Bissingen, Germany) with Dürr Chemistry (Röntgen Spezial-Set für Dürr Automat XR24).



Figure 3.1: Standardized PSP radiographs of the cadaver left lower molar region at various exposure times. Digora 8 bit, Vistascan 12 bit with and without a dedicated periodontal filter and the Vistascan 16 bit were the four PSP groups compared.

Two examples of the radiographic set-up are given in Figure 3.1 and 3.2: the four PSP configurations (Figure 3.1) and the two CCD (Figure 3.2) systems exposed at increasing exposure time using the DC unit.

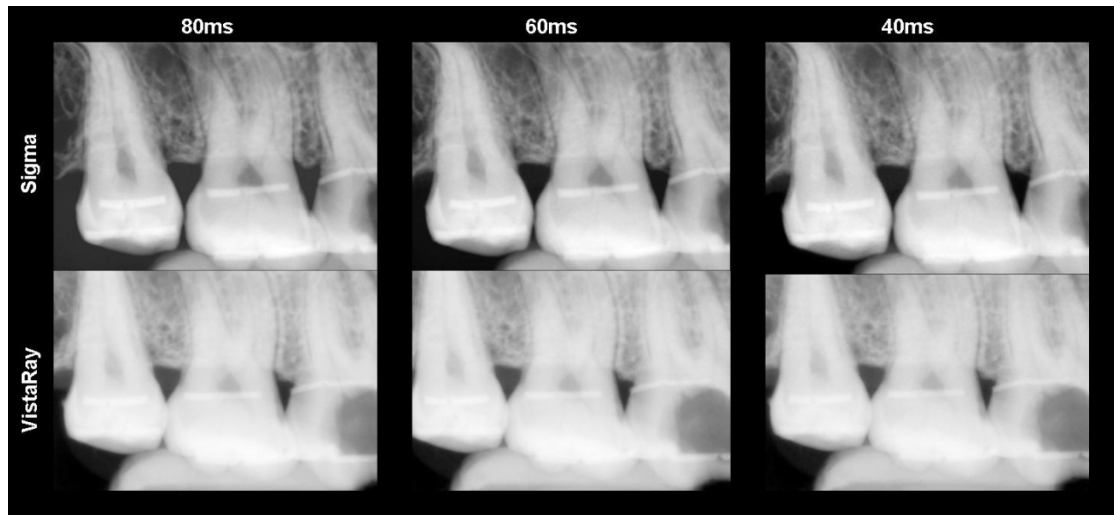


Figure 3.2: Standardized CCD radiographs of the right upper molar area from the dry skull (with gutta percha fragments as fiducials) at decreasing exposure times. The Sigma CCD 12 bit sensor and the VistaRay 14 bit CCD were the two groups included in the analysis.

Radiographic assessments: measurement accuracy and subjective evaluation

The intraoral radiographs from all possible x-ray tube, image receptor and exposure time combinations were evaluated by three observers specialized in oral imaging, during several sessions with two-day intervals in the darkened room of the previous chapter to prevent ambient light influence. Two training sessions were organized prior to the final observations for calibration of the observer measurement method. Conventional films were placed in film mounts (coded random order) to minimize surrounding light and were analyzed with countertop illuminators (Universal Viewer 6"x12" 240 V with magnifier, Dentsply International, York, PA, USA). The digital radiographs were all exported in Tagged Image File Format (TIFF) for observer assessment without loss of information. The blinded digital radiographs were imported into the Emago advanced, V.3.5.2. software (Oral Diagnostic Systems, Amsterdam, The Netherlands) and displayed in the darkened room of the previous chapter, in a random order on three standardized notebooks with 17 inch TFT based LCD monitors (contrast ratio 750:1) having anti-reflective layers, same screen resolution (1440 x 900 pixels) and contrast and brightness levels.

Chapter 3: The influence of image receptor on periodontal measurements

For the alveolar bone level measurements, thirty-one periodontal sites were measured per image receptor and x-ray tube combination at every single exposure time. The observers measured the CEJ to alveolar bone distance using the measurement tools of the Emago advanced software or for the conventional films, using a digital sliding caliper (Mitutoyo, Andover, UK), both at accuracy to the nearest 0.1 mm (which was the most precise setting for the digital measurements). These could then be compared to the gold standard.

For the subjective evaluations, delineation of lamina dura, crater visibility, furcation involvement visibility, depiction of trabecular bone and radiographic contrast were categorized with an ordinal scale, ranging from 0 to 3 (0=not possible to evaluate the criterion, 1=bad, 2=medium, 3=good).

Statistical methodology

Table 3.1 gives an overview of the number of measurements per combination of image receptor – x-ray tube and exposure time used in this report. For the conventional AC unit, 5 groups (two film types, two PSP types and one CCD sensor) were included in the analysis, For the more modern DC tube, 4 groups were distinguished for PSP and 2 for CCD. The subjective ratings consisted of only one measurement or rating per skull for each receptor-tube combination and exposure level.

Table 3.1: Overview of image receptors used in this study and the number of periodontal bone level measurements made by each observer for each combination with exposure level. Differences between combinations are due to missing landmarks on certain radiographs. A total of 1732 measurements were done by each observer.

Receptor	Type	X-ray Tube	20 ms	40 ms	60 ms	80 ms	120 ms	160 ms	Total
<i>Dentus M2</i>	<i>E-speed film</i>	AC 70kV	29	29	29	29	29	29	174
<i>Insight</i>	<i>FE-speed film</i>	AC 70kV	29	29	29	29	29	29	174
<i>Vistascan*</i>	<i>12bit PSP</i>	AC, DC 70kV	31+ 62	31+ 62	31+ 62	31+ 62	31+ 62	31+ 62	558
<i>Vistascan perio</i>	<i>16bit PSP</i>	DC 70kV	31	31	31	31	31	31	186
<i>Digora</i>		AC, DC 70kV	31+ 31	31+ 31	31+ 31	31+ 31	31+ 31	31+ 31	372
<i>Optime</i>	<i>8bit PSP</i>	DC 70kV	31+ 31	31+ 31	31+ 31	31+ 31	31+ 31	31+ 31	372
<i>Sigma</i>	<i>12bit CCD</i>	DC 70kV	27 + 27	27 + 27	27 + 27	27 + 27	0	0	216
<i>VistaRay</i>	<i>14bit CCD</i>	DC 70kV	13	13	13	13	0	0	52
Total			311	89	311	311	244	244	1732

* images were saved and assessed both in original format and after application of a dedicated periodontal filter (for DC only)

For accuracy (absolute distance from the GS), comparisons between groups were made at specific mAs levels separately in the main analysis (cfr previous report), cast into a survival analysis framework. In addition a Cox regression model was used when exposure levels were common to the compared groups. Interaction between both was verified to determine if the differences between groups depended on exposure level.

For the subjective measurements, non parametric tests were used given the lower number of measurements compared to the accuracy analysis. However, the Kruskal-Wallis test followed by the Mann-Whitney for pair-wise comparisons did not take into account the clustered structure of the data and p-values therefore should be interpreted carefully.

In all analyses p-values smaller than 0.05 for accuracy and 0.01 for subjective ratings are considered significant. All analyses have been performed using SAS software, version 9.2 of the SAS System for Windows (SAS Institute Inc 2008).

RESULTS

Measurement accuracy

Digital receptors

Comparison between the PSP receptors (Digora 8 bit, Vistascan 12 bit without and with periodontal filter, Vistascan 16 bit) and CCD sensors (Sigma 12 bit and VistaRay 14 bit) revealed differences in accuracy depending on the exposure level ($p=0.0003$). As such, statements about differences between groups should take into account the exposure level. Figure 3.3 represents the percentage accuracy (percentage of measurements, y-axis) for deviations from the GS (x-axis) for the six groups at various exposure levels.

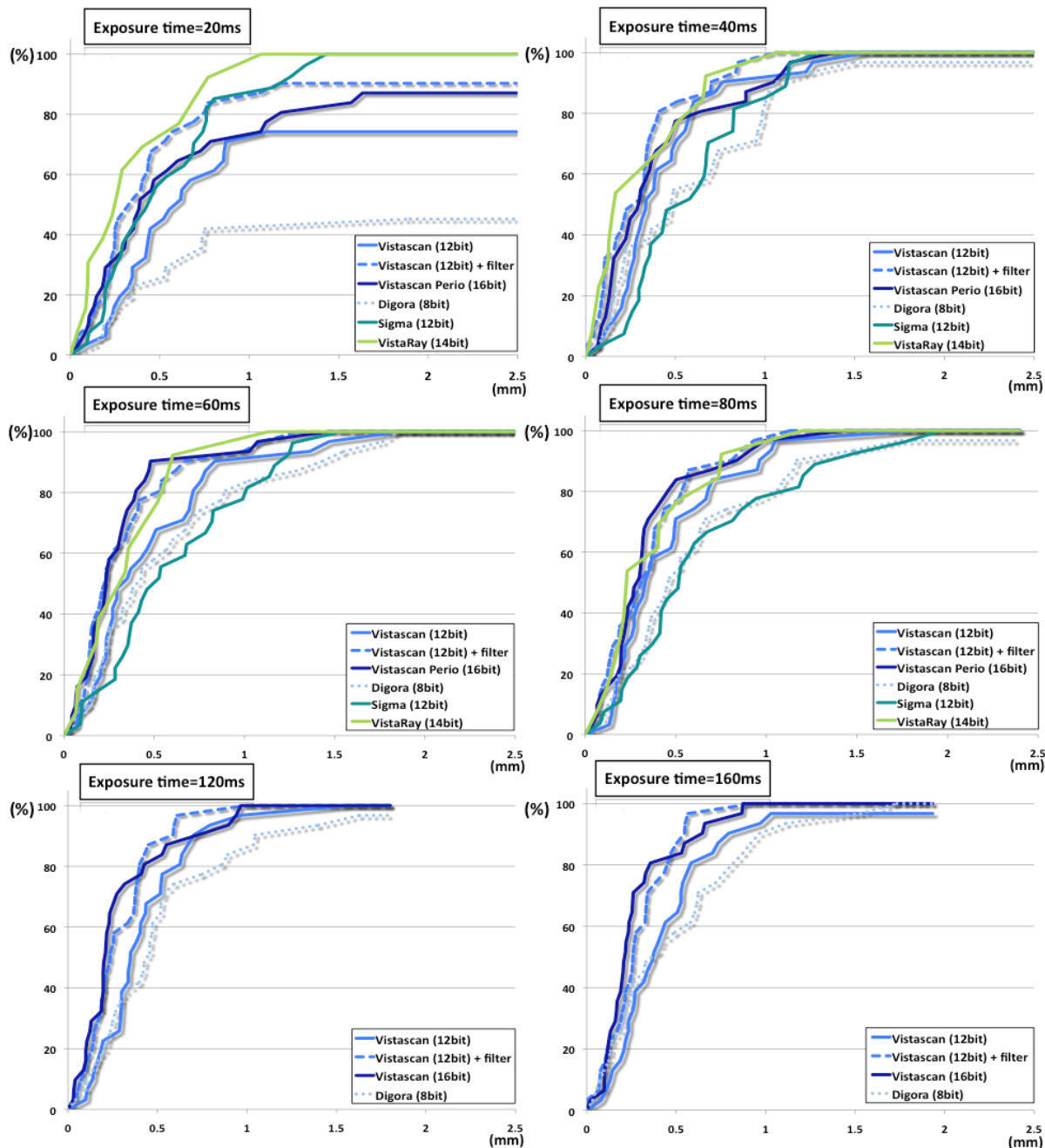


Figure 3.3: Graphic representation of the survival analysis framework: the four PSP groups and two CCD groups were plotted by the distance from the gold standard (x-axis) and the percentage of bone level measurements within these deviations (y-axis). The faster the curve increases for a certain group, the higher the accuracy.

The faster the curve increases, the higher the accuracy. Hence, the lowest accuracy was perceived for the Digora 8 bit, which was significant with almost every group at almost every exposure level, but the strength was more outspoken at lower exposure levels. Table 3.2 summarizes the significant differences at the different exposure levels.

Table 3.2: Results of the survival analysis framework with Cox regression. The model compares the accuracy between various groups within ranges of exposure level. The significant differences in bold indicate a greater accuracy for the first group versus the second one, except when indicated by [*] which demonstrates greater accuracy for the second group. The [x] represents missing combinations.

Receptor	Group	Exposure Time					
		20 ms	40 ms	60 ms	80 ms	120 ms	160 ms
PSP	Vistascan 12bit vs Digora 8bit	p<0.01	p>0.05	p>0.05	p<0.05	p<0.05	p>0.05
	Vistascan 16bit vs Digora 8bit	p<0.0001	p<0.01	p<0.01	p<0.001	p<0.0001	p<0.001
	Vistascan 16bit vs Vistascan 12bit	p>0.05	p>0.05	p<0.05	p>0.05	p<0.01	p<0.01
	Vistascan 12bit + filter vs Vistascan 12bit	p<0.001	p<0.05	p<0.001	p<0.05	p<0.01	p<0.0001
	Vistascan 12bit + filter vs Digora 8bit	p<0.0001	p<0.0001	p<0.001	p<0.0001	p<0.0001	p<0.001
	Vistascan 12bit + filter vs Vistascan 16bit	p>0.05	p>0.05	p>0.05	p>0.05	p>0.05	p>0.05
	VistaRay 14bit vs Sigma 12bit	p>0.05	p<0.05	p<0.05	p>0.05	x	x
	PSP vs CCD	Digora 8bit vs Sigma 12bit	p<0.0001*	p>0.05	p>0.05	p>0.05	x
	Digora 8bit vs VistaRay 14bit	p<0.0001*	p<0.05*	p<0.05*	p>0.05	x	x
	Vistascan 12bit vs Sigma 12bit	p<0.05*	p>0.05	p>0.05	p>0.05	x	x
	Vistascan 12bit vs VistaRay 14bit	p<0.01*	p>0.05	p>0.05	p>0.05	x	x
	Vistascan 12bit + filter vs Sigma 12bit	p>0.05	p<0.001	p<0.01	p<0.01	x	x
	Vistascan 12bit + filter vs VistaRay 14bit	p>0.05	p>0.05	p>0.05	p>0.05	x	x
	Vistascan 16bit vs Sigma 12bit	p>0.05	p>0.05	p<0.01	p<0.01	x	x
	Vistascan 16bit vs VistaRay 14bit	p>0.05	p>0.05	p>0.05	p>0.05	x	x

For the PSP receptors, when restricting attention to ms>20 and ignoring possible interaction between exposure and group, there was still a significant difference in accuracy between the groups:

- the accuracy of Digora 8 bit was significantly lower than for the three other groups (p<0.0001 compared to Vistascan 12 bit with filter and Vistascan 16 bit, p<0.05 compared to Vistascan 12 bit);
- the accuracy for Vistascan 12 bit was significantly lower than Vistascan 12 bit with filter (p<0.0001) and Vistascan 16 bit (p<0.01);
- there was no significant difference between Vistascan 12 bit with filter and Vistascan 16 bit (p>0.05).

For the CCD sensors, when ignoring the interaction between exposure time and receptor groups, there was a significant difference between both groups with the highest accuracy for VistaRay CCD 14 bit compared to Sigma 12 bit CCD ($p < 0.01$).

Dosimetric threshold values

The mAs levels of the 6 groups were associated to their respective skin doses and plotted against their median accuracy (Figure 3.4).

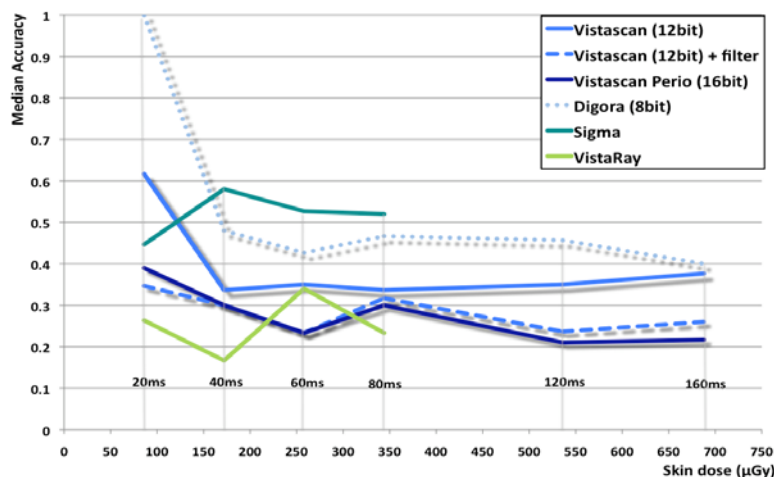


Figure 3.4: Median accuracy (absolute distance from gold standard) of the six digital groups plotted by entrance skin dose (exposure time). Outlying median accuracies (medians higher than 1) were given an arbitrary value of 1. The threshold skin dose levels are given in Table 4.3.

The results from our previous report were confirmed where accuracy increased for all PSP receptors at rising exposure times and remained constant for the CCD sensors. Table 3.3 shows the dosimetric threshold values at which measurement accuracy was within 0.5 and 1 mm deviation from the GS.

Table 3.3. Dosimetric threshold values for periodontal bone level measurement accuracy at 0.5 and 1 mm deviation from the gold standard. At 1 mm deviation accuracy, 50% lower skin doses were found when using systems with at least 12 bit grayscale. For 0.5 mm error margin, application of a dedicated filter on Vistascan 12 bit or using the Vistascan 16 bit seemed to allow reducing the required skin dose with approximately 50% for PSP systems, while the CCD sensors did not result in any apparent dose differences. This tendency was also seen when using the AC tube: 8 bit PSP required similar doses as the 2 film types.

Accuracy	Receptor	Sub-type	DC		AC	
			mAs	µGy	mAs	µGy
0,5 mm	Film	Agfa E-speed	x	x	0.96	444.6
		Kodak FE-speed	x	x	0.96	444.6
	PSP	Digora 8 bit	0.28	176.3	0.96	444.6
		Vistascan 12 bit	0.28	176.3	0.32	133.3
		Vistascan 12bit +filter	0.14	86.7	x	x
	CCD	Vistascan 16 bit	0.14	86.7	x	x
Sigma 12 bit		0.14	86.7	0.16	54.5	
		VistaRay 14 bit	0.14	86.7	x	x
			0-51%		70-88%	

1 mm	Film	Agfa E-speed	x	x	0.64	257.4
		Kodak FE-speed	x	x	0.64	257.4
	PSP	Digora 8 bit	0.28	176.3	0.64	257.4
		Vistascan 12 bit	0.14	86.7	0.32	133.3
		Vistascan 12 bit +filter	0.14	86.7	x	x
	CCD	Vistascan 16 bit	0.14	86.7	x	x
		Sigma 12 bit	0.14	86.7	0.16	54.5
	VistaRay 14 bit	0.14	86.7	x	x	
					0-51%	48-79%

For PSP, a 50% dose reduction could be estimated when using the PSPs with a dynamic range of 12 bit or higher for periodontal bone level measurements at maximum 1mm deviation. When considering 0.5 mm deviation as the maximal error margin, the same was true when using Vistascan 12 bit +filter or higher. For CCD, no immediate dose savings could be estimated given the high accuracy at very low exposure times.

Digital receptors versus film (AC tube)

Above results are confirmed when using an AC x-ray tube (see Figure 3.5) although the possible dose savings seemed slightly larger than with the DC tube.

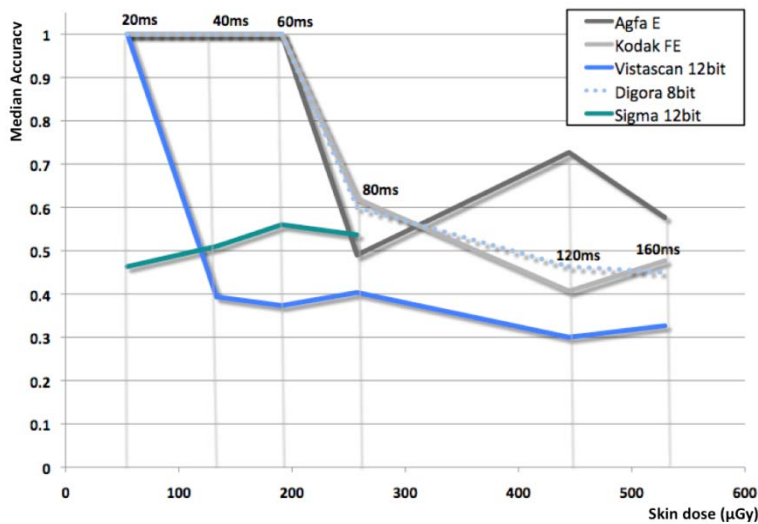


Figure 3.5: Median accuracy of Vistascan 12 bit PSP, Digora 8 bit PSP and Sigma 12 bit CCD in comparison with two film speed types using an AC x-ray generator. The Digora 8 bit PSP behaved similar to the two film types while the other two digital receptors were more accurate at low exposure times.

Table 3.3 shows between 48-78% dose reduction estimates when using Vistascan 12 bit compared to Digora 8 bit and 79-88% when using the 12 bit CCD sensor compared to film or PSP. The threshold skin doses for periodontal bone level measurements using the two films were equal to the ones of the 8bit PSP system. More detailed results on the effect of x-ray tube can be found in our previous report.

Subjective quality evaluation

The mean scores for the PSP and CCD groups are plotted by exposure time for each subjective criterion in Figure 3.6.

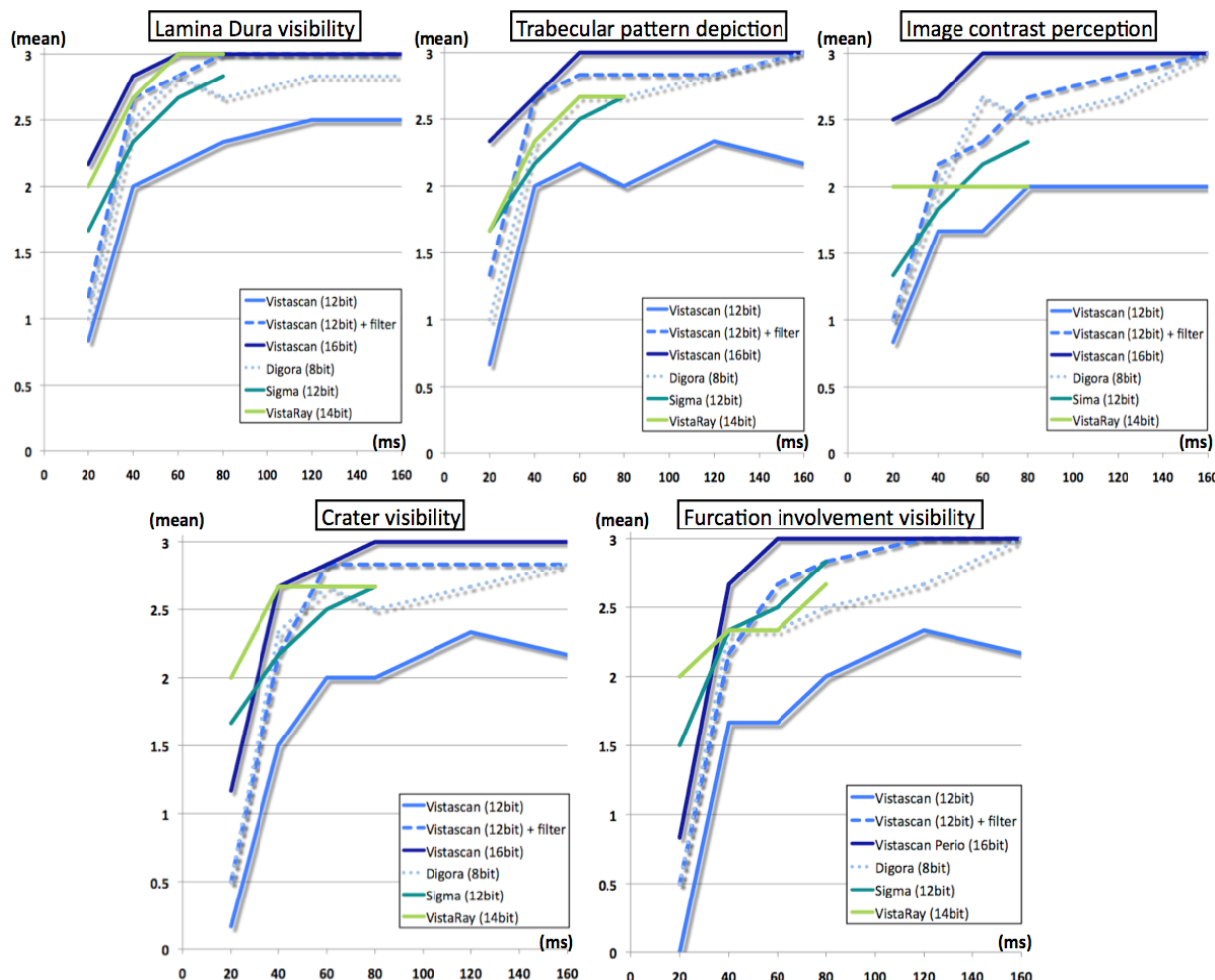


Figure 3.6: For each subjective criterion, the means of the ordinal scores of each group were plotted by exposure time. The scores for most subjective ratings are similar for all groups. Non parametric tests were used to determine any differences between the groups (see Table 3.4).

The p-values of the Kruskal-Wallis tests per observer for each rating are given in Table 3.4. For CCD no significant differences were observed for the different sensors. For PSP however, irrespective the type of rating and observer, the lowest score was systematically given to Vistascan 12 bit without filter (mostly significant with the other groups when using Mann-Whitney) and the highest to Vistascan 16 bit (mostly not significant).

Table 3.4: Kruskal-Wallis tests for subjective ratings of lamina dura (LD) and trabecular pattern (BQ) visibility, image contrast perception (C) and crater (CR) and furcation (FU) visibility for each observer. The p-values in bold indicate significant differences for PSP and further Mann-Whitney tests were used for pair-wise group comparison of the different PSP systems.

		LD	BQ	C	CR	FU
Obs1	PSP	p>0.01	p>0.01	p<0.01	p>0.01	p>0.01
Obs2		p<0.01	p<0.01	p<0.0001	p>0.01	p>0.01
Obs3		p>0.01	p>0.01	p<0.001	p>0.01	p>0.01
Obs1	CCD	p>0.01	p>0.01	p>0.01	p>0.01	p>0.01
Obs2		p>0.01	p>0.01	p>0.01	p>0.01	p>0.01
Obs3		p>0.01	p>0.01	p>0.01	p>0.01	p>0.01

Variable	Receptor	Sub-Type	DC-tube	
LD	PSP	Digora 8bit	0.28	176.3
		Vistascan 12bit	0.28	176.3
		Vistascan 12bit + filter	0.28	176.3
		Vistascan 16bit	0.14	86.7
	CCD	Sigma 12bit	0.28	176.3
		VistaRay 14bit	0.14	86.7
BQ	PSP	Digora 8bit	0.28	176.3
		Vistascan 12bit	0.28	176.3
		Vistascan 12bit + filter	0.28	176.3
		Vistascan 16bit	0.14	86.7
	CCD	Sigma 12bit	0.28	176.3
		VistaRay 14bit	0.28	176.3
C	PSP	Digora 8bit	0.28	176.3
		Vistascan 12bit	0.56	343.9
		Vistascan 12bit + filter	0.28	176.3
		Vistascan 16bit	0.14	86.7
	CCD	Sigma 12bit	0.42	257.8
		VistaRay 14bit	0.14	86.7
CR	PSP	Digora 8bit	0.28	176.3
		Vistascan 12bit	0.42	257.8
		Vistascan 12bit + filter	0.28	176.3
		Vistascan 16bit	0.28	176.3
	CCD	Sigma 12bit	0.28	176.3
		VistaRay 14bit	0.14	86.7
FU	PSP	Digora 8bit	0.28	176.3
		Vistascan 12bit	0.56	343.9
		Vistascan 12bit + filter	0.28	176.3
		Vistascan 16bit	0.28	176.3
	CCD	Sigma 12bit	0.28	176.3
		VistaRay 14bit	0.28	176.3

When considering a minimum ordinal score of 2 (=medium visibility) for all variables, estimated dose reductions were comparable to the ones with the bone level measurements (Table 3.5).

Table 3.5: Threshold skin doses with a minimal ordinal score of 2 for the subjective ratings lamina dura (LD) and trabecular pattern (BQ) visibility, image contrast (C) perception, crater (CR) and furcation (FU) involvement visibility. For most ratings of PSP radiographs, only Vistascan 16 bit scored well at lower skin doses (approximately 50% dose savings, in bold). Similarly for the CCD sensors, most criteria seemed to allow lower threshold doses when using the VistaRay 14 bit system. Note that contrast perception scored well at the lowest threshold skin doses for these two systems.

DISCUSSION

For the PSP systems, when ignoring the possible interaction of exposure time intervals and investigating all radiographic measurements (for 20 to 160 ms), significant differences were found between the four PSP types namely Digora 8 bit, Vistascan 12 bit, Vistascan 12 bit + filter, Vistascan 16 bit. When considering exposure time as a contributing factor, significant differences were still found (see Table 3.2) where the highest accuracy was perceived for Vistascan 12 bit + filter and Vistascan 16 bit. Therefore, when plotting the results by the actual skin dose (see Table 3.3 and Figure 3.5), a 50% lower dose could be estimated when using Vistascan 12 bit + filter or Vistascan 16 bit for a measurement error within 0.5 mm deviation. When setting the threshold value at 1 mm deviation, again 50% dose reduction was seen but this time already when using the 12 bit system or higher compared to 8 bit. This indicated that contrast resolution may play an important factor in the detection of periodontal bone height. Wenzel et al (2007) investigated the influence of bit depth of PSP systems on caries diagnosis and did not seem to find any significant differences when using higher bit depths. However, this study described classification of caries rather than bone level measurements and extracted teeth were used as simulation. No earlier studies could be found describing this for periodontal diagnosis.

For the CCD systems, significant differences were found between the two groups being Sigma CCD 12 bit and VistaRay CCD 14 bit, with highest accuracy for VistaRay CCD 14 bit, especially at higher exposure times. However, this did not translate in any form of dose savings given the already high accuracy of these solid-state sensors at very low exposure times. It did again indicate that contrast resolution may influence accuracy in the detection of local bone height. Heo et al (2008) examined the influence of CCD sensor bit depth in determination of endodontic file positioning and found that 12 bit images were preferred over 8 bit images. No other studies to our knowledge have investigated higher bit depths with solid-state sensors.

When comparing the use of PSP plates to CCD sensors for these specific periodontal diagnostic tasks, it was found that 50% lower doses were achievable when using the 12 or 14 bit CCD sensors compared to PSP 8 bit, (1 mm deviation error margin), but none when using higher PSP bit depths. In our previous report

(Vandenberghe et al 2010), no dose reduction was found when comparing PSP to CCD sensors using a DC tube, but no distinction between different contrast resolutions was made. Therefore, this higher contrast resolutions often attributed to newer technology should be considered for exposure guidelines of digital systems. These results were confirmed when comparing the PSP groups to conventional films using an AC tube (see Figure 3.5). Here, the Digora 8 bit PSP behaved like the two conventional film types (see Table 3.3) and thus no apparent dose savings could be seen when using this PSP system compared to conventional film. The 32-56% dose reduction of PSP compared to film in our previous report was therefore also dependent of the PSP resolution (Vandenberghe et al 2010). It must be noted that the median accuracy in Figure 3.4 and 3.5 was mostly higher for the PSP systems than the solid-state sensors.

Although contrast resolution may thus influence periodontal diagnosis, other important parameters in the intraoral radiographic chain are the imaging software, the display screen resolution, ambient light (Hellén-Halme et al 2008) and the resolving power of the human eye. While standard computer monitors can only image 256 gray shades, the human eye can also only discern approximately 10 lp/mm or 60 shades of gray at once without any aids (Künzel et al 2003). When using higher bit depths, the acquired information can still be imaged using image enhancement algorithms. In addition, medical displays or newer high resolution non-medical computer displays can also image more gray shades (Kimpe et al 2007). In this study, evaluation of digital images was standardized with same ambient light conditions, while images were exported at maximal bit depth in a standard software for radiographic assessments on LCD monitors with same screen resolution (1440 x 900 pixels) and brightness settings. Unfortunately, the screens in this study could only display 8 bit and window-level adjustments were not allowed (except the application of the dedicated periodontal filter for Vistascan 12bit). However, for most sensors, prior to display of the radiographic image and right after image acquisition, manufacturer defined pre-processing algorithms may already influence the actual display of the radiograph in the accompanying software. This can explain why higher accuracies were observed at higher bit depth in this study without the use of window-level functions. Also, when the Vistascan 12 bit images were processed with a dedicated periodontal filter, higher accuracy was perceived comparable to the one of Vistascan

16 bit PSP plates. Baksi (2008) found that enhanced PSP images provided better visibility of periodontal structures but resulted in comparable measurement accuracy. However, no details on filter or contrast resolution of the PSP system used were provided. It may well be that dedicated filtering thus only influences accuracy when using higher bit depths. Eickholz et al (1999) and Wolf et al (2001) also did not find any significant differences when using digital enhancement, although they used digitized conventional films with a 10 bit flatbed scanner. Li et al (2007) also did not find any differences for bone level measurements using enhanced images but exposure time was fixed and additional information is lacking. Further studies should therefore investigate the influence of image processing, especially when using smaller bit depths.

For the subjective ratings of the digital radiographs, the variables lamina dura visibility, trabecular pattern depiction, contrast perception and furcation and crater involvement visibility seemed to score alike and were comparable to the accuracy measurements. No significant differences were found for CCD but for PSP the lowest scores were given to the Vistascan 12 bit, which is different from the accuracy measurements where Digora 8 bit scored the least. However, non parametric tests do not take into account the clustered datasets used in this study and only careful assumptions could be made. In general, all receptors score well for the subjective criteria and a threshold level of 2 on a 3-point rating scale is too limited for accurate statements.

Lastly, it is crucial to respect the ALARA (as low as reasonably achievable) principle for periodontal diagnosis especially since it is a discipline where often radiographs or full mouth series (FMX) are required from the patient. The added value of two-dimensional intraoral radiographs for periodontal diagnosis is still often questions in literature (Müller & Eger 1999, Tugnait et al 2000, Mol 2004) and 3D modalities have proven to be of significant help when assessing crater and furcation involvements (Vandenberghe et al 2008, Walter et al 2009). The low dose of the latter (Roberts et al 2009) is often even lower than an FMX using E-speed film or when using incorrect radiographic techniques (Gibbs 2000, Ludlow et al 2008). Therefore, even though many different technologies are overwhelming the dental market, it is still outermost important to establish digital intraoral radiographic guidelines.

CONCLUSION

This study is the second part of a comprehensive in-vitro study assessing periodontal bone level measurement accuracy and subjective image quality using different x-ray generators and image receptors. In the first report, the influence of x-ray generator on specific exposure settings for conventional and digital sensors has been described. In this second study, the influence of the type of image receptor on exposure levels for periodontal diagnosis was described.

It can be concluded from these results that the type of PSP or solid-state sensor itself played an additional role in the radiographic diagnosis of bone loss. For PSP, 50% dose savings could be estimated when using high contrast resolution systems starting at 12 bit. The use of a dedicated periodontal filter did seem to deliver higher measurement accuracy. The highest accuracy was perceived for Vistascan 16bit where 100% of the measurements were within 0.5 mm deviation. For CCD, the highest accuracy was found for VistaRay 14 bit, where 100% of the measurements were within 0.5 mm deviation. No dose savings could be estimated between the two solid-state sensors given their high accuracy at low exposure times. The findings seemed to indicate that higher contrast resolution may play an important role in alveolar crest depiction and bone level measurements.

ACKNOWLEDGMENTS

I would like to thank the observers for the many observations made, Joris Nens for his help with the dosimetry measurements and Steffen Fieus for the statistical analysis.

Chapter 4:

The influence of tube potential on periodontal measurements

This chapter has been published as:

Vandenberghe B, Jacobs R. The influence of tube potential on periodontal bone level measurements and subjective image quality using a digital PSP sensor. J Oral Maxillofac Res 2010;1:e5

INTRODUCTION

Intraoral radiographs are often a necessary adjunct in the diagnosis of periodontal diseases regarding extent estimation of alveolar bone loss and visualization of important structures like periodontal ligament space, lamina dura or trabecular pattern (Tugnait et al 2000, Mol 2004, Bragger 2005). However, the outcome of this radiographic evaluation is not only depending on exposure parameters but also on image receptor type and viewing conditions (Borg et al 1996, Brettle et al 1996, Borg et al 2000, Pfeiffer et al 2000, Berkhout et al 2004, Bhaskaran et al 2005, Wenzel et al 2007, Hellén-Halme et al 2008, Heo et al 2008, Heo et al 2009, Vandenberghe et al 2009). Accuracy of alveolar bone level measurements on conventional or digital radiographs has been found to lie within 1 to 2 mm deviation (Pepelassi & Diamanti-Kipiotti 1997, Eickholz & Hausman 2000, Pecoraro et al 2005), the latter resulting in similar (Borg et al 1997, Pecoraro et al 2005, Hendriksson et al 2008) or greater accuracy (Kaepler et al 2000, Jorgenson et al 2007, Li et al 2007). This discrepancy in literature is most likely due to the many variables in the radiographic chain, the limited standardization of previous studies and the continuously improving technology. Only one of these studies actually investigated a range of exposure times for alveolar bone level measurements (Borg et al 1997). In addition, no studies could be found investigating beam energy on periodontal bone measurements. These factors are crucial though since they directly influence radiographic contrast (Curry et al 1990, Frederiksen 2004). For caries diagnosis, Svenson and Petersson (1991) have demonstrated no significant difference in diagnostic accuracy between premolars and molars using conventional films exposed at varying tube voltages, although accuracy increased for molars at higher kilovoltage (kV). Similarly, the alveolar crest and the associated accuracy of alveolar bone level measurements may be influenced by different tube voltages since the thickness of the alveolar crest is variable and often affected by small changes in mineral bone density. Furthermore, when considering possible dose savings especially when using digital sensors, laboratory studies have suggested acceptable image quality at a wide range of kV settings (Goshima et al 1996, Hayakawa et al 1996, Kitagawa & Farman 2004).

The purpose of the present study was to investigate the possible influence of two different tube voltages on the measurement accuracy of alveolar bone levels using a digital photostimulable storage phosphor (PSP) system (intraoral digital phosphor plates).

MATERIALS AND METHODS

Two human skulls containing multiple bone loss sites (including irregular crater patterns) were obtained with permission from the Department of Anatomy (Katholieke Universiteit Leuven, Leuven, Belgium) and selected for this study. The first skull was obtained from an adult cadaver head with soft tissues, both upper and lower cadaver jaw were fixed in a 10% formalin solution. The second subject used was a dry adult skull covered with custom-made soft tissue simulation. The latter consisted of melted paraffin wax, Mix D, having similar attenuation properties to human soft tissues (White 1977), and which was modelled over the maxilla and mandible (see Figure 4.1).

For alveolar bone level assessments, measurements from the cemento-enamel junction (CEJ) to the alveolar crest were chosen for the cadaver jaws, but gutta percha fiducials were glued onto the dry skull's teeth since dehydration of the CEJ could increase observer errors in identifying the measurement landmark. Small fragments with a central indentation were thus glued onto the labial and palatal/lingual surfaces of the teeth so their end- or midpoints could be used for mesial and distal or central bone level measurements. Physical measurements of the alveolar bone levels around each subject's teeth (mesial and distal, both oral and buccal) were obtained by two observers (department of oral imaging) using a digital sliding calliper (Mitutoyo, Hants, UK) at the nearest 0.01 mm accuracy. This was done prior to soft tissue simulation and

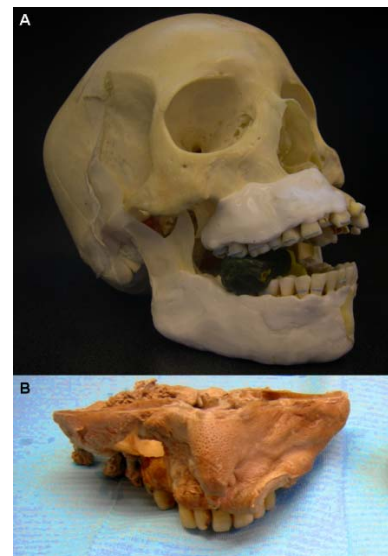


Figure 4.1: A) Radiographic protocol of the dry adult skull. The soft tissues were simulated with synthetic material (in white), bone loss fiducials were introduced made from gutta percha fragments and rigid occlusal imprints ensured reproducibility. B) Maxillary cadaver jaw with formalin fixed tissues.

radiographic exposure for the dry skull, but after radiographic exposure and flap surgery for the cadaver jaws. The observer's averaged measurements could then function as the gold standard (GS) for the radiographic evaluations.

Standardized periapical radiographs were made using a PSP receptor (Vistascan, Dürr Dental GmbH, Bietigheim-Bissingen, Germany) and a multipulse x-ray generator (Prostyle Intra, Planmeca Oy, Helsinki, Finland) at two different kV settings (63 and 70 kV), 8 mA, decreasing exposure times (160 ms, 120 ms and 80 ms) and 30 cm focal-film distance. Reproducible projection geometry was ensured by utilizing the paralleling technique with aiming devices and bite blocks (XCP, RINN Corporation, Elgin, IL, USA) individualized with waxed imprints of the teeth. For each jaw region (front-premolar-molar), the bite blocks were covered with heated green thermoplastic impression compound (Green Sticks, Kerr Corporation, Orange, CA, USA) for imprinting of the occlusal patterns. A mechanically interlocking rectangular (4 cm x 3 cm) collimator (Universal Collimator, RINN Corporation, Elgin, IL, USA)

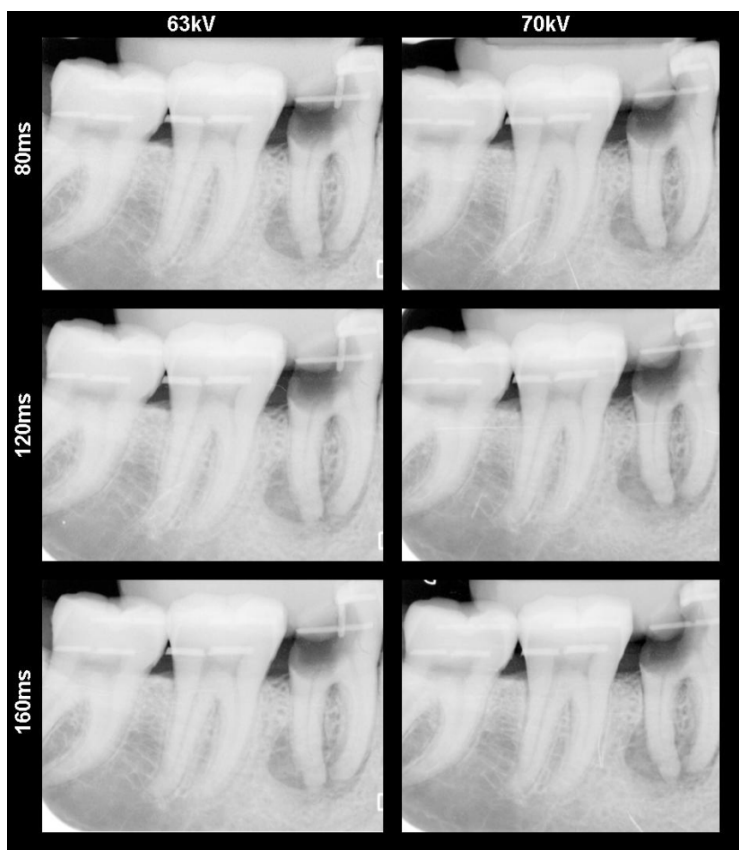


Figure 4.2: Standardized PSP radiographs of the dry skull's mandibular molar region. The images were obtained using two different tube voltages, 63 kV and 70 kV, at decreasing exposure times.

was mounted onto the tube end. A total of 72 radiographs (3 exposure times x 2 kV settings x 12 periapical skull regions) were thus obtained from the skull jaws for this study. Imaging plates were read out using the Vistascan laser scanner (Dürr Dental GmbH, Bietigheim-Bissingen, Germany) at high resolution (20 lp/mm), erased using the strong illumination unit, and exported in Tagged Image File Format (TIFF) for randomization and evaluation with Emago advanced, V.3.5.2. image analysis software (Oral Diagnostic

Systems, Amsterdam, Netherlands). An example of the radiographic set-up is given in Figure 4.2.

Thirty-two periodontal bone loss sites, including infrabony defects and furcation involvements, were chosen for the radiographic measurements and assessed by three observers specialized in oral imaging, after three calibration sessions. Alveolar levels were measured with the software tools to the nearest 0.1 mm, in a room with reduced ambient light, on three 17 inch LCD monitors having antireflective layers and same screen resolution (1440 x 900 pixels). Contrast and brightness settings were set to similar percentages. No image enhancement tools were allowed to adjust the images. Furthermore, the observers were asked to provide subjective ratings of lamina dura delineation, depiction of trabecularization, contrast perception and crater and furcation involvement visibility, using an ordinal scale from 0 to 3 (1 = bad, 2 = medium, 3 = good, 0 = not possible to properly evaluate the variable).

Statistical analysis

In total, 192 radiographic measurements per observer were compared to the gold standard. A 15% repeat of measurements (n=32) was done at a 1 week interval. Measurement consistency between and within observers was determined. The absolute differences (radiographic measures-physical measures (GS)) from the 3 observers were then averaged for further analysis. Multiple regression analysis of the dependent variable periodontal bone measurement and independent variables kV and exposure time was carried out at a significance level of 5%. For the subjective measurements, non parametric statistics were used given the ordinal nature of the data. The variables kV and exposure time were analyzed by a Friedman ANOVA test. All statistical analyses were carried out using SPSS V.13.0. statistical software (SPSS Inc., Chicago, IL, USA) and MedCalc v.9.3.2 (MedCalc Software bvba, Mariakerke, Belgium).

RESULTS

Measurement accuracy

Inter-observer consistency of the 192 periodontal bone measurements was determined and the reliability analysis demonstrated an intraclass correlation coefficient (ICC) of 0.959 (95% confidence interval (CI) with 0.948 and 0.968 as upper and lower bound respectively). Since high correlation was found, the measurements between observers could be averaged for further analysis. No intra-observer effect was found when comparing the 15% repeat of measurements (ICC=0.956, 0.912 – 0.979 at 95% CI).

Table 4.1 shows the descriptive statistics of the absolute differences from the GS for the different variables. Measurement deviations ranged from 0.00 to 2.00 mm from the gold standard. The standard deviation (SD) for all variables was found to be consistent. The bar chart of the absolute differences in Figure 4.3 revealed a similar pattern for both kVs and although mean deviations seemed to decrease at rising exposure time, this effect was only minimal since the mean's range was smaller than 0.1 mm.

Table 4.1: Descriptive statistics of the periodontal bone level measurements (in mm) for the variables kV (irrespective exposure time) and exposure time (irrespective kV).

Descriptives	kV		Exposure time		
	kV 63	kV 70	80 ms	120 ms	160 ms
Sample-size	96	96	64	64	64
Minimum	0.00	0.00	0.00	0.00	0.00
Maximum	1.97	2.00	1.80	2.00	1.97
Mean	0.44	0.44	0.47	0.45	0.41
95% CI	0.373 - 0.505	0.374 - 0.515	0.385 - 0.54	0.360 - 0.530	0.327 - 0.501
Standard Deviation	0.33	0.35	0.32	0.34	0.35

CI=confidence interval of the mean

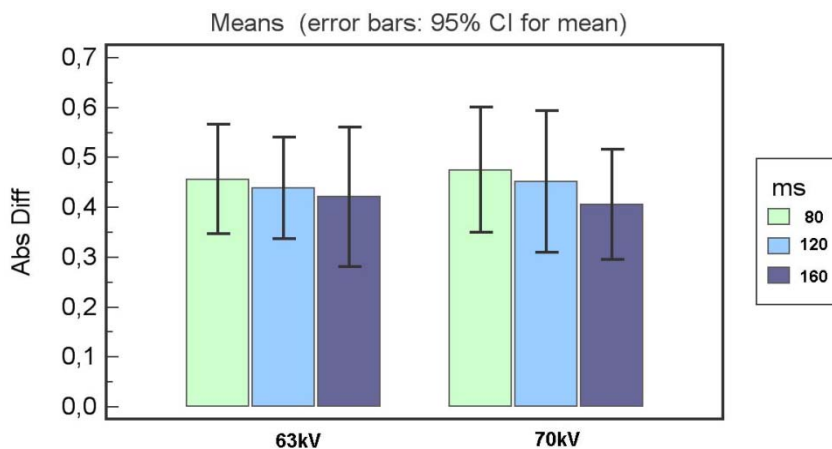


Figure 4.3: Bar chart for the absolute differences (abs diff in mm, y-axis) of the radiographic measurements from the gold standard. The means and error bars at a 95% confidence interval (CI) are shown for the different exposure times (ms), clustered by the two kV settings (x-axis).

The multiple regression equation revealed no significant influence of the independent variables kV (63 and 70) ($P = 0.915$) and exposure time (80 ms, 120 ms, 160 ms) ($P = 0.382$) on the periodontal bone measurements at a significance level of 5%. When ignoring exposure time, 90.3% of the 70kV measurements and 96.8% of the 63 kV ones were within a clinically acceptable threshold level of 1 mm deviation (see Figure 4.4). When reducing the clinical threshold to 0.5 mm, 66.1% for 70 kV and 66.7% for 63 kV were found to be within this limit. Although no significant difference was found between the two kV settings, the curve in Figure 4.4 increases slightly faster for 63 kV, indicating higher but insignificant accuracy.

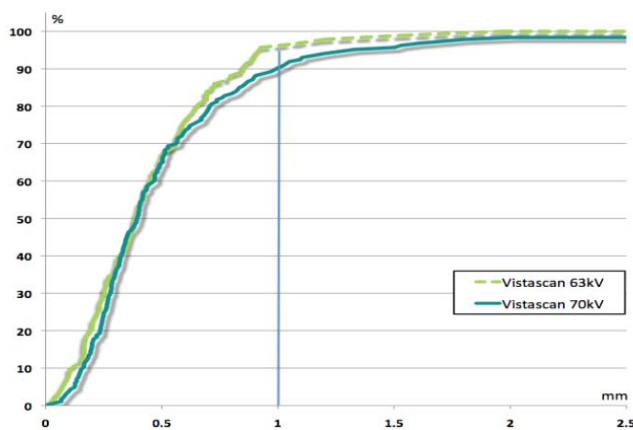


Figure 4.4: Percentage of measurements (y-axis) falling within a specific distance from the gold standard (X-axis), ignoring exposure time. At least 90% of measurements were 1mm deviation. A kV of 63 resulted in a slightly higher accuracy at this threshold level.

Subjective quality evaluation

The results of the Friedman ANOVA test are presented in Table 4.2. The 6 groups compared were the combinations of the two kV settings (63 and 70 kV) with the three exposure times (80, 120 and 160 ms). No significant differences were found for the subjective ratings lamina dura ($P = 0.416$) or trabecular pattern visibility ($P = 0.125$), contrast perception ($P = 0.186$), crater ($P = 0.953$) and furcation ($P = 0.156$) involvement visibility using the different kV or exposure time settings.

Table 4.2: Results of the Friedman ANOVA test for the ordinal ratings. The subjective ratings for lamina dura (LD), trabecular depiction (BQ), contrast perception (CO), crater (CR) and furcation (FU) involvement visibility did not differ significantly for the 6 different groups (the two kV settings and three exposure times)

Subj. Ratings	Mean Rank (1-6)						N	Chi-Square	Df	Asymp Sig
LD	3.08	3.58	3.58	3.58	3.58	3.58	6	5.000	5	0.416
BQ	2.33	3.25	3.25	3.75	3.75	4.67	6	8.629	5	0.125
CO	3.00	3.00	3.00	3.50	4.50	4.00	6	7.500	5	0.186
CR	3.33	3.33	3.33	3.33	3.83	3.83	6	1.111	5	0.953
FU	2.83	2.33	3.83	3.33	4.33	4.33	6	8.000	5	0.156

1=70kV 80 ms, 2=63kV 80 ms, 3=70kV 120 ms, 4=63kV 120 ms, 5=70kV 160 ms, 6=63kV 160 ms

The bar chart from the ordinal scores of the trabecular pattern depiction variable (see Figure 4.5) did reveal higher scores at rising exposure times, although this was found to be insignificant. The same applies for the kV setting of 63 compared to 70 kV. All other variables had similar bar charts.

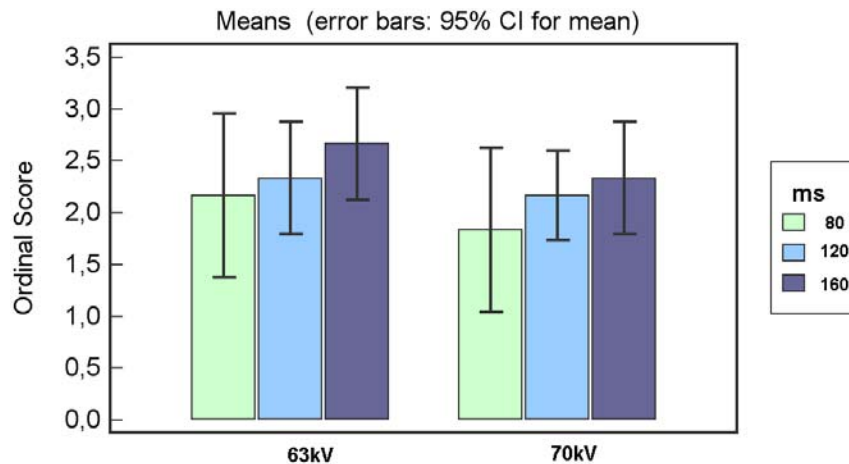


Figure 4.5: Bar chart for the subjective quality ratings of trabecular pattern depiction. Ordinal scores of the observers (y-axis) are plotted by exposure times (ms) and clustered by kV (x-axis).

DISCUSSION

The main objective in this study was to determine the influence of two kV settings (63 kV and 70 kV) on periodontal bone level measurement accuracy using a digital PSP receptor. Furthermore, since exposure time directly affects radiographic contrast, a small range of exposure times was used to investigate this influence.

The results of the present study revealed that no significant difference was found for the two kV settings, and neither for the different exposure times. Although no other studies have compared kV settings for alveolar bone measurement accuracy, our findings confirm certain laboratory studies on different tube voltages (Goshima et al 1996, Hayakawa et al 1996, Kitagawa & Farman 2004). These studies however investigated wide kV ranges for direct digital receptors rather than for PSP sensors, but all conclude that the sensors operate well at various kV settings with highest contrast at low kV settings, just like conventional film. But also some in vitro studies have demonstrated similar findings. De Almeida et al (2003) –using dry skulls and an aluminium step-wedge- studied the effect of various exposure times and kV settings on subjectively rated image quality of four different digital sensors and demonstrated no significant difference between 60 and 70 kV for the PSP system at a wide range of exposure times. Kaeppler et al (2007) also concluded the same for two tube voltages on the visibility of simulated decayed and peri-implant

lesions on dry human skulls using a PSP receptor. Both mentioned studies were based on subjective ratings though, but this is similar to our secondary findings, the subjective ratings for lamina dura, trabecular pattern, contrast, crater and furcation involvement visibility, which scored alike for both tube voltages. Our results do suggest a small preference for the 63 kV setting, for both measurement accuracy (defined as bone level measurement from the gold standard) and subjective ratings, although this was not significant. Helmrot et al (1994) found that when using multipulse x-ray generators or faster films, degradation of radiographic contrast is seen and may need a 5 to 8 kV decrease for counteracting this phenomenon. Since digital receptors are often more sensitive than conventional films, this may play a role, especially at very low exposure times. Further research is thus needed since the minimal exposure time used in this study was 80 ms.

Although there may be some confusion on what the clinically acceptable deviation for bone loss measurements may be, it has been reported that 0.5-1 mm deviation should be accomplished when using a correct standardized radiographic set-up (Tugnait et al 2000, Mol 2004, Bragger 2005). When considering a 1 mm deviation, 90.3% and 96.8% of the measurements in this study for respectively 70 and 63 kV fell within this range, which is similar to other studies (Pepelassi & Diamanti-Kipiotti 1997, Eickholz & Haussman 2000, Pecoraro et al 2005). Also the excellent intra- and inter-observer consistency found were indicative of an adequate measurement method. However, the limitations in this study were the use of a single digital receptor and a limited exposure range. Further studies thus need to be conducted investigating tube voltage influence on measurement accuracy at lower exposure times and using PSP as well as direct digital receptors. Finally, also newer detector technology having higher bit depths -which theoretically would allow higher contrast levels- and/or higher screen resolutions may further improve the accurate depiction of the alveolar crest or other important dental tissues.

CONCLUSION

This study demonstrated no significant difference between radiographic measurements of periodontal bone levels on digital PSP radiographs made with two different tube voltages, 63 or 70 kV. When decreasing exposure time from 160 ms to

120 ms or 80 ms, no significant difference between these voltages was either found. For subjective ratings of lamina dura, trabecular pattern, crater and furcation involvement visibility or contrast perception, similar findings were found.

3D Imaging Modalities for Periodontal Diagnosis

PART II



Chapter 5:

Bone loss measurements on 2D and 3D panoramic reconstructions

This chapter has been published as:

Vandenberghe B, Jacobs R, Yang J. Diagnostic validity (or acuity) of 2D CCD versus 3D CBCT-images for assessing periodontal breakdown. Oral Surg Oral Med Oral Pathol Oral Radiol Endod 2007;104:395-401

INTRODUCTION

Intraoral radiography is the most common imaging modality used for diagnosing periodontal bone defects. However, intraoral radiography is 2-dimensional (2D) and the amount of bone loss can be underestimated due to projection errors (Zulqarnain & Almas 1998, Eickholz & Hausmann 2000, Schliephake et al 2003, Mol 2004, Brägger 2005) or observer errors in identifying reliable anatomical reference points (Benn 1990, Mol 2004, Brägger 2005). Assessing pre-surgical bone levels and changes in post-periodontal treatment often requires three-dimensional (3D) information. A previous study showed that combination of 2D with 3D imaging provides a better pre-operative assessment of implant-site (Jacobs et al 1999). The introduction of digital intraoral imaging and cone beam computed tomography (CBCT) may bring new potentials for periodontal diagnosis and treatment planning (Jeffcoat & Reddy 2000).

Intraoral digital imaging not only reduces radiation exposure compared to conventional film, but also optimizes assessment of oral structures, improving the accuracy of periodontal diagnosis (Sanderink 1993, Vandre & Webber 1995, Brettle et al 1996, Lim et al 1996, Jacobs & Gijbels 2000, Kaeppler et al 2000, Mol 2000, van der Stelt 2000). Conventional computed tomography (CT) provides 3D information, but the dose remains quite high. The recent development of CBCT reduces this radiation exposure significantly (Tsiklakis et al 2005, Ludlow et al 2006, Scarfe et al 2006).

Over the past 15 years there have been many publications concerning the applications of digital intraoral radiography, but few of these have dealt with its validity to monitor periodontal bone lesions (Young et al 1996, Eickholz et al 1999, Paurazas et al 2000, Kitagawa et al 2003, Cury et al 2004, Pecoraro et al 2005). The same scenario applies to the use of CBCT for periodontal indications (Kobayashi et al 2004, Almog et al 2006, Guerrero et al 2006, Misch et al 2006). Many questions regarding both digital intraoral imaging and CBCT need to be addressed: Are periodontal bone levels, lamina dura and bone craters well visualised on both imaging modalities? How accurate are these imaging techniques in assessment of the bone levels and defects? Can the availability of 3D images assist the diagnosis of the bone loss and defects? Therefore, the overall aim of this study was to validate

applications of digital intraoral imaging and CBCT in determination of the periodontal bone loss and defects. We hypothesized that both digital intraoral radiography and CBCT would allow accurate assessment of periodontal bone levels.

MATERIALS AND METHODS

Thirty periodontal bone levels or defects of 2 adult human skulls, a cadaver head and a dry skull, were evaluated by using intraoral digital radiography (CCD, Schick Technologies, New York, USA) and CBCT (i-Cat, 12 bit, Imaging Sciences International, Pennsylvania, USA). The upper and lower jaws of the cadaver head were fixed with 10% formalin and functioned as a clinical subject. The adult human dry skull was covered with a soft tissue substitute, Mix D (White 1977) and used as a simulation.

For the intraoral protocol, the paralleling technique was applied in a standardized exposure set-up. A film holding system (XCP, RINN Corporation, IL, USA) was used. To obtain identical images, bite blocks were covered with waxed imprints of the anterior, premolar and molar regions (see Figure 5.1). Images were obtained with a size #2 charged coupled device (CCD) intraoral digital sensor and a direct current (DC) x-ray unit (Heliodent DS, Sirona Dental Systems LLC, Charlotte, NC). Exposure settings were 60 kVp with 0.28, 0.42 and 0.56 mAs respectively (40, 60 and 80 ms x 7 mA). A rectangular (4 cm x 3 cm) collimator (Universal Collimator, RINN Corporation, Elgin, IL, USA) was used. The focus-receptor distance was 30 cm.

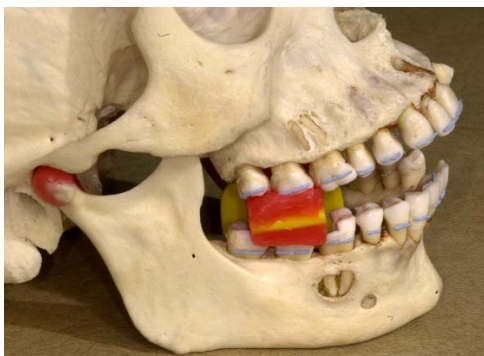


Figure 5.1: Standardized exposure set-up: dry skull with gutta-percha markers and waxed imprints before covering the jaws with soft tissue substitute.

For CBCT, the occlusal plane of the jaw bones was positioned horizontally to the scan plane and the midsagittal plane was centered. The field-of-view (FOV) or the beam diameter at the surface of the image receptor (beam height) was

adjustable. The protocols were set to visualize the entire jaws, giving between 54 and 159 slices of 0.4 mm thickness (approximately between 20 and 60 mm beam height). Images were obtained at 120 kVp and 23.87 mAs with a typical voxel size of 0.4 mm (see Figure 5.2).

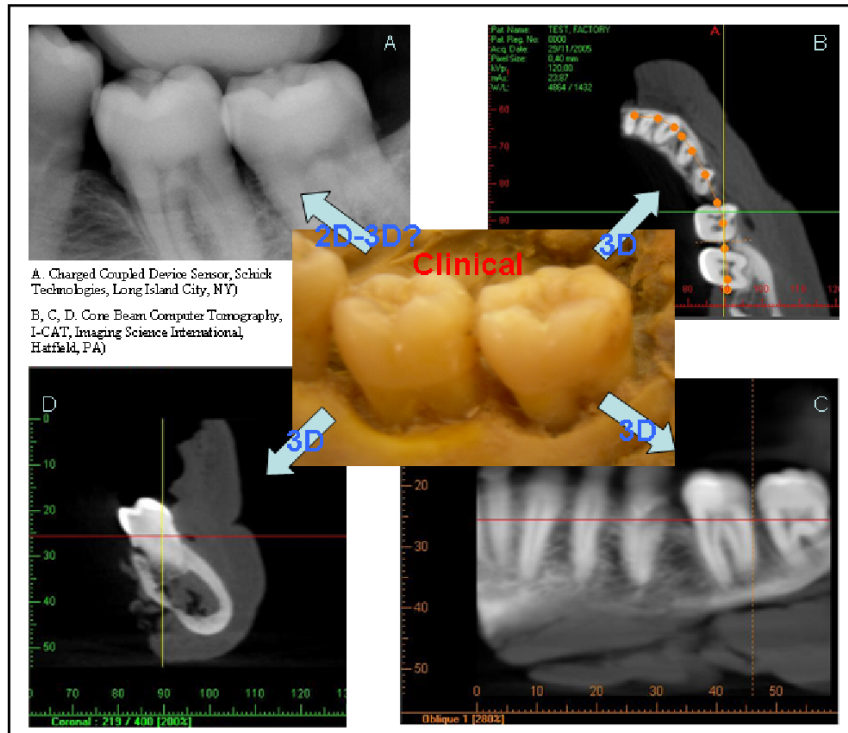


Figure 5.2: Digital x-ray images of molar region from the lower cadaver jaw. 1) Two-dimensional CCD image 2) CBCT axial slice 3) CBCT coronal slice 4) CBCT panoramic view (oblique). Observers described the defects using both imaging modalities (CCD and CBCT) and comparison was done to the gold standard, which was obtained after removing the soft tissues (center).

Periodontal bone levels and defects visualised with both imaging modalities were assessed by three observers (post graduate students at the Oral Imaging Centre). Images were viewed in a darkened room on three notebooks (Sony Vaio VGN A417m, Sony Belgium, Zaventem) with 17-inch LCD monitors and the same screen resolution (1440 x 900 pixels). Intraoral 2D images were displayed in a random order with the Emago advanced, V.3.5.2. software in Tagged Image File Format (TIFF). CBCT images were viewed with the I-CAT software (Xoran CAT V.2.0.21, Xoran Technologies Inc, Ann Arbor, MI, USA). Linear bone level measurements were carried out on a panoramic view obtained from an oblique line on the axial plane with a standard slice thickness of 5.2 mm. Measurement tools on both programs were used to obtain the data. Delineation of lamina dura, defect description, contrasts and bone quality were also analysed by the three observers, using an ordinal scale.

Physical measurements of the skulls were considered as the gold standards for further accuracy assessment of both imaging modalities. For the cadaver jaws,

the gold standard was obtained after image acquisition, by flap surgery to allow physical measurements using a digital sliding caliper (Mitutoyo, Andover, UK). For the dry skull however, gold standards were obtained, before adding soft tissue substitute and image acquisition. Mesial, central and distal bone levels and bone crater depths on the oral and vestibular sides of each selected tooth were measured. Because of dehydration of the dry skull, the faded cemento-enamel junction (CEJ) could not be used as a reference point as in the formalin-fixed cadaver jaws. Therefore, radiopaque gutta-percha fragments with a small central indentation were glued onto the respective teeth to serve as standardized fiducials. A group of nineteen teeth and thirty sites, including linear defects, three-dimensional craters and furcation involvements, was selected for comparison and statistical analysis.

Statistical analysis

Bone levels of the selected sites, measured on the digital intraoral images, were compared with the directly measured gold standards. Exposure settings, imaging methods, and observers were used as independent variables and bone levels and defects as the dependent ones. The gold standard was obtained by averaging the scores of two observers. Intraclass correlation showed no observer effect for these scores.

The acquired data were first scanned for outliers and tested for normality. As normality could not be found even after transformation, non parametric statistics were utilized for the analyses (Siegel 1956, Afifi & Clark 1984). The observer effect was tested with the Kruskal Wallis test and showed no significant difference among the three observers ($p > 0.05$). A 15% repeat of measurements was done at an interval of two weeks and a high reliability was found amongst every observer (interval of 0.986 to 0.997 with 95% confidence and a single measure intraclass correlation coefficient of 0.987). Those measurements were then averaged for further calculations (see Table 5.1). All statistical analyses were carried out using the absolute values of these measurements. For comparison between 2D CCD technique and CBCT, it was justified to use the Wilcoxon Signed Rank test since the measurements were done on different imaging modalities. To test the optimal intraoral exposure settings for comparison, the Friedman ANOVA test was applied (Siegel 1956).

Table 5.1: Absolute differences between averaged observer measurements and direct measurements of ten selected sites for each exposure setting and both imaging modalities. When looking at the exact un-averaged values of these scores, underestimations slightly predominated (53%) compared to overestimations (46%).

Measurement on tooth (in mm)	Heliodent	Heliodent DS	Heliodent DS	I-CAT
	DS 0.56 mAs	0.42 mAs	0.28 mAs	
Mandibular right first molar distal	0.70	0.40	0.20	0.20
Maxillary left central incisor distal	1.03	0.76	0.99	0.13
Maxillary left lateral incisor mesial	1.20	1.33	1.23	0.42
Maxillary left canine mesial	0.23	0.49	0.19	0.18
Maxillary left canine distal	0.37	0.04	0.31	0.18
Maxillary left first molar mesial	0.77	1.17	0.67	0.26
Maxillary left first molar crater	0.26	0.46	0.19	0.96
Maxillary left first molar furcation	0.64	1.14	0.94	0.17
Maxillary left second molar crater	0.68	0.65	0.82	1.67
Mandibular left first molar crater	1.63	1.66	1.66	0.37

Furthermore, subjective analysis of five dependent variables (lamina dura, bone quality, contrast, craters and furcation involvements) on both imaging modalities was conducted. They were scored with an ordinal scale from 0 to 3 (where 0=lack of visibility, 1= poor, 2=medium, 3=good). This ordinal data was processed using non parametric statistics and yielded no observer effect. Again the same test were used, however, when comparing 2D images versus 3D CBCT, the Wilcoxon Signed Rank (Siegel 1956) test was not used for the variables craters and furcation involvements. CBCT image data sets for these variables were interpreted by the observers using extra planes to describe the bone defects. Related to the discrepancy between 2D and 3D data sets, the Mann Whitney test was used to test these variables (Siegel 1956). The statistical analyses were done with SPSS V.13.0. statistical software (SPSS Inc., Chicago, IL, USA).

RESULTS

Linear bone level measurements

Table 5.1 shows absolute linear measurement deviations of periodontal bone levels from the direct measurements (gold standard). The deviations for intraoral radiography ranged from 0.19 to 1.66 mm and 0.13 to 1.67 mm for CBCT. Further analyses revealed no significant difference between the two imaging modalities ($p=0.161$, Table 5.2). The currently applied range of exposure settings for intraoral

radiography, yielded no significant difference in accuracy performance (p=0.425, Table 5.2) as such that it was justified to compare all of these to CBCT imaging.

Table 5.2: Results of the Wilcoxon Signed Rank test for the two different imaging modalities and of the Friedman test for the different settings (the three different exposure times)

	CCD+Heliodent DS vs I-CAT Wilcoxon Signed Rank Test		Heliodent DS 40,60 & 80 ms Friedman Test
Z	-1.070	ChiSq	1.712
Exact Sig.	0.161	Df	2.000
		Asymp.Sig.	0.425

Since each observer made 30 intraoral radiographic measurements (3 settings), a total of 90 measurements were obtained from all the observers. Amongst these measurements, 48 (53%) were underestimated and 42 (47%) were overestimated. For CBCT the 30 measurements (only 1 setting) had the same ratio of underestimation (16 of 30 measurements, 53%) and overestimation (14 of 30 measurements, 47%) as intraoral radiographs. Figure 5.3 is a graphic representation of the exact un-averaged values in Table 5.1, showing only minor difference between over- and underestimation.

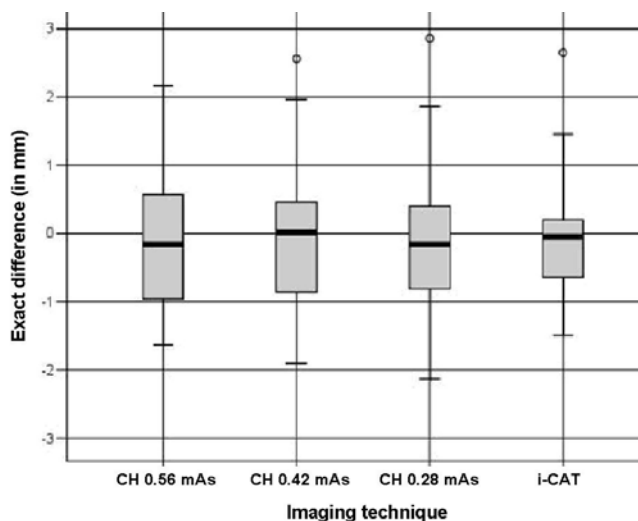


Figure 5.3: Boxplot of exact differences between gold standard measurements and observer linear bone level measurements (Table 5.1). The chart showed median (black line), interquartile range (boxes) and extreme values within different settings of the CCD set-up or the CBCT data. The boxes range between -1 and 1 mm, which represented minor differences from the direct measurements. Overall values were slightly more negative (especially the boxes), showing slightly more underestimation of bone loss. (CH=CCD+Heliodent DS)

Quality rating

Data analysis of the two imaging modalities yielded a significantly better outcome for the intraoral radiographic images regarding lamina dura, contrast and bone quality. On the other hand, for the variables craters and furcation involvements, the morphological descriptions of the periodontal defects were more clearly depicted by using CBCT (p=0.018). This implied that CBCT was more accurate for 3D crater and furcation visualization compared to intraoral digital imaging. Figure 5.4 represents the average values scored for both imaging modalities.

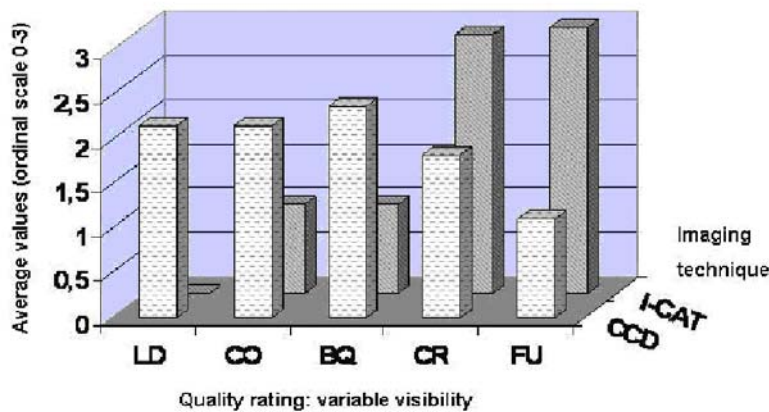


Figure 5.4: Variable comparisons between 2D (CCD) and 3D (CBCT) imaging modalities. Observers found that the lamina dura were well delineated on the CCD images and not visible on CBCT. Contrast and bone quality were also scored better on the digital intraoral radiographs. Periodontal craters and furcation involvements were better visualized on CBCT.

DISCUSSION

As seen in the results, linear bone level measurements were similar with 2D intraoral digital and 3D CBCT images. Both imaging modalities had same over- and under-estimation rates for periodontal bone defects. Bone craters and furcation involvements were better depicted on CBCT than on intraoral images. This could be because CBCT provides multi-planar slices and 3D information. However, because of the lower resolution, CBCT scored less than the intraoral images in contrast, bone quality, and delineation of lamina dura. This indicated that the current CBCT system could not replace intraoral radiography for periodontal assessment. In fact combination of both imaging modalities could benefit periodontal bone assessment and assist presurgical treatment planning.

Radiation dose is always a concern for using conventional CT. However, radiation dose of CBCT was reported up to 15 times less than conventional CT (Scarfe et al 2006). Recent studies reported that CBCT systems only require 4 to 15 times the dose of standard panoramic image (Ludlow et al 2006) or only the dose of a film based full mouth radiographic examination (FMX) (Scarfe et al 2006). An FMX in the USA varies from 18 to 22 intraoral radiographs with a dose range of 13 to 100 μSv (White 1992, Gibbs 2000). Effective dose of CBCT, starting at 36.9 μSv , was in the range of the FMX (Ludlow et al 2006, Scarfe et al 2006). Furthermore, Scarfe et al (2006) reported about dose reduction when using smaller FOV examinations. The 9 inch FOV of the i-CAT images (69 μSv) should be capable of visualizing both jaws and providing all necessary information for periodontal treatment planning of implants. The images require 8 times the dose of a standard panoramic image (1.9-11 μSv). If more information is required in a broader area, the 12 inch FOV (135 μSv)

should be used, but in that case the radiation dose would rise till 15 times a standard panoramic image dose (Scarfe et al 2006).

Since the radiation dose of CBCT is lower than conventional CT, there is growing concern of its over-consumption and radiation safety. In our opinion, the use of CBCT should still be carefully justified (diagnostic benefit and risk to be balanced). The imaging system must be performed by experienced and trained dentists. As low as reasonably achievable (ALARA) radiation safety principle must be followed. In the current study, a low exposure setting of CBCT (only 23.87 mAs and 0.4 mm voxel size) was used. More studies with a large sample size in the future will determine ideal exposure settings, which optimize the image quality and lower the radiation exposure further.

The present study found that CBCT had higher quality rating on bone crater and furcation involvement assessment while contrast, bone quality and delineation of lamina dura were rated lower than for digital intraoral radiography. We would like to suggest that the currently tested model of CBCT should only be used to relatively more complex periodontal treatment planning, such as prognostic planning and surgery of complex periodontal defects and potential use of dental implants.

Previous studies show that periodontal bone level measurements are reproducible on conventional film-based radiography, while examiners' agreements is not enhanced by using intraoral digital imaging systems (Pecoraro et al 2005). Nevertheless, the latter reduce radiation exposure and offer potentials for image analysis, optimisation and quantification, such as contrast enhancement, periodontal filtering and digital subtraction (Vandre & Webber 1995, Young et al 1996, Jeffcoat & Reddy 2000, Mol 2000, Cury et al 2004). These dynamic functions can aid periodontal diagnosis as well. However, when compared to CBCT, digital intraoral radiography is still a 2D technique with limitation of presenting three-dimensional periodontal defects, particularly the buccal and lingual aspects of bone loss (Zulqarnain & Almas 1998, Eickholz & Hausmann 2000, Schliephake et al 2003). In the present study we actually attempted to reduce the radiation dose as much as possible while keeping full diagnostic capabilities to offer a clinically applicable comparison to CBCT. The lowest settings applied (0.28 mAs at 60 kV) were still able to visualize the periodontium with the same accuracy and thus these can be further recommended for the present tube specifications.

All linear measurements in this study were done using a standardized dry skull and a cadaver head, after in vitro pilot-testing of the precision of the method. A standardized repositioning and stabilisation was guaranteed by an individually adapted stent material, serving as a rigid occlusal key during exposure. This set-up allowed avoidance of any projection error and correct fiducials visualisation. The standardised and reproducible image of the reference points was confirmed by the high accuracy scoring and the good intra- and inter-observer agreement in the present report. When defining accuracy in terms of clinical measurement, a certain discrepancy between actual bone level and radiographically estimated bone level has to be admitted and considered as clinically acceptable. Small or big errors in locating the CEJ and the alveolar crest can respectively lead to over- and underestimation of disease prevalence (Brägger 2005). This can even lead to inappropriate planning for further treatment or unnecessary surgery. Considering that a 0.5 mm discrepancy can be admitted clinically, both 2D CCD and 3D CBCT are accurate enough in respectively 60% and 67% of the measures. A 1 mm discrepancy even leads to respectively 82% and 90% accuracy.

Lastly, validation of these imaging modalities has been done by a comparison in detectability of anatomical or pathological features, but the final test will be how well any of them will have effect on treatment decisions and treatment outcome.

CONCLUSION

CBCT allowed similar periodontal bone level measurements as digital intraoral radiography. Bone craters and furcation involvements were better depicted on CBCT, while contrast, bone quality, and details of lamina dura were scored better on digital intraoral radiography. A selective use of both imaging modalities might thus aid periodontal diagnosis and treatment planning. However, selection criteria are needed to define the conditions and specific indications for use of 2D and/or 3D imaging modalities in periodontology.

ACKNOWLEDGMENTS

The authors thank Roslyn Gorin, M.A. (Statistical Application Manager, Computer Sciences, Temple University, Philadelphia, PA) for her help with the statistical analyses.

Chapter 6:

3D topographic assessment of crater and furcation involvements

This chapter has been published as:

Vandenberghe B, Jacobs R, Yang J. Detection of periodontal bone loss using digital intraoral and CBCT images: an in-vitro assessment of bony and/or infrabony defects. *Dentomaxillofac Radiol* 2008;37:252-60

INTRODUCTION

Currently clinical probing and intraoral radiography are the main diagnostic tools for periodontal diseases. However, several studies have shown limitations for both techniques in assessment of periodontal bone loss (Benn 1990, Young et al 1996, Fuhrmann et al 1997, Zulqarnain & Almas 1998, Müller & Eger 1999, Eickholz & Hausmann 2000, Jeffcoat & Reddy 2000, Tugnait et al 2000, Schliephake et al 2003, Mol 2004, Brägger 2005). One of the major drawbacks is surely the lack of three-dimensional (3D) information for assessment as well as classification of periodontal bone defects, especially the infrabony defects and furcation involvements. Infrabony defects are also referred to as bony craters*, which are usually saucer-shaped with 3 or 4 bony walls remaining. Furcation involvements refer to the periodontal defects among the multi-rooted teeth where roots diverge. Correct interpretation of these defects is crucial to predict prognoses of periodontally affected teeth as well as to make adequate treatment planning (Young et al 1996, Fuhrmann et al 1997, Eickholz et al 1999, Müller & Eger 1999, Kaeppler et al 2000, Paurazas et al 2000, Tugnait et al 2000, Cury et al 2004, Kobayashi et al 2004, Pecoraro et al 2005, Almog et al 2006, Deas et al 2006, Guerrero et al 2006, Misch et al 2006, Vandenberghe et al 2007^a). Those non-linear bone defects are namely the main cause for tooth loosening or missing and are not often addressed in research on validation of radiographic modalities for periodontal diagnosis. Measurements of crater depth from the cemento-enamel junction or specific fiducials, like assessment of linear bone loss, do not provide enough information on the 3D defect nature, although this could be essential for periodontal therapy. Different types and degrees of these infrabony defects may have specific prognoses and often require different treatment procedures (Müller et al 1995). Unfortunately, especially the upper molars are listed as most difficult for diagnosis and prognostic planning on 2D images (Svardstrom & Wennstrom 2000), as the root morphology and maxillary sinus overlap will surely cause anatomic masking. Radiographic aids like a furcation arrow have been proven to have limited value in predicting furcation lesions (Deas et al 2006). Considering the limitations of the existing diagnostic methods and the three-

* For description of bony defects, we will be using the general term crater in this article which can refer to 1-walled, 2-walled, 3-walled or 4-walled defects or any combination of these.

dimensional nature of many periodontal bone defects, the current diagnostic approach needs further improvement (Young et al 1996, Fuhrmann et al 1997, Müller & Eger 1999, Tugnait et al 2000) for early diagnosis of these crater-like and furcation defects.

Cone beam computed tomography (CBCT) is a recently developed imaging modality. It can provide 3D information of dentition as well as its supporting structures. When compared to a conventional computed tomography (CT), CBCT considerably reduces radiation exposure to patients (Tsiklakis et al 2005, Ludlow et al 2006, Scarfe et al 2006). Application of this new imaging modality with combination of existing 2D digital intraoral radiographs may offer new perspectives on periodontal diagnosis and treatment planning (Jacobs et al 1999, Misch et al 2006, Vandenberghe et al 2007^a).

Therefore, the purpose of this study was to explore the diagnostic value of CBCT in determination and classification of the three-dimensional topography of periodontal bone craters and furcation involvements. We hypothesized that CBCT would allow more accurate assessment of the periodontal bone defects than intraoral radiography. This study was a continuation of our previous research on assessment of linear bone loss with CBCT (Vandenberghe et al 2007^a).

MATERIALS AND METHODS

Forty-one periodontal non-linear bony defects from two adult human skulls, a cadaver head and a dry skull, were evaluated by using intraoral digital radiography (CCD sensor, Schick Technologies, NY, USA) and CBCT (i-Cat, 12 bit, Imaging Sciences International, Hatfield, Pennsylvania, USA). The upper and lower jaws of the cadaver head were fixed with 10% formalin and functioned as a clinical subject. The adult human dry skull was covered with a soft tissue substitute, Mix D (White 1977), and used as a simulation.

For the intraoral protocol, images were obtained with a size #2 charged coupled device (CCD) intraoral digital sensor and a direct current (DC) x-ray unit (Heliodont DS, Sirona Dental Systems LLC, Charlotte, NC, USA) combined with a rectangular (4 cm x 3 cm) collimator (Universal Collimator, RINN Corporation, Elgin, IL, USA). The focus-receptor distance was 30 cm. The paralleling technique was

applied in a standardized exposure set-up with film holding system (XCP, RINN Corporation, Elgin, IL, USA) and standardized bite blocks (see Figure 6.1). The exposure setting was 60 kVp with 0.28 mAs (40 ms x 7 mA).

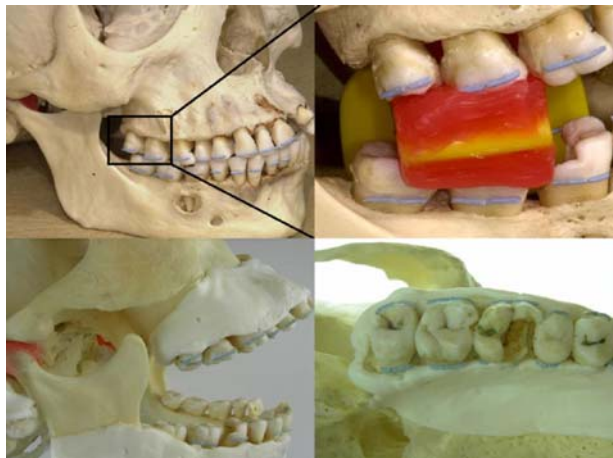


Figure 6.1: Standardized exposure set-up: dry skull with gutta-percha markers (for linear bone loss assessment in our preceding study) and waxed imprints before covering the jaws with soft tissue substitute. Non linear defects were present around almost all teeth. A clearly visible defect is seen on the third maxillary molar.

For CBCT scanning, the occlusal plane of the jaw bones was positioned horizontally to the scan plane and the midsagittal plane was centred. The field-of-view (FOV) or the beam diameter at the surface of the image receptor (beam height) was adjustable and set to visualize the entire jaws, giving between 54 and 159 slices of 0.4 mm thickness (approximately between 20 and 60 mm beam height). Images were obtained using a low-dose protocol, being 120 kVp and 23.87 mAs with a typical voxel size of 0.4 mm (see Figure 6.2).

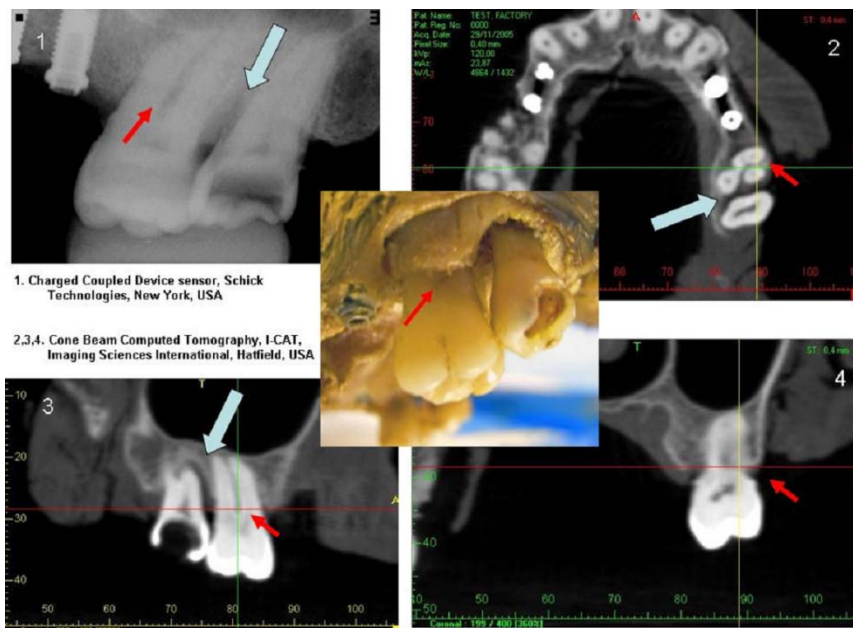


Figure 6.2: Digital x-ray images of molar region from the upper cadaver jaw. 1) Two-dimensional CCD image, 2) CBCT axial slice, 3) CBCT coronal slice and 4) CBCT panoramic view (oblique). Observers described the defects using both imaging modalities (CCD and CBCT) and comparison was done to the gold standard, which was obtained after removing the soft tissues (center). The small arrows indicate a furcation involvement which was overestimated by the three observers on the 2D CCD radiograph.

The larger arrows indicate a mesial 3-walled periodontal bone defect which was marked as 1-walled on the 2D CCD image.

Assessment of the periodontal bony defects using both imaging modalities was done by three observers (a post graduate student in radiology and two radiology faculty members, Temple University School of Dentistry, Philadelphia, USA). Each of them in turn viewed the images in a darkened room on a notebook with 17 inch LCD monitor and high screen resolution (1440 x 900 pixels). Intraoral 2D images were displayed with the Emago advanced, V.3.5.2. software in Tagged Image File Format (TIFF). Dedicated filtering and grey scale enhancement methods were allowed to analyze the selected sites. CBCT images were viewed with the I-CAT software (Xoran CAT V.2.0.21., Xoran Technologies Inc. 2005). Analysis was carried out using coronal, sagittal and axial slices of 0.4 mm each, through the selected teeth. Measurement tools on both programs were used for furcation classification, if necessary.

A group of ten teeth in the molar region of upper and lower jaws, containing forty-one sites, including mesial and distal three-dimensional crater defects and vestibular and oral (for maxillary molars vestibular, mesial and distal) furcation involvements, was selected for comparison and statistical analysis. Physical descriptions on the skull models were considered as the gold standards for further accuracy assessment of both imaging modalities. For the cadaver jaws, the gold standard was obtained after image acquisition, by flap surgery to allow physical description and classification. Furcation classification was done by using a periodontal probe. For the dry skull however, gold standards were obtained, prior to adding soft tissue substitute and image acquisition.

Statistical analyses

Bone defects and crater involvements of the selected sites, observed on the digital intraoral and CBCT-images, were compared with the gold standards. Imaging methods and observers were used as independent variables and bone crater and furcation involvements as the dependent ones. The latter were classified by an ordinal scale from 0 to 4 (no defect, 1-walled, 2-walled, 3-walled and 4-walled) and from 0 to 3 (no furcation involvement, class I, class II and class III) respectively. The gold standard was obtained by averaging the scores of two observers. Intra-class correlation showed no observer effect for these scores.

Because of the ordinal nature of the acquired data, non parametric statistics were utilized for the analyses (Siegel 1956, Afifi & Clark 1984). The observer effect for both dependent variables was tested with the Kruskal Wallis test and showed no significant difference among the three observers ($p>0.05$). A 50% repeat of measurements was done at an interval of one week and a high reliability was found amongst every observer (interval of 0.986 to 0.997 with 95% confidence and a single measure intra-class correlation coefficient of 0.987). Those measurements were then averaged for further calculations (see Table 6.1).

Table 6.1: Crater assessment: gold standard versus CCD and CBCT assessment. The ordinal scale represents classifications (0, 1, 2, 3 and 4-walled defects). The table shows the averaged values of three observers as no observer effect was found. For CCD only 25% of the craters compared to 88% of them for CBCT matched the gold standard.

Crater	Gold Standard	2D CCD	3D CBCT
Mandibular right first molar mesial	0	0	0
Mandibular right first molar distal	2	2	2
Mandibular right second molar mesial	0	0	0
Mandibular right second molar distal	3	0	3
Mandibular right third molar mesial	0	0	0
Maxillary right first molar mesial	3	1	3
Maxillary right first molar distal	3	0	3
Maxillary right second molar mesial	2	1	2
Maxillary right second molar distal	2	2	1
Maxillary right third molar mesial	2	0	2
Maxillary right third molar distal	2	0	2
Mandibular left first molar mesial	2	2	2
Mandibular left first molar distal	1	2	1
Mandibular left second molar mesial	3	0	2
Mandibular left second molar distal	3	1	3
Maxillary left second molar mesial	3	3	3
Maxillary left second molar distal	2	1	2
Maxillary left third molar mesial	3	1	3
Maxillary left third molar distal	1	2	1

When comparing gold standard, 2D images and 3D CBCT-images, the Kruskal Wallis test was used to test the variables (Siegel 1956). The statistical analyses were done with SPSS V.13.0. statistical software (SPSS Inc., Chicago, IL, USA).

RESULTS

Craters

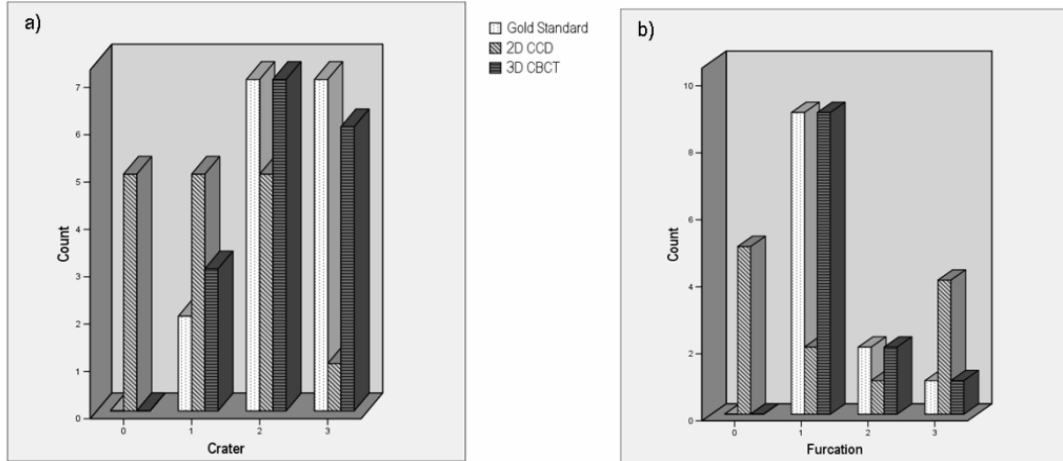
Table 6.1 is a summary of the observations of the selected crater sites. The gold standard versus 2D intraoral digital imaging and 3D CBCT assessment of the crater sites and their mean values are shown. The 0 values in the gold standard, representing absence of craters and furcation involvements, were excluded from the statistical analyses as no different values were scored with both techniques, yielding thus a 100% specificity for this variable for 2D and 3D imaging.

The gold standard versus 2D digital intraoral images and 3D CBCT were compared using the Kruskal Wallis test. There was a significant difference ($p=0.001$) between the gold standard and the imaging modalities. Further exploration through the Mann Whitney test showed that this was due to the 2D intraoral imaging technique, which was significantly different from the gold standard ($p=0.001$, see Table 6.2). Table 6.2 also demonstrated the significant difference ($p=0.002$) between the 2D and the 3D imaging techniques in assessment of craters. Figure 6.3a is a graphic representation of the values in Table 6.1, showing frequency counts of gold standard, 2D CCD and 3D CBCT images.

Table 6.2: Kruskal Wallis test and Mann Whitney test for accuracy assessment of the two imaging techniques. The 2D intraoral technique was significantly different from the gold standard for both dependent variables. The significant differences between both 2D and 3D images showed more accurate assessment of craters and furcation involvements by the 3D CBCT images.

		GS vs 2D CCD	GS vs 3D CBCT	2D CCD vs 3D CBCT	GS versus 2D CCD versus 3D CBCT	
<u>Crater</u>	Z	-3.264	-0.471	-2.950	ChiSq	13.387
	Exact Sig.	0.001	0.374	0.002	Df	2
					Exact Sig.	0.001
<u>Furcation</u>	Z	-0.430	0.000	-0.430	ChiSq	0.269
	Exact Sig.	0.322	0.608	0.322	Df	2
					Exact Sig.	0.892

Figure 6.3: Bar charts of the averaged observer data showing frequency counts of the gold standard, 2D CCD and 3D CBCT images. a) crater classification (0=no defect, 1=1-walled, 2=2-walled, 3=3-walled) b) furcation classification (0=no involvement, 1=class I, 2=class II and 3= class III). Both graphics show more precise classifications using CBTC as the frequency counts lie close to the gold standard. They both reveal that for 2D CCD images, many craters and furcation involvements were not detected.



From Table 6.1 we found that for intraoral digital imaging, 31% of the present defects were not detected. Only 25% of the observations had the same class as the gold standards. A tendency to overestimate the crater involvement is seen in 62% of the sites and only 13% are underestimations. For CBCT however, all crater involvements were visible. Observations deviated only slightly, 12% of overestimations and 88% were correctly classified. We found no significant difference between the gold standards and this 3D imaging modality ($p=0.374$, Table 6.2).

Furcation involvement

Table 6.3 shows the observations of the selected furcation sites. The ordinal scale was adjusted to a 0 to 3 scale (see Figure 6.3b) for statistical analyses. Again the 0 values of the gold standard were excluded from the statistical analyses.

Table 6.3: Furcation assessment: gold standard versus CCD and CBCT assessment. Classification in main classes is given (0=no defect, 1/2/3=class IA/IB/IC, 4/5/6=class IIA/IIB/IIC, 7/8/9=class IIIA/IIIB/IIIC). Again the averaged values of three observers are shown as no observer effect was found. Subclasses were not used in statistical analyses because of the nature of the ordinal scale. Intraoral images could not distinct vestibular from oral furcation involvements. Fifty-eight percent of the furcation involvements were detectable with the CCD technique and only 25% of them were correctly classified. In the contrary CBCT allowed 100% detection and correct classification of furcation involvements.

Furcation	Gold Standard	2D CCD	3D CBCT
Mandibular right first molar vestibular	1	7	1
Mandibular right first molar oral	4	7	4
Mandibular right second molar vestibular	0	0	0

Chapter 6: 3D topographic assessment of crater and furcations

Mandibular right second molar oral	0	0	0
Mandibular right third molar vestibular	0	0	0
Mandibular right third molar oral	0	0	0
Maxillary right first molar mesial	1	0	1
Maxillary right first molar distal	0	0	0
Maxillary right first molar vestibular	1	0	1
Maxillary right second molar mesial	0	0	0
Maxillary right second molar distal	0	0	0
Maxillary right second molar vestibular	1	0	1
Mandibular left first molar vestibular	0	0	0
Mandibular left first molar oral	1	1	1
Mandibular left second molar vestibular	0	0	0
Mandibular left second molar oral	4	0	4
Maxillary left second molar mesial	1	4	1
Maxillary left second molar distal	7	7	7
Maxillary left second molar vestibular	1	7	1
Maxillary left third molar mesial	0	0	0
Maxillary left third molar distal	1	0	1
Maxillary left third molar vestibular	1	1	1

However, for this variable, the Kruskal Wallis test and subsequently the Mann Whitney test revealed no significant differences among the gold standard and two imaging modalities. Hence, the data of both variables were explored and revealed normal variations in the medians of the crater data (gold standard=2, CCD=1 and CBCT =2), but a constant value of 1 for the furcation involvement data. This limitation explained the unexpected results for furcation involvements and therefore further analyses including cross-tabulations and Chi-square tests of the furcation involvement data were made. Table 6.4 shows that based on frequency counts significant difference was found for the furcation involvement variable between the 2D CCD images and the gold standard ($p=0.006$, Table 6.4)

Table 6.4: Chi-square tests of both variables. The crater outcome matched the Mann Whitney test outcome with a significant difference when comparing 2D CCD image classification to the gold standard. Although the Mann Whitney test in Table 6.2 shows no significant difference for the furcation involvement variable, a significant difference based on frequency counts was found between 2D CCD image classifications and the gold standards.

		GS versus 2D CCD	GS versus 3D CBCT	2D CCD versus 3D CBCT
<u>Crater</u>	Chi-Sq Value	11.119	0.277	16.250
	Df	3	2	6
	Exact Sig.	0.009	1.000	0.010
<u>Furcation</u>	Chi-Sq Value	11.588	0.000	18.300
	Df	3	2	6
	Exact Sig.	0.006	1.000	0.003

With intraoral CCD images, 58% of the furcation involvements were detectable. Even for those detectable ones, only 25% were correctly classified and the misclassification counts were as high as 75% (33% of overestimations and 42% of underestimations). Also, it was not possible to distinct vestibular from oral furcation involvements. For CBCT, 100% of the furcation involvements were visible and they were all correctly classified. Based on these frequency counts no significant difference was found ($p=1.000$, Table 6.4) between the gold standard and 3D CBCT images in assessment of furcation involvements.

DISCUSSION

The recent attention for cone beam CT requires validation of this technology for diagnostic purposes. For periodontal diagnosis, the present results revealed a better depiction of bone craters and furcation involvements on CBCT than on intraoral images. Also, vestibular and oral bone defects, as well as maxillary trifurcations were easily assessed by CBCT images. This architecture remains problematic to visualize through typical intraoral images, despite various efforts to optimize their diagnostic value. These images left the observers more to guessing than accurately assessing the existing craters and furcation involvements. Only 69% of the crater defects and 58% of the furcation involvements were identified on the intraoral CCD images, in contrast to a 100% detectability for both defects on the CBCT image data. These findings are comparable to following studies. Misch et al (2006) found that only 67% of the artificially created infra-bony defects were diagnosed on intraoral images. Fuhrmann et al (1997) found that only 21% of the artificial furcation involvements were identified on dental radiographs and 100% through high resolution CT.

While the use of digital intraoral radiography has not been found to be superior to conventional radiography for periodontal linear measures (Pecoraro et al 2005), it cannot be ignored that it offers at least two essential benefits being radiation dose reduction and image analysis for improved bone diagnostics (Mol 2000, van der Stelt 2000). With regard to the first benefit, we actually attempted to reduce the intraoral radiographic dose as much as possible while keeping full diagnostic capabilities. The method and exposure settings used in the present study have been tested and validated in our previous report (Vandenberghe et al 2007^a). The second benefit of

digital intraoral images, indeed, may allow for image optimisation and quantification, such as contrast enhancement, periodontal filtering and digital subtraction (Young et al 1996, Jeffcoat & Reddy 2000, van der Stelt 2000, Cury et al 2004, Mol 2000). These dynamic functions may aid periodontal diagnosis. However, it is widely accepted that the two-dimensional nature of the images, whether these are conventional or digital, prevents a diagnosis of the entire spatial bone defect. Whenever such a three-dimensional diagnosis might be possible, it may hold an important potential to better assess prognosis of individual teeth and thus obtain a more efficient treatment planning.

In the present study, we confirmed the hypothesis that CBCT would allow more accurate assessment of the periodontal bone defects than intraoral radiography. Dedicated periodontal filtering may aid bone level measurements but not crater and furcation assessment. When compared to CBCT, digital intraoral radiography is still a 2D technique with limitation of presenting three-dimensional periodontal defects, particularly with regard to the buccal and lingual aspects of bone loss (Zulqarnain & Almas 1998, Eickholz & Hausmann 2000, Schliephake et al 2003). Our observers were not able to distinguish vestibular from oral bony defects. The maxillary trifurcations could hardly be detected or interpreted.

Of course, this more accurate assessment by CBCT is mainly due to the fact that CT technology provides multi-planer slices and 3D information. The innovative cone beam technology of this imaging technique finally allows lower radiation doses, which will be able to expand its further use. Radiation dose of CBCT was reported up to 15 times less than conventional CT (Scarfe et al 2006). Recent studies reported that CBCT systems only require 4 to 15 times the dose of standard panoramic image (Tsiklakis et al 2005) or only the dose of a film based full mouth radiographic examination (FMX) (Scarfe et al 2006). An FMX in the USA varies from 18 to 22 intraoral radiographs with a dose range of 13-100 μ Sv (White 1992, Gibbs 2000). Effective dose of CBCT, starting at 36.9 μ Sv, was in the range of the FMX (Tsiklakis et al 2005, Scarfe et al 2006). Furthermore, Ludlow et al (2006) reported about dose reduction when using smaller FOV examinations. Since the radiation dose of CBCT is lower than conventional CT, there is growing concern of over-consumption of CBCT and its radiation safety. In our opinion, the use of CBCT should still be carefully justified (diagnostic benefit and risk are balanced), if optimised exposure

protocols (following the ALARA principle, as low as reasonably achievable) are considered. This can be guaranteed if the image acquisition and further interpretation are performed by specialists in this field. In the current study, a low dose protocol of CBCT (only 23.87 mAs and 0.4 mm voxel size) was used. More studies with a large sample size in the future will determine ideal exposure settings, which optimize the image quality and lower the radiation exposure further.

The currently used software of CBCT requires a certain amount of experience which leads to the most optimal assessment of anatomical features. The growing possibility of real 3D reconstruction of the CBCT images by more precise algorithms will even improve this by making it easier to interpret the three dimensions of crater and furcation involvements. Figure 6.4 shows 3D reconstruction images and manipulations of one of the selected regions (see Figure 6.2) on the cadaver jaws.

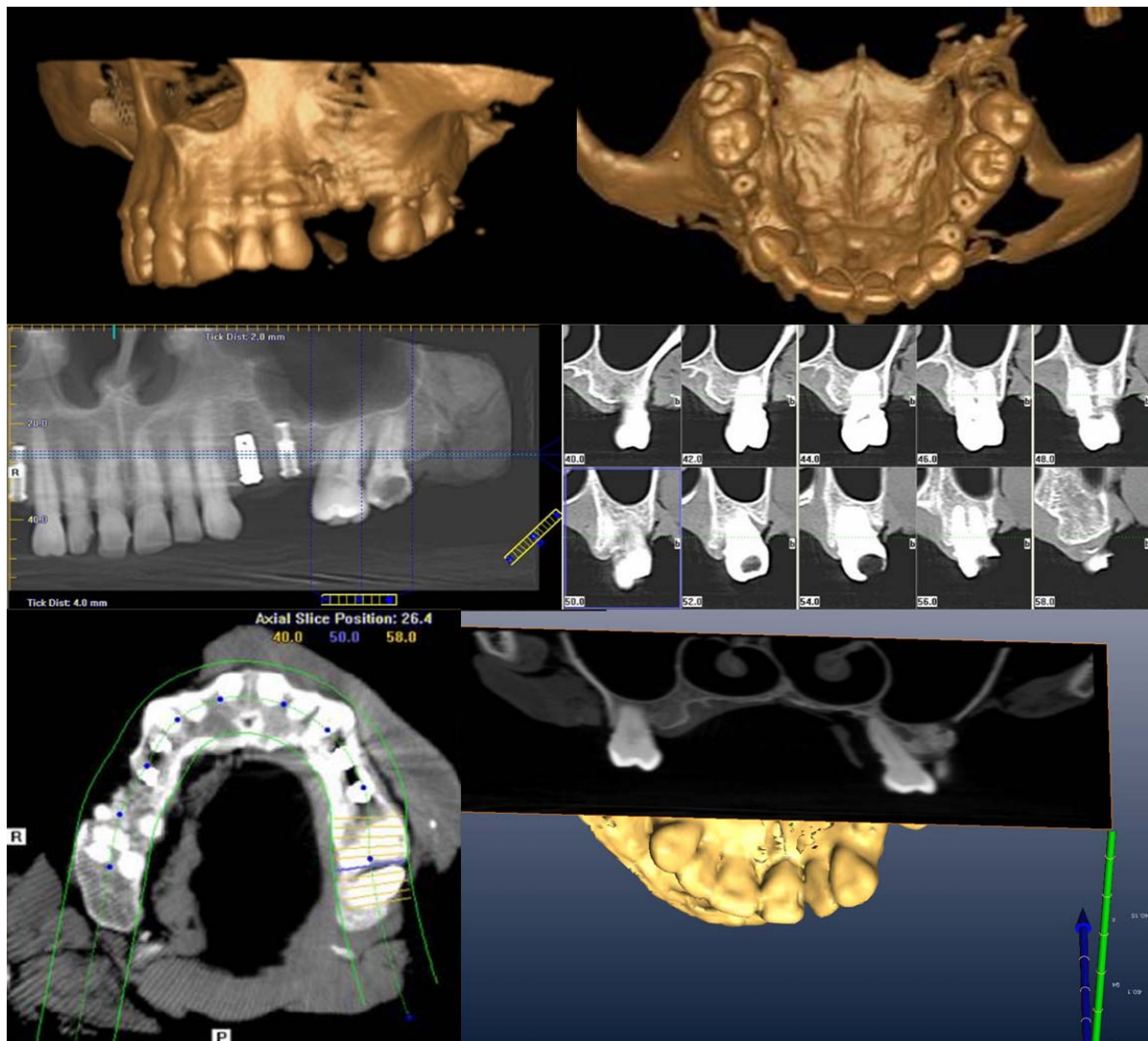


Figure 6.4: Three-dimensional reconstruction images of the same molar region as in Figure 6.2, using different software packages.

In the preceding part of this study, linear bone loss was found similar to intraoral CCD assessment using CBCT images (Vandenberghe et al 2007^a). However, because of the lower resolution, CBCT were scored less than the intraoral images in contrast, bone quality, and delineation of lamina dura. This indicated that the current CBCT system could not replace intraoral radiography for periodontal assessment. In fact combination of both imaging modalities could benefit periodontal bone assessment and assist pre-surgical treatment planning. We would like to suggest that the currently tested model of CBCT should only be used to relatively more complex periodontal treatment planning, such as prognostic planning and surgery of complex periodontal defects and potential use of dental implants.

All observations in this study were done using a general classification system. Periodontal defects were given the general name of crater and classified as 1-walled, 2-walled, 3-walled and 4-walled in the most apical depth of the lesions. This way we followed the common classification proposed by Karn et al (1984) but avoided the sometimes difficult nomenclature of crater, trench, moat, ramp, plane or combinations of these. Furcation involvements were classified looking at the horizontal component proposed by Hamp et al (1975) (class I, II and III) and the vertical component proposed by Tarnow et al (1984) (subclass A, B and C). However, because of the discrepancy of the assigned ordinal data to this scale, only the main classes were used for the statistical analysis. The classification proposed by Rosenberg et al (1985) for maxillary trifurcations was left aside as the three bifurcations were assessed separately. Most of these classifications might have been based on clinical, surgical and 2-D radiological information.

Finally, validation of these imaging modalities has been done by comparison in detectability of anatomical or pathological features, but the ultimate test would lie on how much these features impact on treatment decisions and treatment outcome. Therefore, further long time clinical studies would be required.

CONCLUSION

CBCT allowed more accurate assessment of bone craters and furcation involvements than digital intraoral radiography. This study might help in establishing

selection criteria for different imaging modalities in assessment of periodontal bone loss and further assist in periodontal diagnosis and treatment planning.

ACKNOWLEDGMENTS

We would like to thank Roslyn Gorin, M.S., Statistical Application Manager, Department of Computer Sciences, Temple University for her help with the statistical analyses.

Chapter 7:

Bone loss measurements on 3D orthogonal slices

This chapter has been published as:

Vandenberghe B, Jacobs R, Yang J. Topographic assessment of periodontal craters and furcation involvements by using 2D digital images versus 3D cone beam CT: an in-vitro study. Chin J Dent Res 2007;10:21-29

INTRODUCTION

Studies have shown that early detection of periodontal disease is important in the prevention of tooth loss and/or for the patient's general health (Slots 2003, Oliveira Costa et al 2007). However, current diagnostic approaches including clinical probing and intraoral radiography, have shown several limitations in their reliability (Benn 1990, Hefti 1997, Zulqarnain & Almas 1998, Eickholz & Hausmann 2000, Jeffcoat & Reddy 2000, Schliephake et al 2003, Mol 2004, Brägger 2005). Clinical probing is dependent on the probing force, while periapical radiographs or bitewings may over- or underestimate the amount of bone loss due to projection errors. One of the main drawbacks of intraoral radiography is overlap of anatomical structures and lack of three-dimensional (3D) information. This often hinders a true distinction between the buccal and lingual cortical plate and complicates the evaluation of periodontal bone defects, especially the infrabony lesions, also denoted as craters, and furcation involvements.[†]

Several efforts for optimizing these diagnostic tools have been made over the past few years. Unfortunately, electronic probes have not demonstrated more advantages over manual probing (Quirynen et al 1993, Khocht & Chang 1998). Digitalization of intraoral radiographs has considerably reduced radiation dose and made digital subtraction radiography (DSR) possible for lesion follow-up (Jeffcoat & Reddy 2000, van der Stelt 2000, Cury et al 2004). However, intraoral radiography remains essentially a two-dimensional (2D) imaging technique with lack of information on the 3D defect nature of infrabony lesions. Conventional computed tomography (CT) solves this problem by providing axial slices throughout the object of interest, but has major drawbacks including high radiation dose, high cost and low resolution (Sukovic 2003, Ludlow et al 2006, Scarfe et al 2006). In order to enforce this 3D assessment of bone defects, the current diagnostic approach needs further improvement for early diagnosis of periodontal disease (Müller & Eger 1999, Fuhrmann et al 1997, Tugnait et al 2000, Deas et al 2006).

Cone beam computed tomography (CBCT) is a recently developed imaging modality. When compared with conventional CT, CBCT considerably reduces

[†] For description of bony defects, we will be using the general term crater in this article which can refer to 1-walled, 2-walled, 3-walled or 4-walled defects or any combination of these.

radiation exposure to patients (Sukovic 2003, Ludlow et al 2006, Scarfe et al 2006). Although there has been limited publications concerning CBCT for periodontal assessment, application of this new imaging modality with combination of existing 2D digital intraoral radiographs may offer new perspectives on periodontal diagnosis and treatment planning (Guerrero et al 2006, Misch et al 2006, Vandenberghe et al 2007^{a,b}).

The purpose of this study was to explore the diagnostic value of CBCT in the determination of periodontal bone loss, including the 3D topography of infrabony defects. Since bone loss can be subdivided into linear and non-linear loss, the study was divided into two respective parts, the first dealing with the assessment of periodontal bone height and the second part with the evaluation and classification of 3D topography of periodontal bone craters and furcation involvements. We hypothesized that both imaging techniques would allow accurate assessment of bone loss and that CBCT would allow more accurate evaluation of the non-linear periodontal bone defects than intraoral radiography. This study was a continuation of our previous reports on the potential of CBCT for periodontal diagnosis (Vandenberghe et al 2007^{a,b}).

MATERIALS AND METHODS

Assessment of bone levels through anatomical marker measurements and the evaluation or classification of non-linear bony defects were implemented on intraoral digital radiographs (Schick CDR[®], Schick Technologies, Long Island City, NY) and CBCT images (i-Cat[™], 12 bit, Imaging Sciences International, Hatfield, PA).

Two carefully selected and processed adult human skulls containing multiple periodontal defects were used for the measurement and observation of 71 selected sites. The first skull, a cadaver head with upper and lower jaws fixed by a 10% formaldehyde aqueous solution (formalin), functioned as a clinical subject. A second human dry skull was covered with a soft tissue substitute, Mix-D, and used for simulation (White 1977). In order to assess bone levels, the cemento-enamel junction (CEJ) could only be used as a reference point for the formalin-fixed jaws. Because of dehydration of the dry skull, standardized fiducials were introduced as a substitute for the faded CEJ. Radiopaque gutta-percha fragments with a small central indentation

were glued onto the buccal and lingual surfaces of the respective teeth (see Figure 7.1).



Figure 7.1: Clinical simulation by processing a dry skull. Gutta-percha markers, used as fiducials for bone loss assessment, were glued onto the vestibular/oral sides of every tooth (a). After measuring gold standards, the dry skull could be covered with soft tissue substitute (b). Intraoral images were obtained using standardized bite blocks containing waxed imprints of the teeth (c). After in vitro pilot-testing of these rigid occlusal keys, a standardized set-up was obtained which allowed correct fiducial visualization and projection geometry.

Intraoral digital images were obtained using the paralleling technique in a standardized exposure set-up with a size 2 charged coupled device (CCD) sensor and a direct current (DC) x-ray unit (Heliodent[®] DS, Sirona Dental Systems GmbH, Bensheim, Germany). A rectangular (4 cm x 3 cm) collimator and film holding system (Universal Collimator and XCP[®], Dentsply RINN, Elgin, IL) with standardized bite blocks were used. The focus-detector distance was 30cm. The exposure setting was 60 kVp with 0.28 mAs (40 ms x 7 mA). For CBCT scanning, the occlusal plane of the jaw bones was positioned horizontally to the scan plane and the midsagittal plane was centred. The beam height at the surface of the image receptor was adjustable and set to visualize the entire jaws (approximately between 20 and 60 mm beam height), giving between 54 and 159 slices of 0.4 mm thickness. A low-dose protocol of 120 kVp and 23.87 mAs (20 sec pulsed scanning and a 7 mA current) and a 0.4 mm voxel size were used for image acquisition (see Figure 7.2).

Three observers (a Medical Imaging Master and PhD student and two radiology faculty members, Temple University, School of Dentistry, Philadelphia, PA) randomly measured periodontal bone levels and classified the defects, while seated at a 60 cm distance of a 17 inch LCD high-resolution screen (1440 x 900 pixels) of a Sony Vaio[®] VGN A417m computer (Sony Corporation, Tokyo, Japan). Intraoral 2D images were displayed with the Emago[®] software (Emago Advanced V.3.5.2., Oral Diagnostic Systems (ACTA), Amsterdam, Netherlands) in Tagged Image File Format (TIFF). CBCT images were viewed with the i-CAT software (Xoran CAT V.2.0.21.,

Xoran[®] Technologies Inc., Ann Arbor, MI, USA). Measurement tools on both programs were used for assessing bone levels and for furcation classification, if necessary.

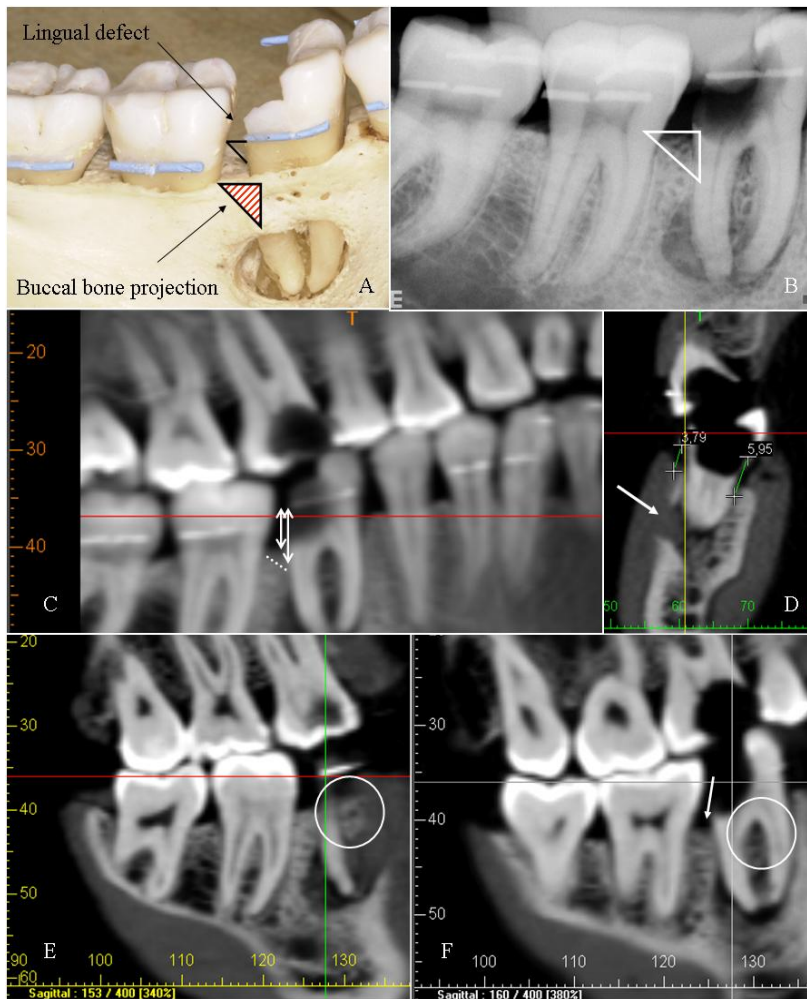


Figure 7.2: Periodontal assessment of the mandibular right first molar. Before covering the dry skull with soft tissue substitute, the gold standard of bone levels and defect topography were taken. On the distolingual side of the selected tooth, (A) a large defect, which could be difficult to assess on (B) 2D intraoral radiographs due to overlap of the buccal bone plate, was clearly seen. (C) Using a panoramic reconstruction of CBCT slices for bone level assessment, measurements were not significantly different from those on CCD images. However, the same projection overlap is seen (dotted line shows the possible defect border). (D) When measuring on individual coronal or sagittal slices of 0.4 mm, buccal and lingual levels or defects can clearly be separated (also note the buccal plate

perforation shown by the arrow). Using these separate CBCT slices, ((E) sagittal slice 153 and (F) sagittal slice 160) a clear 3D effect is obtained, allowing accurate crater topography assessment and furcation involvement evaluation (E/F: both circles show the bone levels around the bifurcation; the arrow in F shows the crater delineation).

The acquired measurement data and periodontal defect classifications were compared to the gold standard. The latter were based on blinded determination of physical measurements and classifications on the skull models by two of the observers. Mesial, central and distal bone levels and bone crater depths on the oral and vestibular sides of each selected tooth were measured. The gold standard of the cadaver jaws was obtained after image acquisition by flap surgery to allow physical measurements using a digital sliding calliper (Mitutoyo, Andover, Hants, UK), description and classification. Furcation classification was done using a furcation

probe. For the dry skull however, gold standards were obtained, prior to adding soft tissue substitute and image acquisition.

In the first part of this study, 43 sites including linear defects, three-dimensional craters and furcation involvements, were chosen out of 20 randomly selected teeth for assessment on intraoral CCD and CBCT images, and the obtained bone height measurements were subsequently compared with the gold standards. Measurements on the CBCT software were carried out on a panoramic reconstruction view (the same for each observer) with a default slice thickness of 5.2 mm, large enough to visualize the specific fiducials and the bone perpendicular to it (see Figure 7.2C). Those CBCT measurements were repeated afterwards on cross-sectional slices of 0.4 mm (see Figure 7.2D). Subjective quality assessment of lamina dura delineation, contrasts, bone quality and defect description was performed using an ordinal scale, ranging from 0 to 3 (where 0=lack of visibility, 1=poor visibility, 2=medium visibility, 3=good visibility).

In the second part of the study, a group of 11 teeth in the molar region of upper and lower jaws, containing 28 mesial or distal craters and buccal and lingual (or for maxillary molars buccal, mesial and distal) furcation involvements, was selected for comparison to the gold standard. Crater and furcation involvement classifications on CCD and CBCT images were given an ordinal scale from 0 to 4 (no defect, 1-, 2-, 3- and 4-walled) and from 0 to 3 (no furcation involvement, class I, class II and class III) respectively (Hamp et al 1975, Karn et al 1984, Tarnow & Fletcher 1984). Analysis was carried out on both programs and for CBCT, using coronal, sagittal and axial slices of 0.4 mm each, through the selected infrabony defects (see Figure 7.2E).

Statistical analysis

43 selected sites were measured by 3 observers on the digital intraoral CCD and CBCT images and compared with the gold standards. Imaging methods and observers were used as independent variables and bone levels measurements as the dependent variables. Although these data were not ordinal, we opted for non-parametric tests (Wilcoxon signed-rank test for comparison of absolute differences with gold standard of CCD versus CBCT measurements) as no normality could be found in the measurement data, even after transformation (Siegel 1956, Afifi & Clark

1984). For the quality rating on images of both modalities, the ordinal data of the dependent variables was compared using the Wilcoxon signed-rank test except for crater and furcation visibility on CBCT cross-sectional slices, for which the Mann-Whitney test was applied considering a discrepancy between the 2D and 3D data.

28 craters and furcation involvements were classified by the same observers on both modalities and compared with the gold standards. Imaging method and observers were the independent and crater and furcation involvement the dependent variables. Comparison of the ordinal data from the gold standards, CCD and CBCT was carried out using the Kruskal-Wallis test. All statistical analyses were done with SPSS® V.13.0. statistical software (SPSS Inc., Chicago, IL, USA).

RESULTS

The results of the reliability analyses and the Kruskal-Wallis tests for observer-effect evaluation are given in Table 7.1. No intra- or interobserver effect was found when analyzing the gold standard, CCD and CBCT measurements or classifications from the three observers. This made averaging of the observer data possible for further calculations.

Table 7.1: Overview of intra- and interobserver-effects. To test the reliability among observer measurements and classifications on CCD (2D) and CBCT (3D) images, a 15% repeat was done at an interval of two weeks. The intraclass correlation coefficients (ICC) and 95% confidence intervals (CI) show high reliability for all observations. The results of the Kruskal-Wallis test show no significant difference ($p > 0.05$) between observers for all measurements and classifications. Gold standards of crater and furcation classification did not differ among and between observers.

	Observer-effect				
	Reliability Analysis (INTRA)		Kruskal Wallis test (INTER)		
	ICC	95% CI	ChiSq	Df	Asymp Sig
GS measurements	0.934	0.928 to 0.984	0.283	1	0.595
2D/3D measurements	0.713	0.675 to 0.914	0.301	2	0.860
2D/3D crater classifications	0.775	0.849 to 0.951	0.117	2	0.943
2D/3D furcation classifications	0.958	0.976 to 0.992	0.027	2	0.987

Part 1: bone level measurements & quality rating

Table 7.2 shows that no significant difference was found ($p = 0.165$) when comparing the intraoral CCD bone level measurements with those on the panoramic

reconstruction image of the CBCT data with 5.2 mm slice thickness. However, when comparing the absolute differences with the gold standards of the CCD measurements with those of the 0.4 mm cross-sectional CBCT slices, a significant difference was found between both modalities (p=0.006).

Table 7.2: Comparison of the gold standards (GS), 2D CCD and 3D CBCT data. The Wilcoxon signed-rank test was used to compare measurements on intraoral CCD images and those on a 5.2 mm panoramic reconstruction image (CBCT1) or 0.4 mm thin cross-sectional slices (CBCT2) of CBCT images. A high significant difference was found between both modalities for CBCT2 (p=0.006). However, further exploration through the Mann-Whitney test did not reveal any significant differences of the measurements with the gold standard for both modalities.

		Wilcoxon Signed Rank Test		Mann Whitney Test	
		Z	Exact Sig	Z	Exact Sig
Measurements	CCD versus CBCT1	-1.419	0.165	/	
	CCD versus CBCT2	-2.455	0.006	GS versus CCD	-0.384 0.708
				GS versus CBCT	-0.185 0.857

Although further analysis through the Mann Whitney test did not reveal a significant difference between the raw data (actual measurements) of the gold standard and the CCD or CBCT data, further investigation of the latter test will indicate the cause of the differences in the nature of the data. The descriptive statistics show a smaller deviation range and mean error for the CBCT measurements on 0.4 mm cross-sectional slices compared with those for CCD images or those on the CBCT panoramic reconstruction image.

Table 7.3: Descriptive statistics of the measurements for bone level assessment. CBCT1 are the measurements on the panoramic reconstruction CBCT image of 5.2 mm slice thickness, CBCT2 on CBCT cross-sectional slices of 0.4 mm. The mean error (compared with the gold standards), minimum and maximum are given. Over- and underestimations tend to be equally dispersed, except for CBCT2 where a slightly higher overestimation rate is seen. If admitting a clinically acceptable measurement discrepancy of 1 mm, the percentages of the CBCT2 measurements run up to 100%.

	CCD	CBCT1	CBCT2
mean error	0.56	0.47	0.29
min (in mm)	0.01	0.03	0.04
max (in mm)	1.65	1.69	0.9
%overestimations	50	52	63
%underestimations	50	48	37
%measurements<1mm	87	90	100

This is also indicated by the ranks for CBCT measurements on cross-sectional slices of 0.4 mm. 27 negative ranks (CBCT-gold standard difference < CCD-gold standard difference), 13 positive ranks (CCD-GS < CBCT-GS differences) and 1 tie reveal that 63% of the measurements were closer to the gold standard using cross-sectional CBCT images and only 33% were closer to the gold standard using CCD images. Figures 7.3 and 7.4 are graphic representations of the exact and absolute differences from the gold standards. Table 7.3 gives an overview of descriptive statistics for the three methods.

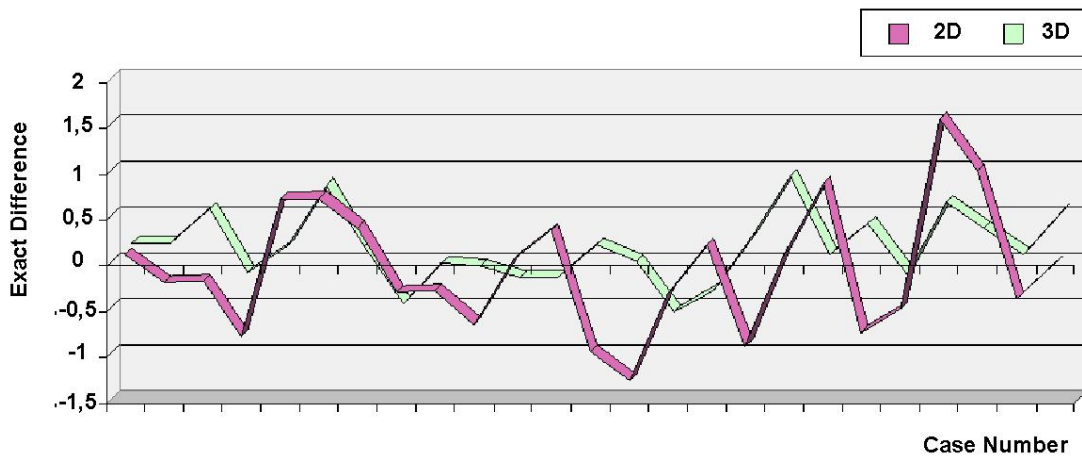


Figure 7.3: Line chart derived from the measurement data. The lines represent the exact difference from the gold standard of the bone level measurements on both 3D cross-sectional CBCT slices and 2D CCD, allowing visualization of over- and underestimations and measurement deviations.

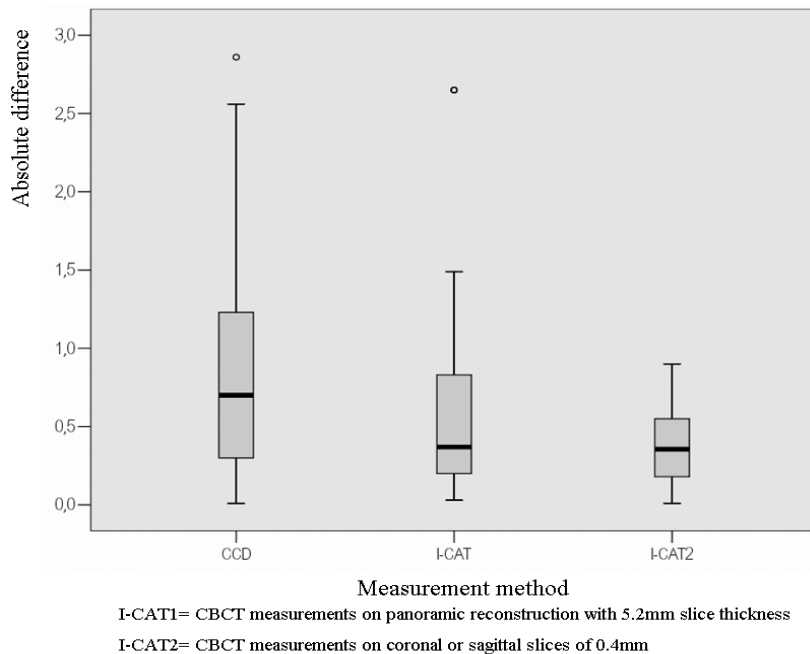


Figure 7.4: Box plots of absolute differences between the gold standard bone level measurements and the observer measurements on different modalities. The chart shows median (black line), interquartile range (boxes) and extreme values. The values of i-CAT2 clearly show the least deviation. (i-CAT1 = CBCT measurements on panoramic reconstruction with 5.2 mm slice thickness, i-CAT2 = CBCT measurements on coronal or sagittal slices of 0.4 mm)

Deviations for intraoral radiography ranged from 0.01 to 1.65 mm, for CBCT panoramic measurements deviations ranged from 0.03 to 1.69 mm and for CBCT cross-sectional measurements they ranged from 0.04 to 0.9 mm. The latter are all under 1 mm deviation and 80% of them under 0.5 mm. For CCD, deviations were over 1 mm in 13% of the cases and less than 0.5 mm in 63% of the sites. Over- and underestimations were both 50% for CCD, with a mean of 0.56mm for the overestimations and 0.55 mm for the underestimations (see Table 7.3). Over- and underestimations on the CBCT panoramic image had the same ratio with a mean of 0.47 mm. A tendency to overestimate (63%, with a mean of 0.34 mm) was seen compared to the underestimations (37%, with a mean of 0.24 mm) for cross-sectional measurements.

The quality rating yielded a significantly better outcome for the intraoral radiographic images regarding lamina dura, contrast and bone quality (see Figure 7.5).

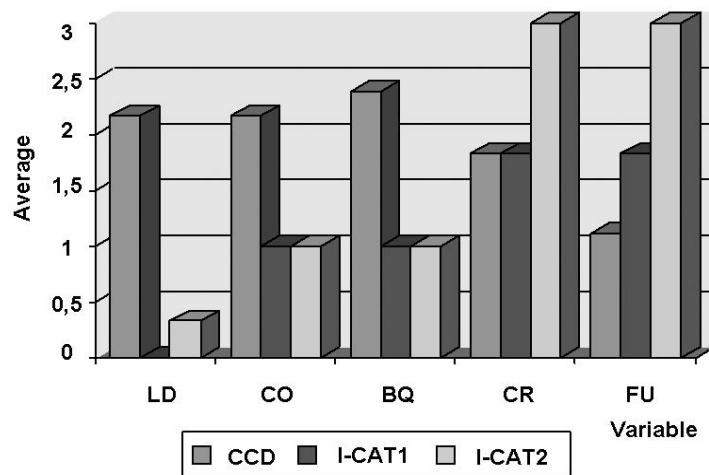


Figure 7.5: Quality assessment: variable comparison for the CCD ratings and the two CBCT ratings. The lamina dura (LD) were well delineated on the CCD images and (almost) not visible on CBCT. CCD also scored better for the variable contrast (CO) and bone quality (BQ) but only periodontal craters (CR) and furcation involvements (FU) were better visualized on CBCT cross-sectional slices (i-CAT2) compared to CCD or CBCT panoramic reconstruction images of 5.2 mm (i-CAT1).

Crater and furcations visibility were not scored differently for CCD and the CBCT panoramic image. However, when using the CBCT cross-sectional slices, the morphological descriptions of the periodontal defects were more clearly depicted by using CBCT ($p=0.014$). Further exploration of these findings was tested in Part 2 of this article.

Part 2: craters and furcations

For both the crater and the furcation variable, a significant difference was found with the Kruskal-Wallis test between the observations on the 2D intraoral images, the CBCT slices and the gold standard (respectively $p=0.008$ and $p=0.017$). When using the Mann-Whitney test to determine which one is significantly different from the gold standard, we found for that both variables CCD classifications of infra-bony defects are inferior when compared to CBCT assessment ($p=0.04$ for crater and $p=0.036$ for furcation involvements). On the intraoral digital images, 29% of the craters and 44% of the furcation defects were not detected and only 29% and 20% of the variables, respectively, were correctly classified. On the CBCT images however, both defects showed a 100% detectability, while 91% of the craters and 100% of the furcation involvements were correctly classified. Also, on intraoral images, it was not possible to differentiate vestibular from oral furcation involvements.

DISCUSSION

Many investigations of the recent cone beam CT technology have validated its usefulness for several diagnostic purposes like implant planning or orthodontics (Maki et al 2003, Guerrero et al 2006). However, limited studies have been reported on the advantages of CBCT for periodontal diagnosis (Guerrero et al 2006, Misch et al 2006, Vandenberghe et al 2007^{a,b}). The present results demonstrate an equal accuracy of periodontal bone level measurements using intraoral 2D digital CCD images (mean error of 0.56 mm) or using a panoramic reconstruction image with 5.2 mm slice thickness of 3D CBCT data (mean error of 0.47 mm). This panoramic reconstruction provides the user with an overall view and allows quick assessment of the periodontal bone. The slice thickness was set on the default setting of 5.2 mm, large enough to visualize all teeth with their fiducials on one reconstruction. Quality rating on both 2D and 3D images shows a clearly positive outcome for CBCT cross-sectional slices when rating crater and furcation involvement evaluation. The delineation of lamina dura, bone quality and contrast rating remains better for the digital intraoral CCD images, which contain a higher resolution compared to CBCT. These findings are comparable to similar studies. Misch et al (2006) found no significant difference in bone level measurements using periapical F-speed films

(mean error of 0.27 mm) or cross-sectional CBCT slices (mean error of 0.41 mm). The present study therefore based the current comparison on digital image data sets in 2D and 3D. While the use of digital intraoral radiography has not been found to be superior to conventional radiography for periodontal linear measures (Pecoraro et al 2005), it cannot be overlooked since it offers at least two essential benefits such as radiation dose reduction and image analysis for improved bone diagnostics (Jeffcoat & Reddy 2000, van der Stelt 2000, Cury et al 2004). A digital CCD system was therefore used for comparison instead of conventional film. With regard to the first benefit, we attempted to reduce the intraoral radiographic dose as much as possible while keeping full diagnostic capabilities. The method and exposure settings used in the present study have been tested and validated in a previous report (Vandenberghe et al 2007^a). The mean error of the measurements on intraoral CCD images in our results differs slightly from the 0.27 mm deviation found by Misch et al (2006) on conventional film. This deviation could be related to the different methodology used and the sample size of infrabony defect measurements.

Even though the results in this study showed a similar outcome for bone level assessment using both imaging modalities, a conclusion based on CBCT panoramic reconstruction images of 5.2 mm, would not allow complete exploitation of the acquired 3D CBCT data. Therefore, the selected sites were measured again on the 3D CBCT data, but this time on coronal or sagittal images of 0.4 mm through the specific fiducials. This, however, did reveal a better assessment of periodontal bone levels on CBCT cross-sectional slices (mean underestimation of 0.29 mm) than on intraoral CCD images (mean error of 0.56 mm). These findings differ from Misch et al (2006) which could be due to the different CBCT protocol. In contrast to a reconstruction slice of 1mm thickness used in the latter study, the measurements in this present study were done on images of 0.4 mm slice thickness. However, more research, including outcome assessment of various exposure and reformatting protocols and evaluation of the diagnostic validity during clinical follow-up, is required for proper justification of various CBCT applications in dentomaxillofacial radiology. Deviations from the gold standard were only between 0.04 and 0.9 mm for the cross-sectional slices. When defining accuracy in terms of clinical measurement, a certain discrepancy between actual bone level and estimated bone level on radiographs has to be considered as clinically acceptable. Small or big errors in locating the CEJ and

the alveolar crest can respectively lead to over- and underestimation of disease prevalence (Brägger 2005). Considering that a 0.5 mm discrepancy can be seen clinically (Mol 2004, Brägger 2005), 2D CCD is accurate enough in 63% of the measures and 3D CBCT in 80%. A 1 mm discrepancy even leads to 100% accuracy for CBCT in contrary to 87% for CCD.

The above measurements of bone levels included crater depth and furcation measurements from the CEJ or specific fiducials. These data do not provide enough information on the 3D defect nature, which can be crucial to prognosis and treatment planning of periodontally affected teeth. Infrabony defects are the main cause of tooth loosening and loss and are often not addressed in research regarding the validation of radiographic modalities for periodontal diagnosis (Fuhrmann et al 1997, Müller & Eger 1999, Tugnait et al 2000, Deas et al 2006, Guerrero et al 2006, Misch et al 2006, Vandenberghe et al 2007^{a,b}). For these reasons and because of the favourable results for evaluation of infrabony defects on CBCT images seen in the quality rating, a further exploration of this research was conducted to evaluate classification of those defects using both 2D and 3D modalities. After comparing defect classifications to the gold standards, the results show a better depiction of crater and furcation involvements on CBCT than on intraoral digital images. Also, vestibular and oral bone defects, as well as maxillary trifurcations were easily assessed by CBCT images in contrast to a problematic or even impossible evaluation on CCD images. Craters and furcation involvements were all detectable (100%) on CBCT data, while only 71% of the crater defects and 56% of the furcation involvements were identified on the intraoral CCD images. Misch et al (2006) found similar results, showing 100% detection of the artificially created infrabony defects with CBCT and only 67% on intraoral film. Fuhrmann et al (1997) found that only 21% of the artificial furcation involvements were identified on dental radiographs and 100% through high resolution CT.

In the present study, we were able to confirm our hypothesis that CBCT would allow accurate assessment of bone levels and a better description of infra-bony defects than intraoral CCD images. The results show a more precise measurement deviation from the gold standard using CBCT cross-sectional slices. This finding indicated that the current CBCT system may become more influential in the diagnosis of periodontal diseases. When compared with CBCT, digital intraoral radiography

remains a high resolution but 2D imaging technique, thus preventing visualization of the entire periodontal defect. For instance, our observers were not able to distinguish vestibular from oral bony defects. The maxillary trifurcations could hardly be detected or interpreted. However, because of the higher resolution of intraoral radiography, some diagnostic parameters such as bone quality evaluation remain inferior for CBCT. Also, since the radiation dose of CBCT has been reported up to 15 times less than conventional CT (Scarfe et al 2006), only 4 to 15 times the dose of standard panoramic image (Ludlow et al 2006) or only the dose of a film based full mouth radiographic examination (FMX) (Scarfe et al 2006), there is growing concern of over-consumption of CBCT and its radiation safety. Furthermore, Ludlow et al (2006) reported dose reduction when using smaller FOV examinations. In our opinion, the use of CBCT should still be carefully justified (diagnostic benefit and risk are balanced), if optimized exposure protocols (following the ALARA (as low as reasonably achievable) principle) are considered. This can be guaranteed if the image acquisition and further interpretation are performed by specialists in this field. In the current study, a low-dose protocol of CBCT (only 23.87 mAs and 0.4 mm voxel size) was used. More studies in the future with a large sample size will determine ideal exposure settings that optimize the image quality and lower the radiation exposure further.

Considering the several advantages, limitations and risks of both modalities; we would like to suggest that the currently tested model of CBCT should only be used for relatively more complex periodontal treatment planning, such as prognostic planning and surgery of complex periodontal defects and potential use of dental implants. Given the limited number of publications on this subject, more research using a large sample-size for periodontal bone level assessment and clinical studies with perioperative check-up as a gold standard for the bone defects should be conducted. This could further expand the applicability of CBCT in periodontal diagnosis.

In conclusion, CBCT images allowed measurements of periodontal linear and non-linear bone levels on panoramic reconstruction images of 5.2 mm slice thickness that were comparable with intraoral digital radiography. Measurements on cross-sectional slices of 0.4 mm demonstrated a more accurate assessment, which is due to the inherent 3D character of the CBCT data and absence of overlapping

structures. CBCT showed more potential in the morphological description of periodontal bone crater and furcation involvements. However, because of the lower resolution compared to intraoral digital images, details like trabecular pattern were better visualized using intraoral radiography.

CBCT allowed more accurate assessment of bone craters and furcation involvements than digital intraoral radiography. These findings may offer perspectives for further studies in balancing radiation dose and gather information in order to help establishing selection criteria for assessment of periodontal bone loss. These findings may also be used for further research on accurate periodontal diagnosis and treatment planning, especially when surgery is involved.

ACKNOWLEDGMENTS

We would like to thank Roslyn Gorin, M.S., Statistical Application Manager, Department of Computer Sciences, Temple University for her help with the statistical analyses. We would also like to thank Drs. Htin Gyaw and Adnan Saleem, the faculty members at Division of Oral and Maxillofacial Radiology, Temple University School of Dentistry for their assistance in measurements. This manuscript was a finalist in the Research Award Competition at the 16th International Congress of Dentomaxillofacial Radiology, Beijing, China.

Chapter 8:

General discussion and
conclusions

The present thesis determined the accuracy of 2D and 3D imaging techniques in the diagnosis of periodontal diseases. **Part I** investigated the diagnostic yield of digital intraoral radiographic systems for periodontal assessments. **Part II** assessed the accuracy of the newly introduced low-dose 3D CBCT for the same periodontal parameters.

METHODOLOGY

In vitro specimens

For the clinical assessment of radiographic parameters –whether for periodontal diagnosis or other dental applications- research is mostly limited to *in vitro* studies. A good simulation of the *in vivo* situation is therefore required. One of the most important radiographic landmarks for periodontal diagnosis is the alveolar crest depiction which is prone to demineralization or breakdown due to periodontal infections (Lindhe et al 2003). This degree of breakdown is difficult to simulate and we therefore opted to work with naturally occurring periodontal defects. Many studies have used dried human skull samples for investigating different radiographic parameters that may influence periodontal assessments (Borg et al 1997, Kaeppler et al 2000, Gomes-Filho et al 2007, Baksi 2008) but this has one major limitation. Since soft tissues of the orofacial region also influence the primary x-ray beam and therefore the radiographic contrast or grey scale levels (Souza et al 2004), it is desirable to complement dry skull samples with some form of soft tissue simulation. In previous studies, water has often been used as a simulation material (Richards & Webber 1963, White 1977), but given the intraoral radiographic protocol for this research, another equivalent was needed. The custom-made (Sanderink 1987) synthetic material, Mix D, used in this thesis consisted of paraffin wax, polyethylene, magnesiumoxide and titaniumoxide (White 1977) and is a common simulation material for radiographic studies. The paraffin-based material was melted to 180 degrees Celsius and modelled over the upper and lower jaws of the dry skull, including the alveolar crest. Furthermore, radiopaque gutta percha fragments –often used in studies determining radiographic linear measurement accuracy- were glued onto the oral and lingual surfaces of the teeth to use as periodontal measurement landmarks. These fiducials were chosen since the CEJ of dried teeth specimens can

be faded making it less suitable. In addition, the purpose of the research was to investigate diagnostic yields by varying digital radiographic parameters. Therefore, the highest standardization was desirable to obtain reproducible radiographs and assessments (Mol 2004). Still, since dried bone may present slightly different radiographic properties, two cadaver jaws (upper and lower) were selected which had been naturally exposed to periodontal breakdown and contained multiple infrabony defects. Both samples were still covered with their orofacial tissues such as lips, cheeks and tongue and were fixed in a 10% formalin solution. The standardized dry skull with gutta markers and cadaver skull with CEJ fiducials did not show a significant difference in periodontal measurement accuracy at the start of the project and were therefore always considered together as a group of specimens. The excellent inter- and intra-observer reproducibility and minimal measurement deviations described in each chapter confirmed the accuracy of this set-up.

2D Modalities & Assessments

Radiographic reproducibility

For comparison of (digital) radiographic parameters (*see Chapter 2, 3 & 4*), it was even more crucial to obtain reproducible radiographs with identical projection geometry since projection errors largely contribute to observer errors in bone level measurements (Zulqarnain & Almas 1998, Mol 2004). Individual occlusal keys were fabricated onto the intraoral positioning devices. First, a pink modelling wax (Cavex, Haarlem, The Netherlands) was used for the imprints. The baseplates were heated and modelled into cubes to obtain the occlusal keys (Figure 8.1). The radiographic reproducibility was tested after one month by comparing tooth lengths with the baseline radiographs. Repositioning of the teeth in the occlusal keys was inadequate and resulted in deviations, due to the instability of the wax at room temperature and when slightly under pressure. The radiographic set-up was therefore adjusted and a more stable impression material was used, green stent (Green Sticks, Kerr Corporation, Orange, CA, USA). This allowed for accurate projection reproducibility for the whole duration of the project.



Figure 8.1: Occlusal keys for identical radiographic projection geometry: the pink wax on the left proved to be a less stable material than the green stent on the right.

Image analysis

All radiographs in this present thesis were exported into TIFF. This flexible file format allows for lossless compression and is widely accepted for grey scale images (Gürdal et al 2001). It was compatible with the image analysis software used for this project (Emago advanced V.3.5.2, Oral Diagnostic Systems, Amsterdam, The Netherlands) and since file storage was not of any issue, this format was chosen to maintain the grey scale ranges of high resolution radiographic modalities. After calibration, observers viewed the randomly displayed radiographs in sessions of 4 hours during several weeks. Viewing conditions were kept as standardized as possible and image enhancement was not allowed. One could argue that this may have affected the accuracy of measurements with high resolution digital systems. The human eye is only able to distinguish 60 shades of grey at once without additional aids (Künzel et al 2003) while image resolution may also be limited by the display screen contrast, brightness and resolution (Hellén-Halme et al 2008). However, we wanted to keep the assessments as objective as possible given the many parameters to be examined. Especially the influence of exposure time may have been influenced since image enhancement may correct for small over- or under- exposed images. Furthermore, most digital systems perform some kind of pre-processing steps before actual display after acquisition. Still, we chose to investigate the influence of one predefined periodontal filter with the receptor we had different resolution for (Vistascan 12 bit, Dürr Dental GmbH, Bietigheim-Bissingen, Germany). It has been suggested that this filter would allow a better subjective image quality of periodontal ligament space, alveolar crest depiction and bony trabecularization (Yalcinkaya et al 2006).

3D Modalities & Assessments

When making measurements on CBCT data -whether it is for alveolar bone loss or for implant site assessment- it is foremost important to mention that patient positioning is crucial when investigating alveolar bone. When scanning a patient along the occlusal plane, axial slices are obtained parallel this plane, while the reformatted orthogonal cross-sections will be perpendicular to the axial one. Assuming a normal occlusal pattern with normal dental alignment, the sagittal and coronal slice should then be approximately parallel to the central axes of the teeth. This will allow for correct measurements. However, when tilting the scan plane or when certain teeth are abnormally tilted in the dentition, alveolar bone level measurement deviations will increase or decrease because orthogonal reslices are not parallel to the teeth's axes. Figure 8.2 is an example of this phenomenon when a jaw is scanned along the border of the mandibular body in stead of the occlusal plane. Therefore, for part 2 of this thesis, all CBCT scans of the skulls specimens were positioned with their occlusal surfaces aligned parallel to the scan plane.

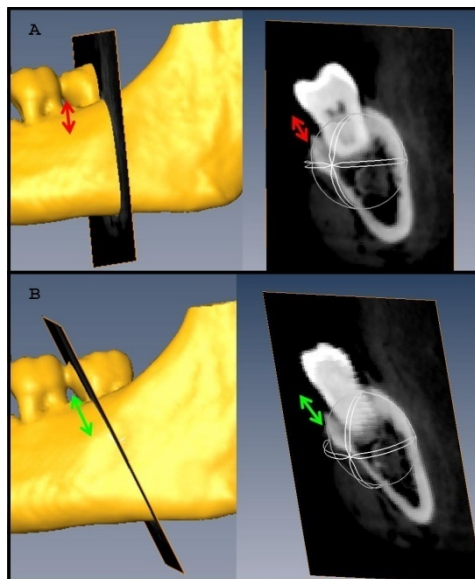


Figure 8.2: (A) CBCT scanning was done by aiming the horizontal positioning line parallel to the mandibular border. Since the molar teeth are inclined, the coronal slice -standard reformatted orthogonally onto the axial- is not parallel to the longitudinal axes of the teeth. (B) By adjusting the coronal slice (oblique reformat), correct measurements, parallel to the teeth's axes, can be done.

The CBCT exposure parameters chosen for this study were 23.87 mAs, 120 kV and 0.4 mm spatial resolution. These parameters are the recommended and therefore most often used clinical protocol balancing exposure and acquired information. A smaller voxel size would allow greater detail, but at the cost of a higher radiation dose. This latter is associated with a higher exposure time which may cause significant motion artefacts. The standard FOV of 13 cm height (and 16 cm diameter)

was used to make the entire jawbones would be imaged. However, in clinical practice, this FOV is too large for the current application since heights of 8 cm may easily contain all necessary periodontal structures of both jawbones (see section Clinical Implications). For the comparison to 2D intraoral diagnosis, we selected only one x-ray detector and x-ray tube for the intraoral protocol. From the first results in **chapter 2**, it was clear that the multipulse or constant potential generator was the most desirable x-ray tube. A solid-state sensor was chosen with an exposure time interval adapted to the tube and receptor type. As found in PART 1 of this research, 2D modalities with inadequate exposure parameters might thus also influence diagnostic tasks and their settings should therefore always first be justified when comparing them to other modalities.

In **chapter 5**, we first compared periodontal measurements with CBCT measurements on 5.2 mm thick panoramic reconstructions. The reason for this is twofold: 1) this new 3D imaging technique requires adequate training for thorough understanding of 3D periodontal anatomy (Carter et al 2008, Horner et al 2009); 2) periodontal assessments of all bony sites around each tooth on 3D cross-sections may be time-consuming and an accurate overview for chair-side evaluation may be a good way to start the radiographic evaluation. The standard slice thickness of 5.2 mm provided us with a good overview, large enough to visualize all the chosen oral or buccal gutta percha fiducials on the dry skull sample. This thickness was then also used for the cadaver jaws. In a way, these panoramic reconstructions rather simulate intraoral radiographs than panoramic images so we expected periodontal measurements to be alike with the intraoral radiographic measurements.

In **chapter 6 and 7**, CBCT assessments were done on 0.4 mm cross-sections to fully exploit the CBCT information. Observers were allowed to scroll through the consecutive slices to determine the exact topography of infrabony defects or to measure periodontal bone levels. For the latter, observer variation may influence the outcome since landmark selection may cause over- or under- estimations of bone levels (Mol 2004). Therefore, calibration sessions were organized to train observers in 3D landmark selection (Figure 8.3) prior to the actual measurements.

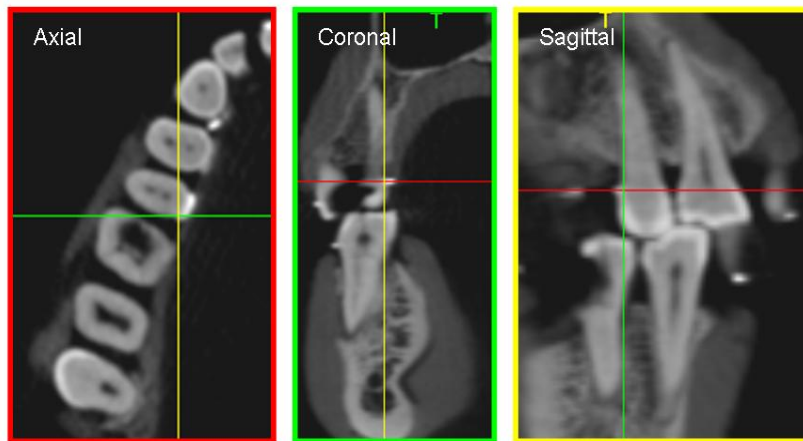


Figure 8.3: CBCT landmark selection for the maxillary second premolar of the dry skull. For the disto-palatal bone level, observers were asked to set the axial slice at the level of the palatal gutta marker. The sagittal and coronal slice were then placed at the respective gutta edges. This then allowed measurements on the coronal or sagittal slice.

2D PERIODONTAL DIAGNOSTIC ACCURACY

Only few studies have assessed the accuracy of digital intraoral radiography for periodontal diagnosis (Borg et al 1997, Müller & Eger 1999, Kaeppler et al 2000, Wolf et al 2001, Pecoraro et al 2005, Deas et al 2006, Jorgenson et al 2007, Li et al 2007) but, more surprisingly, only one study could be found investigating radiographic parameters such as exposure time (Borg et al 1997). In **Part I** of this thesis, it was demonstrated that modern digital systems perform at least similar to conventional film in measuring alveolar bone loss or in the subjective evaluation of periodontal landmarks. However, more importantly, it was found that this accuracy is especially depending on the many radiographic parameters influencing digital imaging. The diagnostic yields of digital receptors are in many ways different than conventional radiography and should be taken into account since not only dose savings may be expected but also overexposure errors may occur when following improper radiographic guidelines.

In **chapter 2**, the influence of x-ray generator was investigated, showing a higher accuracy of HF or DC generators, especially when using low exposure times, although this mostly pertained to PSP receptors. The latter allow using approximately 50% lower exposure times with associated dose savings when using a DC compared to AC generator while maintaining similar accuracy of periodontal measurements. The high sensitivity of modern solid-state sensors still generates adequate radiographic images when using the lower energy levels of these AC generators, thus with no apparent dose savings. The subjective evaluations of periodontal landmarks scored similarly for PSP receptors with high scores when using HF or DC

tubes at 27-60% lower exposure times than AC. But this time also for the CCD receptors and HF or DC combination, these periodontal landmarks scored well at 0-55% the exposure times of AC tubes. Most likely it may thus be concluded that approximately 50% of the exposure times from AC tubes may be used with modern x-ray generators for maintaining radiographic accuracy for periodontal diagnosis with digital receptors. No other studies have investigated this influence but McDavid et al (1982) and Helmrot et al (1994) described dose reductions of respectively 26% and 35-40% when using a DC unit in stead of a conventional AC one, without loss of radiographic contrast. These findings were based on laboratory studies and do not take into account the many clinical diagnostic parameters. Furthermore, the receptor type should also be balanced towards these findings. A last important remark of our study was that periodontal measurement accuracy decreased for CCD sensors when rising exposure time. Since blooming artefacts may deteriorate image quality of CCD sensors at high exposure times (Borg et al 1997, Berkhout et al 2004), we only included exposure times up to 80 ms, in stead of the 160 ms for PSP sensors.

In **chapter 3**, the receptor type was investigated more thoroughly compared to **chapter 2**. The latter did not take into account the specifications of the different receptors used in this research since only three groups were described: film, PSP and CCD. Still, both PSP and CCD sensor groups consisted of receptors with different resolution and one with a dedicated periodontal filter applied to the acquired radiographs. The results of this study did indicate that periodontal measurement accuracy increased when using higher resolution PSP or CCD systems. No other studies have explored the influence of contrast resolution on periodontal diagnosis. Wenzel et al (2008) did not find a significant influence of higher bit depths for the detection of carious lesions, although a classification of caries was used rather than radiographic periodontal measurements. On the contrary, Heo et al (2008) demonstrated improved accuracy of endodontic file length determination when using higher bit depths. Furthermore, the same group (Heo et al 2009) also found that higher bit depths were superior in the detection of subtle radiographic density differences. It thus seem acceptable to conclude that higher bit depths seem to influence diagnostic accuracy when investigating small details like measurements to the nearest 0.1 mm from CEJ to the alveolar crest. This can be confirmed by the results of the subjective evaluation of periodontal landmarks which did not reveal any

significant differences when using higher bit depths. Another finding was that the use of a dedicated periodontal filter significantly improved periodontal measurement accuracy compared to the original images. Although subjective evaluation of the periodontal landmarks did not improve, crater and furcation involvements were scored better on the filtered images. However, other reports have found opposite results. Baksi (2008) found that enhanced PSP images provided better visibility of periodontal structures but resulted in comparable measurement accuracy. However, no details on filter or contrast resolution of the PSP system used were provided. Eickholz et al (1999) and Wolf et al (2001) also did not find any significant differences when using digital enhancement, although they used digitized conventional films with a 10 bit flatbed scanner. Similarly, Li et al (2007) could also not identify any differences for bone level measurements using enhanced images but exposure time was fixed and additional information is lacking. It may well be that some filters may improve accuracy while others do not (Borg 1999). Furthermore, it is likely that the outcome of image filtering depends on the receptor's resolution. Older sensors having 8 bit grey scales may not benefit as much as 12 bit sensors which can inherently display more grey values. Further studies should therefore investigate the influence of image processing, especially in the light of different receptor resolutions.

Finally in **chapter 4**, the influence of tube potential revealed no significant difference when using 63 or 70 kV on periodontal measurement accuracy or subjective ratings. These settings were the only available choices for the specific x-ray tube used, while the remaining x-ray tubes from chapter 1 did not allow kV changes. Still, the results confirmed studies from de Almeida et al (2003) or Kaepler et al (2007) which found no differences between 60 and 70 kV for subjectively rated image quality of four different digital sensors or for the visibility of simulated decayed and peri-implant lesions respectively. Nevertheless, limitations of this study were that only one receptor was used –and no solid state sensor- and lower exposure times should also be investigated.

3D PERIODONTAL DIAGNOSTIC ACCURACY

In **chapter 5**, the periodontal assessments of the skull samples were carried out on 5.2 mm oblique panoramic reconstructions of CBCT scans (simulating a high

resolution panoramic radiography). For the alveolar bone level assessments, measurement deviations were found between 0.13 and 1.67 mm. These were not significantly different from digital intraoral measurements which ranged from 0.19 to 1.66 mm. Furthermore, bone crater and furcation involvements were more clearly depicted using this panoramic reconstructions, but delineation of lamina dura and bony trabecularization were scored better for intraoral radiography.

In **chapter 7**, these measurements on 5.2 mm reconstructed slices were compared with measurements on 0.4mm cross-sections. Deviations for intraoral radiography were 0.01 to 1.65 mm, for 5.2 mm panoramic reconstructions 0.03 to 1.69 mm but for 0.4 mm cross-sections 0.04 mm to 0.9 mm, which revealed a significant difference with the assessments on digital intraoral radiographs. Still, the previous periodontal landmarks scored better for intraoral radiography using a subjective rating scale.

Mengel et al (2005) compared measurements of periodontal defects on periapical radiographs, panoramic films, CT and CBCT in animal and human mandibles to their corresponding histologic specimens. They reported mean height discrepancies of 0.29 mm for intraoral radiographs and 0.16 mm for CBCT. These quite small deviation errors compared to our results are due to the elaborate standardization used in this study: the teeth's occlusal surfaces were ground off for perfect occlusal alignment. Although this does not perfectly simulate the clinical situation, it does reveal the geometric accuracy of CBCT for bone level measurements. This accuracy has been confirmed by Marmulla et al (2005) using an in vitro geometric model to test a head and neck CBCT. They found that variation was 0.13 mm (± 0.09 S.D.) with a maximum deviation of 0.3 mm. Lascala et al (2004) used large measurements of skulls with the same machine and found errors varying from 0.07 mm to 0.2 mm. Misch et al (2006) compared linear measurements of artificially created periodontal defects on CBCT images and periapical radiographs. They report a mean error of 0.41 mm for measurements on CBCT 1 mm cross-sections. Again only a small measurement error was found even though the naturally occurring occlusal planes of dry skulls were used for alignment in the CBCT unit. This indicated that the clinical alignment protocol along the occlusal plane for CBCT acquisition should allow accurate periodontal measurements. This scanning protocol was therefore also used in our in vitro studies. The latter study reports that CBCT

measurements are as accurate (0.41 mean error) as direct measurements using a periodontal probe (0.34 mean error) and as reliable as radiographs (mean error of 0.27) for interproximal areas. Although no difference was found between intraoral radiographs and CBCT, measurements on the latter were done on 1mm cross-sections which limited its accuracy: local bone loss may be very different in these sub-millimetre slices. The same applies for Mol and Balasundaram (2008) who found measurement deviations of 1.16-2.24 mm for assessments on FMX and 0.91-1.95 mm for the ones on CBCT. These authors did also state that an older generation of CBCT was used in this study with limited bit depth. Newer units nowadays have an improved contrast resolution reaching 12 bit or higher. They also mentioned that there was often lack of clarity of the images and that noise may be one of the contributing factors. Above mentioned studies share one important finding: accuracy of alveolar bone level measurements on CBCT images was found as reliable as assessments on intraoral radiographs. In addition, it seems that accuracy may be even higher for CBCT when measurements are done on thin sub-millimetre slices.

In **chapter 6**, the exact topography of infrabony defects was assessed on CBCT sub-millimetre slices (0.4 mm) and intraoral radiography. Observers were allowed to scroll through the data and classify their involvement. The results revealed that CBCT is superior to digital intraoral radiography: 100% of the crater and furcation involvements were detected using CBCT in contrast to respectively 69% and 58%. Misclassifications were as high as 75% on intraoral radiography while for CBCT, all furcations and 88% of the crater involvements were correctly classified. Most other studies did not investigate the exact topographic involvement using CBCT, but only the detectability of infrabony defects (Misch et al 2006, Noujeim et al 2009). In one clinical study from Walter et al (2009), 12 patients with generalized chronic periodontitis were recruited for clinical and radiographic examination. After non-surgical treatment (scaling and rootplaning of pocket ≥ 4 mm) and follow-up, maxillary molars needing periodontal surgery were further examined using CBCT. Treatment recommendations from the clinical and intraoral radiographic exam alone were significantly different than the ones with additional CBCT imaging of the maxillary furcation involvements. The authors concluded that CBCT imaging for maxillary molar's furcation surgery planning is a useful tool and allow a better planning.

For the subjective rating of periodontal landmarks in **Chapter 5 & 7**, our results point out that lamina dura delineation and bony trabecularization is more clearly depicted on intraoral radiographs. No other studies have investigated these ratings on both modalities, but one study from Ozemerich et al (2008) did research the value of CBCT in the detection of the periodontal ligament (PDL) space. Although both intraoral radiographic and CBCT assessments of gaps wider than 200 μm showed a similar accuracy of nearly 100%, gaps smaller than 200 μm were clearly less visible using CBCT. Yet, the slice thickness used in this study was 1 mm which makes these small changes difficult to see. In addition, Liang et al (2009) compared the subjective image quality of five different CBCT units to MSCT and found that image quality was comparable or even superior to MSCT but that the lamina dura delineation, PDL space and trabecularization of bone were the least visible and ratings can vary depending on the CBCT unit. Indeed, CBCT units with new (detector) technology and/or much higher spatial resolution and less noise may provide better results. Figure 8.4 shows axial slices of a cadaver maxillary canine region scanned with 4 different CBCT units and with similar –but not identical- voxel sizes: notice the differences in trabecular pattern depiction.

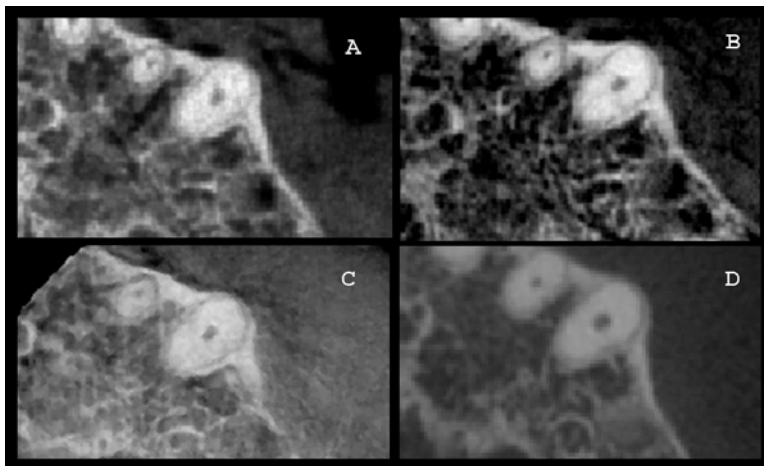


Figure 8.4: Axial slices of an upper cadaver canine region scanned with Scanora 3D (0.2 mm, 85 kV, 8 mA) (A), PaX-Uni3D (0.2 mm, 85 kV, 6 mA)(B), Accuitomo 3D (0.125 mm, 80 kV, 4 mA) (C) and i-CAT next generation (0.25 mm, 120 kV, 5 mA)

FUTURE RESEARCH

Given the multitude of different CBCT models recently introduced, and the many radiographic parameters of CBCT imaging including spatial resolution (voxel-size), energy and exposure (kV and mAs) or FOV, it is important to conduct evidence-based research in order to establish proper diagnostic protocols for periodontal diagnosis, following each radiographer's golden principle: ALARA.

Palomo et al (2008) described radiation dose reductions of CBCT examinations when using the lowest exposure settings. This seems logic, but what is the influence on image quality and does this influence the clinical findings? Therefore, we are currently continuing this research by investigating the influence of 3D exposure parameters on periodontal diagnosis. By lowering kV and mA, by reducing the exposure time and frame count or by varying the voxel size, further dose savings may be anticipated for periodontal diagnosis. Figure 8.5 is an example of the dry skull used in this thesis scanned with different CBCT exposure settings.

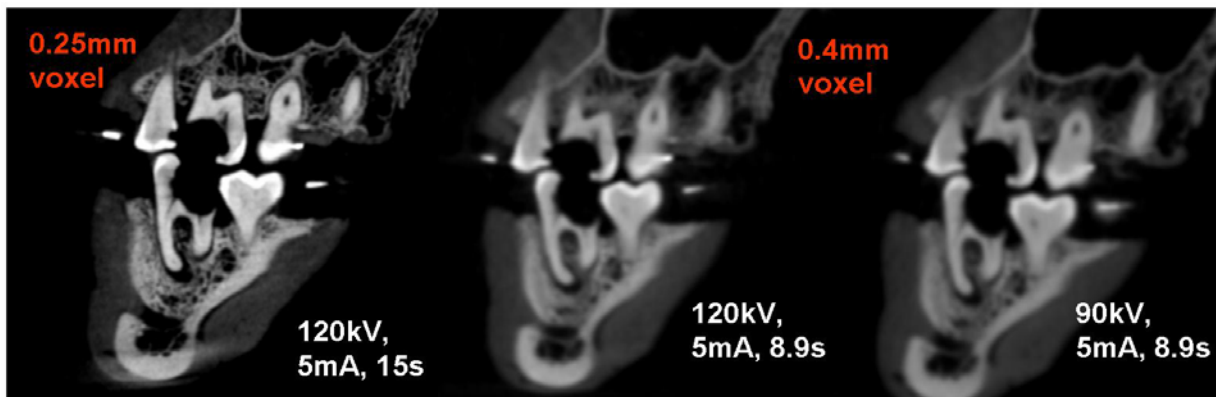


Figure 8.5: Different scanning protocols for the same sagittal slice through the molar region of the standardized dry skull.

But also the other way around one might think to increase the CBCT scan resolution (smaller voxel size, but often at the cost of a higher dose) to further improve measurement accuracy and allow more adequate depiction of periodontal structures (which scored less than intraoral radiography in the present thesis). Furthermore, new detector technology and improved reconstruction algorithms are rapidly changing the available CBCT protocols, allowing increased spatial information while using fewer frames (reduced radiation). However, more clinical studies are needed to investigate the influence of scanning parameters on therapy planning and outcome, and these desired scanning protocols should most importantly also be balanced towards the information required for specific clinical applications (always keeping in mind the ALARA principle). For instance, for image-guided implant treatment using CBCT data, the most crucial factor will be the segmentation accuracy for surface reconstruction of the jaws and accurate fit of the surgical guides. This may require a different scanning protocol than for periodontal bone loss status

assessments (linear measurement accuracy), which may not need the highest spatial resolution.

CLINICAL IMPLICATIONS & CONCLUSIONS

From the present thesis it can be concluded that many radiographic parameters indeed affect the accuracy of 2D or 3D periodontal diagnosis. With the advent of low dose 3D imaging it is outermost important to establish proper intraoral radiographic protocols and revisit current guidelines. In **part I**, dose savings up to 50% can be anticipated for periodontal assessments when using modern x-ray generators in combination with high resolution digital intraoral sensors. This is important since the summed radiation dose of current radiographic diagnostic images for periodontal diagnosis –whether an FMX or a panoramic radiograph supplemented with local periapical radiographs- may easily approach the dose of CBCT examinations (Ludlow et al 2008, Roberts et al 2008). In **part II** of this thesis, it has been demonstrated that periodontal assessments, especially the topographic determination of infrabony defects, were more accurate on CBCT sub-millimetre cross-sections. Nonetheless, certain periodontal landmarks may still better be depicted on intraoral radiographs. Although CBCT has only been available for a few years, its periodontal applications are becoming evident. More evidence-based research is needed for 3D imaging given the many variables of the radiographic protocol before making drastic recommendations. The current findings thus do not indicate to routinely use CBCT for periodontal patients, but rather show that CBCT may be advantageous in certain complex cases requiring more information for treatment planning. Three-dimensional imaging will likely improve patient understanding of their disease, enhance diagnosis and assist clinicians in refining their treatment methods.

In **Chapter 4**, the influence of tube potential on periodontal diagnosis was investigated using an intraoral PSP receptor and a high frequency multipulse x-ray tube. It was concluded that no significant difference was found between these two settings for the radiographic assessments of periodontal bone levels and subjective ratings of periodontal landmarks. However, dose calculations were missing and are therefore included in this appendix. In Figure A.1, the median accuracy and skin doses are plotted by exposure time, revealing similar periodontal measurement accuracy but slightly higher measured skin doses for the 70 kV setting.

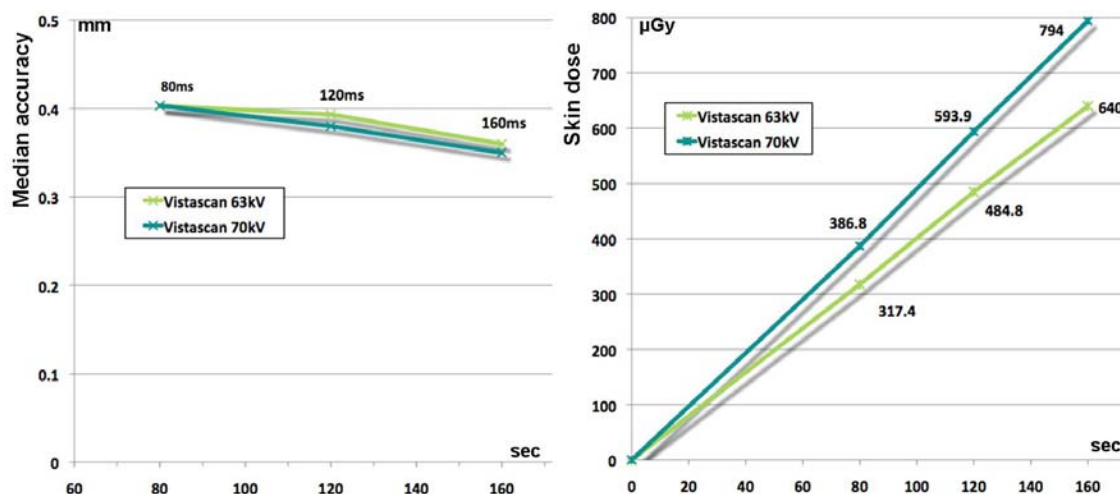


Figure A.1: Median accuracy (left) and skin doses (right) plotted by exposure time for the two different kV (63 and 70 kV) settings.

When considering 0.5 mm an acceptable measurement deviation for periodontal diagnosis, median accuracies for the three mAs settings and both tube voltages were found to be within this limit (see Table A.1). This would allow at least (no lower exposure times were used) 50% lower exposure times than the 160 ms, and approximately 18% dose savings when using the 63 kV setting.

Table A.1: Skin doses for the two kV settings with periodontal measurement accuracy at 0.5 mm. The median accuracy for the different exposure times were all under this threshold value which would allow using 50% lower skin doses (160 vs 80ms). Similarly, 63kV would allow approximately 18% of dose savings while maintaining the same accuracy for periodontal bone level measurements.

Accuracy	Receptor	70 kV		63 kV		Dose Saving
		mAs	µGy	mAs	µGy	
0,5 mm	PSP	0.64	386.8	0.64	317.4	17.9%
		0.96	593.9	0.96	484.8	18.4%
		1.28	794	1.28	640	19.4%
		51.3%		50.4%		18.6%

All subjective ratings scored similar to the periodontal bone level measurements, except for the variable trabecular bone depiction (see Table A.2). When considering a threshold rating of 2 (=medium visibility), this variable needed a higher exposure time (and associated higher skin dose) using the 70 kV setting. Still, given the limited ordinal rating scale, the insignificance found in the statistical analysis and the scores of the other variables it is careful to assume the same 18% dose savings when using 63 kV compared to 70 kV when using the specific PSP and x-ray tube combination.

Table A.2: Skin doses for the two kV settings with a threshold rating of 2 (=medium visibility) for the subjective ratings of lamina dura (LD), trabecular pattern depiction (BQ), contrast perception (C), crater (CR) and furcation (FU) visibility. All variables scored alike using the same threshold skin doses for both kV settings, except the variable BQ.

Variable	70 kV		63 kV		Dose savings
	mAs	µGy	mAs	µGy	
LD	0.64	386.8	0.64	317.4	17.9%
BQ	0.96	593.9	0.64	317.4	46.5%
C	1.28	794	1.28	640	19.4%
CR	0.64	386.8	0.64	317.4	17.9%
FU	0.96	593.9	0.96	484.8	18.4%

Summary

Samenvatting

Summary

Over 50% of the entire population has periodontal (gum) disease. It is one of the leading causes of tooth loss in the elderly population and has a high association with certain systemic diseases. For affected patients, a periodontal status is evaluated every two years for follow-up of the two main periodontal manifestations, bone loss and soft tissue attachment loss. Until now, diagnosis of this status consists of two-dimensional intraoral radiographs for bone loss assessments and clinical probing of attachment loss (soft tissue loss). Both methods have their limitations and are therefore complementary. For instance, projection radiographs are two-dimensional for evaluation of a three-dimensionally expanding disease: local bone loss between neighbouring teeth can namely appear like irregular crater-like destruction, followed by spreading into the bifurcation area of the roots (where the root divides into two or more roots). Surprisingly, current diagnostic approaches have not changed over the past twenty years. Digitalization of intraoral radiography has brought several advantages over conventional film radiography but has only limitedly been explored for periodontal diagnosis. Furthermore, low dose 3D CBCT has been introduced for dental applications which may bring new potential in the detection of periodontal diseases.

Considering the lack of scientific validation and the rising use of 2D digital intraoral radiography as well as 3D CBCT imaging, the overall aim of the present thesis was to compare the accuracy of current 2D digital and 3D imaging techniques for periodontal diagnosis. The first sub-objective was therefore to investigate the diagnostic yield of digital intraoral radiography for periodontal diagnosis and demonstrate an associated improvement in imaging accuracy and quality at reduced radiation exposure compared to conventional film imaging (**Part I**). The second sub-objective was to determine the accuracy of periodontal diagnosis using the recently introduced low-dose 3D CBCT imaging technique (**Part II**).

For 2D imaging, the accuracy of periodontal diagnosis using digital receptors has been found at least as good as conventional films (**Chapter 2 & 3**), although their diagnostic yields are very different and lower doses may be recommended. HF or DC x-ray generators allow more accurate periodontal measurements and reducing exposure times up to 50% compared to older x-ray generators (**Chapter 2**). However,

this is especially depending on the receptor type: for solid-state sensors these dose saving are less apparent given their much higher sensitivity than PSP receptors. Further investigation of the receptor type (**Chapter 3**) revealed that high resolution digital receptors and/or dedicated periodontal filtering may improve periodontal accuracy and allow additional dose savings. Finally, no significant difference was found when using two tube potentials (63 and 70 kV), thus further helping in possible dose savings (**Chapter 4**).

The same periodontal assessments were then done using CBCT imaging. Bone level measurements on CBCT panoramic reconstructions of 5.2 mm thickness were found to be as accurate as 2D digital intraoral radiographs (**Chapter 5**). However, assessments on 0.4 mm cross-sectional CBCT slices were more accurate than 2D (**Chapter 7**). The subjective rating of certain periodontal landmarks like the lamina dura or bony trabecularization did score better on 2D, but most importantly, the bony 3D architecture and topographic classification of infrabony craters and furcation involvements was much more accurate using 3D CBCT (**Chapter 6**). Although more clinical research is needed to confirm these findings, and to determine CBCT's diagnostic yield to establish guidelines, it did reveal that low dose 3D examinations may be beneficial in certain complex cases of periodontal diseases.

Samenvatting

Meer dan de helft van de bevolking lijdt aan parodontitis. Het is meteen een van de belangrijkste redenen voor tandverlies rekening houdend met een vergrijzing van de bevolking en een hoge associatie met verschillende systemische ziektes. Een parodontale status wordt bij parodontitis patiënten om de twee jaar genomen om zowel bot- als zacht weefsel- verlies na te gaan. Tot op heden bestaat deze status uit het nemen van een reeks tweedimensionale intraorale radiografieën voor het opsporen van botverlies en een klinische sondering voor het nagaan van aanhechtingsverlies. Beide methoden hebben een aantal tekortkomingen, dus worden ze complementair gebruikt. Zo is een intraorale radiografie slechts een 2D projectie van het botverlies terwijl dit laatste een 3D dynamisch gebeuren is: lokaal botverlies tussen de tanden kan namelijk een kratervorming patroon vertonen met spreiding naar de bifurcatie regio (splitsing) van de wortels. Echter, de huidige diagnostische technieken hebben de laatste twintig jaar maar weinig verandering ondergaan. Digitalisatie van intraorale radiografie heeft verschillende voordelen met zich meegebracht vergeleken met conventionele film ontwikkeling, maar is slechts zeer beperkt onderzocht geworden in het kader van parodontale diagnose. Bovendien werden recent lage dosis 3D technieken (CBCT) in de tandheelkunde geïntroduceerd, die mogelijks kunnen bijdragen tot een betere parodontale diagnostiek.

Aangezien de beperkte wetenschappelijke validatie en het groeiende gebruik van 2D digitale intraoral radiografie en 3D CBCT beeldvorming, was het globale doel van dit onderzoeksproject de 2D digitale en recente 3D beeldvormingsmodaliteiten te vergelijken voor de detectie van parodontaal botverlies. De eerste subdoelstelling was daarom het onderzoeken van de diagnostische uitkomst van digitale intraorale radiografie voor parodontale diagnose en het aantonen van een geassocieerde verbetering in beeldkwaliteit en accuraatheid aan lagere dosissen vergeleken met film **(Deel I)**. De tweede subdoelstelling was het bepalen van de nauwkeurigheid van parodontale diagnose aan de hand van de recent geïntroduceerde lage dosis 3D CBCT **(Deel II)**.

Voor 2D beeldvorming werd de accuraatheid voor parodontale diagnose aan de hand van digitale receptoren minstens even goed bevonden dan conventionele

films (**Hoofdstuk 2 & 3**), hoewel hun diagnostische uitkomsten verschillen en veel lagere belichtingstijden kunnen aangeraden worden. Hoog frequente wisselstroom of gelijkstroom röntgenbuizen laten meer nauwkeurige parodontale botmetingen toe aan lagere belichtingstijden (tot 50%) vergeleken met oudere röntgenbuizen (**Hoofdstuk 2**). Doch, dit is vooral afhankelijk van het receptor type: voor solid-state sensoren zijn deze lagere dosissen minder beduidend aangezien ze veel gevoeliger zijn dan PSP receptoren. Verder onderzoek naar het receptor type (**Hoofdstuk 3**) toonde aan dat hoge resolutie digitale receptoren en/of parodontale filters (beeldmanipulatie) de accuraatheid van parodontale metingen kon verbeteren en additionele dosis verlagingen kon teweegbrengen. Als laatste parameter werd er geen significant verschil gevonden wanneer twee verschillen buisspanningen aangewend werden (63 and 70 kV), wat dus verder zou kunnen bijdragen tot de dosisverlaging voor parodontale diagnose (**Hoofdstuk 4**).

Dezelfde parodontale metingen werden vervolgens uitgevoerd aan de hand van CBCT beeldvorming. Botmetingen op CBCT panoramische reconstructies van 5.2 mm dikte werden even accuraat bevonden dan op 2D digitale intraorale radiografieën (**Hoofdstuk 5**), maar metingen op CBCT 0.4 mm cross-secties waren toch nauwkeuriger dan op 2D (**Hoofdstuk 7**). De subjectieve scores van bepaalde parodontale structuren zoals de lamina dura of bot-trabecularizatie waren beter voor 2D intraorale radiografie. Belangrijk was dat de 3D bot architectuur en topografische classificatie van parodontale kraters en furcaties correcter werd gediagnosticeerd op basis van 3D CBCT (**Hoofdstuk 6**). Hoewel meer klinisch onderzoek vereist is om deze bevindingen te versterken, en om de diagnostische uitkomst van CBCT te onderzoeken voor de verschillende toepassingen, toonde dit onderzoek aan dat lage dosis 3D onderzoeken voordelig kunnen zijn in bepaalde complexe gevallen van parodontitis.

References

- Afifi AA, Clark V. Computer aided multivariate analysis, 2nd edition. Lifetime learning Belmont, CA, 1984.
- Almog DM, LaMar J, LaMar FR, LaMar F. Cone beam computerized tomography-based dental imaging for implant planning and surgical guidance, Part 1: Single implant in the mandibular molar region. *J Oral Implantol* 2006;32:77-82.
- Analoui M^a. Radiographic image enhancement. Part I: spatial domain techniques. *Dentomaxillofac Radiol* 2001;30:1-9
- Analoui M^b. Radiographic image enhancement. Part II: transform domain techniques. *Dentomaxillofac Radiol* 2001;30:65-77
- Arai Y, Tammissalo E, Iwai K, Hashimoto K, Shinoda K. Development of a compact computed tomographic apparatus for dental use. *Dentomaxillofac Radiol* 1999;28:245-248.
- Araki K, Endo A, Okano T. An objective comparison of four digital intra-oral radiographic systems: sensitometric properties and resolution. *Dentomaxillofac Radiol* 2000;29:76-80.
- Armitage GC; Research, Science and Therapy Committee of the American Academy of Periodontology. Diagnosis of periodontal diseases. *J Periodontol* 2003;74:1237-1247.
- Baksi BG. Measurement accuracy and perceived quality of imaging systems for the evaluation of periodontal structures. *Odontology* 2008;96:55-60.
- Benn DK. A review of the reliability of radiographic measurements in estimating alveolar bone changes. *J Clin Periodontol* 1990;17:14-21.
- Berkhout WE, Beuger DA, Sanderink GC, van der Stelt PF. The dynamic range of digital radiographic systems: dose reduction or risk of overexposure? *Dentomaxillofac Radiol* 2004;33:1-5.
- Bhaskaran V, Qualtrough AJ, Rushton VE, Worthington HV, Horner K. A laboratory comparison of three imaging systems for image quality and radiation exposure characteristics. *Int Endod J* 2005;38:645-652.
- Borg E (1999) Some characteristics of solid-state and photo-stimulable phosphor detectors for intra-oral radiography. *Swed Dent J* 1999;139:1-67.

- Borg E, Attaelmanan A, Gröndahl HG. Subjective image quality of solid-state and photostimulable storage phosphor systems for digital intra-oral radiography. *Dentomaxillofac Radiol* 2000;29:70-75.
- Borg E, Gröndahl HG. On the dynamic range of different X-ray photon detectors in intra-oral radiography. A comparison of image quality in film, charge-coupled device and storage phosphor systems. *Dentomaxillofac Radiol* 1996;25:82-88.
- Borg E, Gröndahl K, Gröndahl HG. Marginal bone level buccal to mandibular molars in digital radiographs from charge-coupled device and storage phosphor systems. An in vitro study. *J Clin Periodontol* 1997;24:306-312.
- Brägger U. Radiographic parameters: biological significance and clinical use. *Periodontol 2000* 2005;39:73-90.
- Brettle DS, Workman A, Ellwood RP, Launders JH, Horner K, Davies RM. The imaging performance of a storage phosphor system for dental radiography. *Br J Radiol* 1996;69:256-261.
- Brown LJ, Löe H. Prevalence, extent, severity and progression of periodontal disease. *Periodontol 2000* 1993;2:57-71.
- Burt B, Research, Science and Therapy Committee of the American Academy of Periodontology. Position paper: epidemiology of periodontal diseases. *JPeriodontol* 2005;76:1406-1419.
- Carter L, Farman AG, Geist J, Scarfe WC, Angelopoulos C, Nair MK, Hildebolt CF, Tyndall D, Shroud M; American Academy of Oral and Maxillofacial Radiology. American Academy of Oral and Maxillofacial Radiology executive opinion statement on performing and interpreting diagnostic cone beam computed tomography. *Oral Surg Oral Med Oral Pathol Oral Radiol Endod* 2008;106:561-562.
- Cury PR, Araujo NS, Bowie J, Sallum EA, Jeffcoat MK. Comparison between subtraction radiography and conventional radiographic interpretation during long-term evaluation of periodontal therapy in Class II furcation defects. *J Periodontol* 2004;75:1145-1149.
- Curry TS, Dowdey JE, Murry RC. Christensen's physics of diagnostic radiology. 4th edn. Lea and Febiger, Philadelphia, 1990, pp 36-60.
- de Almeida SM, de Oliveira AE, Ferreira RI, Bóscolo FN. Image quality in digital radiographic systems. *Braz Dent J* 2003;14:136-141.

- Deas DE, Moritz AJ, Mealey BL, McDonnell HT, Powell CA. Clinical reliability of the “furcation arrow” as a diagnostic marker. *J Periodontol* 2006;77:1436-1441.
- Dreiseidler T, Mischkowski RA, Neugebauer J, Ritter L, Zöller JE. Comparison of cone-beam imaging with orthopantomography and computerized tomography for assessment in presurgical implant dentistry. *Int J Oral Maxillofac Implants* 2009;24:216-225.
- Eickholz P, Hausmann E. Accuracy of radiographic assessment of interproximal bone loss in intrabony defects using linear measurements. *Eur J Oral Sci* 2000;108:70-73.
- Eickholz P, Riess T, Lenhard M, Hassfeld S, Staehle HJ. Digital radiography of interproximal bone loss; validity of different filters. *J Clin Periodontol* 1999;26:294-300.
- Eley BM, Cox SW. Advances in periodontal diagnosis. 3. Assessing potential biomarkers of periodontal disease activity. *Br Dent J* 1998;184:109-113.
- European Commission. The European guidelines on radiation protection in dental radiology. The safe use of radiographs in dental practices. Radiation protection 136. Brussels. 2004.
- Farman AG, Farman TT. A comparison of 18 different x-ray detectors currently used in dentistry. *Oral Surg Oral Med Oral Pathol Oral Radiol Endod* 2005;99:485-489.
- Farman AG, Levato CM, Gane D, Scarfe WC. In practice: how going digital will affect the dental office. *J Am Dent Assoc* 2008;139:S14-19.
- Frederiksen NL. Health physics. In: White SC, Pharoah MJ, editors. *Oral Radiology. Principles and Interpretation*. Mosby, St Louis, 2004, pp. 265-277.
- Fuhrmann RA, Bucker A, Diedrich PR. Assessment of alveolar bone loss with high resolution computed tomography. *J Periodontal Res* 1995;30:258-263.
- Fuhrmann RA, Bucker A, Diedrich PR. Furcation involvement: comparison of dental radiographs and HR-CT-slices in human specimens. *J Periodontal Res* 1997;32:409-418.
- Gahleitner H, Watzek G, Imhof H. Dental CT: imaging technique, anatomy, and pathologic conditions of the jaws. *Eur Radiol* 2003;13:366-367.
- Gibbs SJ. Effective dose equivalent and effective dose: comparison for common projections in oral and maxillofacial radiology. *Oral Surg Oral Med Oral Pathol Oral Radiol Endod* 2000;90:538-545.

- Goldman LW. Principles of CT: Multislice CT. *J Nucl Med Technol* 2008;36:57-68.
- Gomes-Filho IS, Sarmiento VA, de Castro MS, da Costa MP, da Cruz SS, Trindade SC, de Freitas CO, de Santana Passos J. Radiographic features of periodontal bone defects: evaluation of digitized images. *Dentomaxillofac Radiol* 2007;36:257-262.
- Goodson JM. Diagnosis of periodontitis by physical measurement: interpretation from episodic disease hypothesis. *J Periodontol* 1992;63:373-382.
- Goshima T, Goshima Y, Scarfe WC, Farman AG. Sensitometric response of the Sens-A-Ray, a charge-coupled device, to changes in beam energy. *Dentomaxillofac Radiol* 1996;25:17-18.
- Greenstein G, Polson A, Iker H, Meitner S. Associations between crestal lamina dura and periodontal status. *J Periodontol* 1981;52:362-366.
- Guerrero ME, Jacobs R, Loubele M, Schutyser F, Suetens P, van Steenberghe D. State-of-the-art on cone beam CT imaging for preoperative planning of implant placement. *Clin Oral Investig* 2006;10:1-7.
- Gürdal P, Hildebolt CF, Akdeniz BG. The effects of different image file formats and image-analysis software programs on dental radiometric digital evaluations. *Dentomaxillofac Radiol* 2001;30:50-55.
- Hamp SE, Nyman S, Lindhe J. Periodontal treatment of multirrooted teeth. Results after 5 years. *J Clin Periodontol* 1975;2:126-135.
- Hausmann E. Radiographic and digital imaging in periodontal practice. *J Periodontol* 2000;71:497-503.
- Hausmann E, Allen K. Reproducibility of bone height measurements made on serial radiographs. *J Periodontol* 1997;68:839-841.
- Hayakawa Y, Farman AG, Scarfe WC, Kuroyanagi K, Rumack PM, Schick DB. Optimum exposure ranges for computed dental radiography. *Dentomaxillofac Radiol* 1996;25:71-75.
- Hefti AF. Periodontal probing. *Crit Rev Oral Biol Med* 1997;8:336-356.
- Hellén-Halme K, Petersson A, Warfvinge G, Nilsson M. Effect of ambient light and monitor brightness and contrast settings on the detection of approximal caries in digital radiographs: an in vitro study. *Dentomaxillofac Radiol* 2008;37:380-384.

- Helmrot E, Carlsson GA, Eckerdal O. Effects of contrast equalization on energy imparted to the patient: a comparison of two dental generators and two types of intraoral film. *Dentomaxillofac Radiol* 1994;23:83-90.
- Helmrot E, Matscheko G, Carlsson GA, Echerdal O, Ericson S. Image contrast using high frequency and half-wave rectified dental x-ray generators. *Dentomaxillofac Radiol* 1988;17:33-40.
- Hendriksson CH, Stermer EM, Aass AM, Sandvik L, Møystad A. Comparison of the reproducibility of storage phosphor and film bitewings for assessment of alveolar bone loss. *Acta Odontol Scand* 2008;66:380-384.
- Heo MS, Choi DH, Benavides E, Huh KH, Yi WJ, Lee SS, Choi SC. Effect of bit depth and kVp of digital radiography for detection of subtle differences. *Oral Surg Oral Med Oral Pathol Oral Radiol Endod* 2009;108:278-283.
- Heo MS, Han DH, An BM, Huh KH, Yi WJ, Lee SS, Choi SC. Effect of ambient light and bit depth of digital radiograph on observer performance in determination of endodontic file positioning. *Oral Surg Oral Med Oral Pathol Oral Radiol Endod* 2008;105:239-244.
- Horner K, Islam M, Flygare L, Tsiklakis K, Whaites E. Basic principles for use of dental cone beam computed tomography: consensus guidelines of the European Academy of Dental and Maxillofacial Radiology. *Dentomaxillofac Radiol* 2009;38:187-195.
- Jacobs R, Adriansens A, Verstreken K, Suetens P, van Steenberghe D. Predictability of a three-dimensional planning system for oral implant surgery. *Dentomaxillofac Radiol* 1999;28:105-111.
- Jacobs R, Gijbels F. Final report of the minosquare concerted action European commission, EDMIN, Department of Periodontology, KULeuven, Leuven 2000.
- Jeffcoat MK, Reddy MS. Advances in measurements of periodontal bone and attachment loss. *Monogr Oral Sci* 2000;17:56-72.
- Jorgenson T, Masood F, Beckerley JM, Burqin C, Parker DE. Comparison of two imaging modalities: F-speed film and digital images for detection of osseous defects in patients with interdental vertical bone loss. *Dentomaxillofac Radiol* 2007;36:500-505.
- Kaepler G, Dietz K, Herz K, Reinert S. Factors influencing the absorbed dose in intraoral radiography. *Dentomaxillofac Radiol* 2007;36:506-513.

- Kaeppler G, Dietz K, Reinert S. Influence of tube potential setting and dose on the visibility of lesions in intraoral radiography. *Dentomaxillofac Radiol* 2007;36:75-79.
- Kaeppler G, Vogel A, Axmann-Krcmar D. Intra-oral storage phosphor and conventional radiography in the assessment of alveolar bone structures. *Dentomaxillofac Radiol* 2000;29:362-367.
- Karn KW, Shockett HP, Moffitt WC, Gray JL. Topographic classification of deformities of the alveolar process. *J Periodontol* 1984;55:336-340.
- Kashima I. Computed radiography with photostimulable phosphor in oral and maxillofacial radiology. *Oral Surg Oral Med Oral Pathol Oral Radiol Endod* 1995;80:577-598.
- Kassebaum DK, Nummikoski PV, Triplett RG, Langlais RP. Cross-sectional radiography for implant site assessment. *Oral Surg Oral Med Oral Pathol* 1990;70:674-682.
- Khader YS, Albashaireh ZS, Alomari MA. Periodontal diseases and the risk of coronary heart and cerebrovascular diseases: a meta-analysis. *J Periodontol* 2004;75:1046-1053.
- Khocht A, Chang KM. Clinical evaluation of electronic and manual constant force probes. *J Periodontol* 1998; 69:19-25.
- Kimpe T, Tuytschaever T. Increasing the number of gray shades in medical display systems- -how much is enough? *J Digit Imaging* 2007;20:422-432.
- Kitagawa H, Farman AG. Effect of beam energy and filtration on the signal-to-noise ratio of the Dexis intra-oral X-ray detector. *Dentomaxillofac Radiol* 2004;33:21-24.
- Kitagawa H, Scheetz JP, Farman AG. Comparison of complementary metal oxide semiconductor and charge-coupled device intra-oral x-ray detectors using subjective image quality. *Dentomaxillofac Radiol* 2003;32:408-411.
- Klinge B, Petersson A, Maly P. Location of the mandibular canal: comparison of macroscopic findings, conventional radiography, and computed tomography. *Int J Oral Maxillofac Implants* 1989;4:327-332.
- Kobayashi K, Shimoda S, Nakagawa Y, Yamamoto A. Accuracy of measurement in distance using limited cone-beam computerized tomography. *Int J Oral Maxillofac Implants* 2004;19:228-231.
- Künzel A, Scherkowski D, Willers R, Becker J. Visually detectable resolution of intraoral dental films. *Dentomaxillofac Radiol* 2003;32:385-389.

- Langen HJ, Fuhrmann R, Diedrich P, Günther RW. Diagnosis of infra-alveolar bony lesions in the dentate alveolar process with high-resolution computed tomography. Experimental results. *Invest Radiol* 1995;30:421-426.
- Lascalea CA, Panella J, Marques MM. Analysis of the accuracy of linear measurements obtained by cone beam computed tomography (CBCT-NewTom). *Dentomaxillofac Radiol* 2004;33:291-294.
- Li G, Engström PE, Nasström K, Lü ZY, Sanderink G, Welander U. Marginal bone levels measured in film and digital radiographs corrected for attenuation and visual response: an in-vitro study. *Dentomaxillofac Radiol* 2007;36:7-11.
- Liang X, Jacobs R, Hassan B, Li L, Pauwels R, Corpas L, Souza PC, Martens W, Shahbazian M, Alonso A, Lambrichts I. A comparative evaluation of Cone Beam Computed Tomography (CBCT) and Multi-Slice CT (MSCT) Part I. On subjective image quality. *Eur J Radiol* 2009 Apr 30.
- Lim KF, Loh EEM, Hong YH. Intra-oral computed radiography-an in vitro evaluation. *J Dent* 1996;24:359-364.
- Lindh C, Petersson A, Rohlin M. Assessment of the trabecular pattern before endosseous implant treatment: diagnostic outcome of periapical radiography in the mandible. *Oral Surg Oral Med Oral Pathol Oral Radiol Endod* 1996;82:335-343.
- Lindhe J, Lang NP, Karring T (eds). *Clinical Periodontology and Implant Dentistry*. Blackwell Munsgaard, Oxford, 2003.
- Litwiller D. CCD vs CMOS: Facts and Fiction. *Photonics Spectra* 2001;1:154-158.
- Loos B, Nylund K, Claffey N, Egelberg J. Clinical effects of root debridement in molar and non-molar teeth. A 2-year follow-up. *J Clin Periodontol* 1989;16:498-504.
- Ludlow JB, Davies-Ludlow LE, Brooks SL, Howerton WB. Dosimetry of 3 CBCT devices for oral and maxillofacial radiology: CB Mercuray, NewTom 3G and I-CAT. *Dentomaxillofac Radiol* 2006;35:219-226.
- Ludlow JB, Davies-Ludlow LE, White SC. Patient risk related to common dental radiographic examinations: the impact of 2007 International Commission on Radiological Protection recommendations regarding dose calculation. *J Am Dent Assoc* 2008;139:1237-1243.
- Ludlow JB, Platin E, Mol A. Characteristics of Kodak Insight, an F-speed intraoral film. *Oral Surg, Oral Med, Oral Pathol, Oral Radiol Endod* 2001;91:120-129.

- Maki K, Inou N, Takanishi A, Miller AJ. Computer-assisted simulations in orthodontic diagnosis and the application of a new cone beam X-ray computed tomography. *Orthod Craniofac Res* 2003;6 Suppl 1:95-101.
- Manson JD. Lamina dura. *Oral Surg Oral Med Oral Pathol* 1963;16:432-438.
- Marmulla R, Wörtche R, Mühling J, Hassfeld S. Geometric accuracy of the NewTom 9000 Cone Beam CT. *Dentomaxillofac Radiol* 2005;34:28-31.
- McDavid WD, Welander U, Pillai BK, Morris CR. The Intrex—a constant-potential x-ray unit for periapical dental radiography. *Oral Surg, Oral Med Oral Pathol* 1982;53:433-436.
- Mengel R, Candir M, Shiratori K, Flores-de-Jacoby L. Digital volume tomography in the diagnosis of periodontal defects: an in vitro study on native pig and human mandibles. *J Periodontol* 2005;76:665-673.
- Miracle AC, Mukherji SK. Conebeam CT of the head and neck, part 1: physical principles. *AJNR Am J Neuroradiol* 2009;30:1088-1095.
- Misch KA, Yi ES, Sarment DP. Accuracy of cone beam computed tomography for periodontal defect measurements. *J Periodontol* 2006;77:1261-1266.
- Mol A. Image processing tools for dental applications. *Dent Clin North Am* 2000;44:299-318.
- Mol A. Imaging methods in periodontology. *Periodontol 2000* 2004;34:34-48.
- Mol A, Balasundaram A. In vitro cone beam computed tomography imaging of periodontal bone. *Dentomaxillofac Radiol* 2008;37:319-324.
- Mozzo P, Procacci C, Tacconi A, Martini PT, Andreis IA. A new volumetric CT machine for dental imaging based on the cone-beam technique: preliminary results. *Eur Radiol* 1998;8:1558-1564.
- Müller HP, Eger T. Furcation diagnosis. *J Clin Periodontol* 1999; 26: 485-498.
- Müller HP, Eger T, Lange DE. Management of furcation-involved teeth. A retrospective analysis. *J Clin Periodontol* 1995;22:911-917.
- Müller HP, Ulbrich M. Alveolar bone levels in adults as assessed on panoramic radiographs. (I) Prevalence, extent and severity of even and angular bone loss. *Clin Oral Investig* 2005;9:98-104.
- Nyman S, Lindhe J. Examination of patients with periodontal disease. In Lindhe J, Karring T, Lang NP (Ed.), *Clinical periodontology and implant dentistry*, 4th ed, pp403-413, Oxford, Blackwell Munksgaard, 2003.

- Noujeim M, Prihoda T, Langlais R, Nummikoski P. Evaluation of high-resolution cone beam computed tomography in the detection of simulated interradicular bone lesions. *Dentomaxillofac Radiol* 2009;38:156-162.
- Oliveira Costa F, Cota LO, Costa JE, Pordeus IA. Periodontal disease progression among young subjects with no preventive dental care: a 52-month follow-up study. *J periodontol* 2007;78:198-203.
- Oliver RC, Brown LJ, Loe H. Periodontal diseases in the United States population. *J Periodontol* 1998;69:269-278.
- Palomo JM, Rao PS, Hans MG. Influence of CBCT exposure conditions on radiation dose. *Oral Surg Oral Med Oral Pathol Oral Radiol Endod* 2008;105:773-782.
- Pauls V, Trott JR. A radiological study of experimentally produced lesions in bone. *Dent Pract Dent Rec* 1966;16:254-258.
- Paurazas SB, Geist JR, Pink FE, Hoen MM, Steinman HR. Comparison of diagnostic accuracy of digital imaging by using CCD and CMOS-APS sensors with E-speed film in the periapical bony lesions. *Oral Surg Oral Med Oral Pathol Oral Radiol Endod* 2000;89:356-362.
- Papapanou PN. Epidemiology of periodontal diseases: an update. *J Int Acad Periodontol* 1999;1:110-116.
- Papapanou PN & Wennström JL. The angular bony defect as indicator of further alveolar bone loss. *J Clin Periodontol* 1991;18:317-321.
- Pecoraro M, Azadivatan-le N, Janal M, Khocht A. Comparison of observer reliability in assessing alveolar bone height on direct digital and conventional radiographs. *Dentomaxillofac Radiol* 2005;34:279-284.
- Pepelassi EA, Diamanti-Kipiotti A. Selection of the most accurate method of conventional radiography for the assessment of periodontal osseous destruction. *J Clin Periodontol* 1997;24:557-557.
- Pfeiffer P, Schmage P, Nergiz I, Platzer U. Effects of different exposure values on diagnostic accuracy of digital images. *Quintessence Int* 2000;31:257-260.
- Polson AM. The research team, calibration, and quality assurance in clinical trials in periodontics. *Ann Periodontol* 1997;2:75-82.
- Preda L, Di Maggio EM, Dore R, La Fianza A, Solcia M, Schifino MR, Campani R, Preda EG. Use of spiral computed tomography for multiplanar dental reconstruction. *Dentomaxillofac Radiol* 1997;26:327-331.

- Quirynen M, Callens A, van Steenberghe D, Nys M. Clinical evaluation of constant force electronic probe. *J Periodontol* 1993;64:35-39.
- Ramadan AB, Mitchell DF. A roentgenographic study of experimental bone destruction. *Oral Surg Oral Med Oral Pathol* 1962;15:934-943.
- Ramesh A, Ludlow JB, Webber RL, Tyndall DA, Paquette D. Evaluation of tuned-aperture computed tomography in the detection of simulated periodontal defects. *Oral Surg Oral Med Oral Pathol Oral Radiol Endod* 2002;93:341-349.
- Rees T, Biggs NL, Collins CK. Radiographic interpretation of periodontal osseous defects. *Oral Surg Oral Med Oral Pathol* 1971;2:141-153.
- Richards AG, Webber RL. Constructing phantom heads for radiation research. *Oral Surg Oral Med Oral Pathol* 1963;16:683-690.
- Roberts JA, Drage NA, Davies J, Thomas DW. Effective dose from cone beam CT examinations in dentistry. *Br J Radiol* 2009;82:35-40.
- Rohlin M, Akesson L, Hakansson J, Hakansson H, Nasstrom K. Comparison between panoramic and periapical radiography in the diagnosis of periodontal bone loss. *Dentomaxillofac Radiol* 1989;18:72-76.
- Rosenberg MM. Management of osseous defects, furcation involvements, and periodontal-pulpal lesions. Clark JW. ed. *Clinical Dentistry – Periodontal and Oral Surgery Vol 10*, Harper and Row, Philadelphia, 1985, p108-117.
- Ruttimann UE, Qi XL, Webber RL. An optimal synthetic aperture for circular tomosynthesis. *Med Phys* 1989;16:398-405.
- Sanderink GCH. Imaging characteristics in rotational panoramic radiography. Doctoral Thesis, University of Utrecht, 1987, p47-51.
- Sanderink GCH. Imaging: new versus traditional technological aids. *Int Dent J* 1993;43:335-342.
- SAS Institute Inc. *SAS/STAT® 9.2 User's Guide*. Cary, NC: SAS Institute Inc, 2008.
- Scarfe WC, Farman AG, Brand JW, Kelly MS. Tissue radiation dosages using the RVG-S with and without niobium filtration. *Aust Dent J* 1997;42:335-342.
- Scarfe WC, Farman AG, Sukovic P. Clinical applications of cone beam computed tomography in dental practice. *J Can Dent Associ* 2006;72:75-80.
- Schliephake H, Wichmann M, Donnerstag F, Vogt S. Imaging of periimplant bone levels of implants with buccal bone defects. *Clin Oral Implants Res* 2003;14:193-200.

- SedentextCT Project (2009) Radiation protection: cone beam CT for dental and maxillofacial radiology. Provisional guidelines. Available for download at <http://www.sedentext.eu/guidelines>. Accessed 08 Jan 2010.
- Seymour GJ, Ford PJ, Cullinan MP, Leishman S, Yamazaki K. Relationship between periodontal infections and systemic disease. *Clin Microbiol Infect* 2007;13 Suppl 4:3-10.
- Siegel. Non parametric statistics for the behavioural sciences. McGraw-Hill series in Psychology, New York, USA, 1956.
- Slots J. Update on general health risk of periodontal disease. *Int Dent J* 2003;53:200-207.
- Souza PH, da Costa NP, Veeck EB. Influence of soft tissues on mandibular gray scale levels. *Braz Oral Res* 2004;18:40-44.
- Suetens P. Fundamentals of medical imaging. Cambridge University Press, New York, 2002.
- Sukovic P. Cone beam computed radiography in craniofacial imaging. *Orthod Craniofac Res* 2003;6 Suppl 1:31-6.
- Svärdström G, Wennström JL. Periodontal treatment decisions for molars: an analysis of influencing factors and long-term outcome. *J Periodontol* 2000;71:579-585.
- Svenson B, Petersson A. Influence of tube voltage on radiographic diagnosis of caries in premolars and molars. *Swed Dent J* 1991;15:245-50.
- Tarnow D, Fletcher P. Classification of the vertical component of furcation involvement. *J Periodontol* 1984;55:283-284.
- Tsiklakis K, Donta C, Gavala S, Karayianni K, Kamenopoulou V, Hourdakos CJ. Dose reduction in maxillofacial imaging using low dose Cone Beam CT. *Eur J Radiol* 2005;56:413-417.
- Tsuchida R, Araki K, Endo A, Funahashi I, Okano T. Physical properties and ease of operation of a wireless intraoral x-ray sensor. *Oral Surg Oral Med Oral Pathol Oral Radiol Endod* 2005;100:603-608.
- Tugnait A, Clerehugh V, Hirschmann PN. The usefulness of radiographs in diagnosis and management of periodontal diseases: a review. *J Dent* 2000;28:219-226.

- Tugnait A, Clerehugh V, Hirschmann PN. Use of the basic periodontal examination and radiographs in the assessment of periodontal diseases in general dental practice. *J Dent* 2004;32:17-25.
- Tyndall DA, Brooks SL. Selection criteria for dental implant site imaging: a position paper of the American Academy of Oral and Maxillofacial radiology. *Oral Surg Oral Med Oral Pathol Oral Radiol Endod* 2000;89:630-637.
- van der Stelt PF. Principles of digital imaging. *Dent Clin North Am* 2000;44:237-48.
- Vandenberghe B, Bud M, Sutanto A, Jacobs R. The use of high-resolution digital imaging technology for small diameter K-file length determination in endodontics. *Clin Oral Investig* 2009, Epub May 19.
- Vandenberghe B, Corpas L, Bosmans H, Yang J, Jacobs R. A comprehensive in-vitro study of image accuracy and quality for periodontal diagnosis. PART 1: The influence of x-ray generator on periodontal measurements using conventional and digital receptors. *Clin Oral Investig* 2010 (submitted).
- Vandenberghe B^a, Jacobs R, Yang J. Diagnostic validity (or acuity) of 2D CCD versus 3D CBCT-images for assessing periodontal breakdown. *Oral Surg Oral Med Oral Pathol Oral Radiol Endod* 2007;104:395-401.
- Vandenberghe B^b, Jacobs R, Yang J. Topographic assessment of periodontal craters and furcation involvements by using 2D digital images versus 3D cone beam CT: an in-vitro study. *Chin J Dent Res* 2007;10:21-29.
- Vandenberghe B, Jacobs R, Yang J. Detection of periodontal bone loss using digital intraoral and cone beam computed tomography images: an in vitro assessment of bony and/or infrabony defects. *Dentomaxillofac Radiol* 2008;37:252-260.
- Vandre RH, Webber RL. Future trends in dental radiology. *Oral Surg Oral Med Oral Pathol Oral Radiol Endod* 1995;80:471-478.
- Walter C, Kaner D, Berndt DC, Weiger R, Zitzmann NU. Three-dimensional imaging as a pre-operative tool in decision making for furcation surgery. *J Clin Periodontol* 2009;36:250-257.
- Webber RL, Horton RA, Tyndall DA, Ludlow JB. Tuned-aperture computed tomography (TACT). Theory and application for three-dimensional dento-alveolar imaging. *Dentomaxillofac Radiol* 1997;26:53-62.

- Wenzel A, Haiter-Neto F, Gottfredsen E. Influence of spatial resolution and bit depth on detection of small caries lesions with digital receptors. *Oral Surg Oral Med Oral Pathol Oral Radiol Endod* 2007;103:418-422.
- White DR. Phantom materials for photons and electrons. The Hospital Physicists' Association, Radiotherapy Topic Group. *Scientific Report Series* 1977;20:1-30.
- White SC. 1992 assessment of radiation risk from dental radiography. *Dentomaxillofac Radiol* 1992;21:118-126.
- Wolf B, von Bethlenfalvy E, Hassfeld S, Staehle HJ, Eickholz P. Reliability of assessing interproximal bone loss by digital radiography: infrabony defects. *J Clin Periodontol* 2001;28:869-878.
- Yalcinkaya S, Künzel A, Willers R, Thoms M, Becker J. Subjective image quality of digitally filtered radiographs acquired by the Dürr Vistascan system compared with conventional radiographs. *Oral Surg Oral Med Oral Pathol Oral Radiol Endod* 2006;101:643-651.
- Yang J, Cavalcanti MG, Ruprecht A, Vannier MW. 2-D and 3-D reconstructions of spiral computed tomography in localization of the inferior alveolar canal for dental implants. *Oral Surg Oral Med Oral Pathol Oral Radiol Endod* 1999;87:369-374.
- Young SJ, Chaibi MS, Graves DT, Majzoub Z, Boustany F, Cochran D, et al. Quantitative analysis of periodontal defects in a skull model by subtraction radiography using a digital imaging device. *J Periodontol* 1996;67:763-769.
- Zulqarnain BJ, Almas K. Effect of x-ray beam vertical angulation on radiographic assessment of alveolar crest level. *Indian J Dent Res* 1998;9:132-138.

Professional career

Bart Vandenberghe (°18 October 1981) obtained his Master degree in Dentistry in 2005, with the distinct grade of "best integrated clinical patient treatment". His master thesis dealt with digital intraoral radiography, which strengthened his interest in oral imaging. To continue his academic training, he obtained the degree of Master in Medical Imaging at the K.U.Leuven and spent three years in the United States of America as research scholar at Temple University in Philadelphia (2005-2006) and at Tufts University in Boston (2007). Shortly after, he was recruited by the University of Maryland, where he spent more than a year (2007-2008) in the department of Diagnostic Sciences and Pathology as Visiting Assistant Professor. He was course director of Radiology for the first year dental and dental hygiene students and was responsible for the advanced imaging lectures in Implantology. Furthermore, he provided oral pathology advice and became actively involved in Guided Surgery. He is working on many research projects (national and international collaborations) with a specific focus on digitalization, 3D modalities and advanced planning methods, which shows his passion for the overlap of oral imaging and restorative dentistry. Bart Vandenberghe was finalist for the Research Award of the International Dentomaxillofacial Radiology Association in 2007 in Beijing, China, and is reviewer for several international journals as well as editorial board member of the eJournal of Oral & Maxillofacial Research. Besides his academic endeavors, he organized a first dental mission for the Tierra Bomba Organization in 2007, where he provided dental care and dental preventive education at the local school on the island of Tierra Bomba, Colombia. Currently, he finalized a research grant in 3D Cone Beam imaging at the K.U.Leuven, is working part-time as a scientific collaborator at the department of Prosthetic Dentistry and starting up a private training center in Oral Imaging.

PUBLICATIONS

Peer-reviewed journals

- Vandenberghe B, Jacobs R, Yang J. Detection of periodontal bone loss using digital intra-oral and CBCT images: an in-vitro assessment of bony and/or infrabony defects. *Dentomaxillofac Radiol* 2008;37:252-60
- Vandenberghe B, Jacobs R, Yang J. Diagnostic validity (or acuity) of 2D CCD versus 3D CBCT-images for assessing periodontal breakdown. *Oral Surg Oral Med Oral Pathol Oral Radiol Endod* 2007;104:395-401
- Vandenberghe B, Jacobs R, Yang J. Topographic assessment of periodontal craters and furcation involvements by using 2D digital images versus 3D cone beam CT: an in-vitro study. *Chin J Dent Res* 2007;10:21-29
- Vandenberghe B, Bud M, Jacobs R. The use of high resolution digital CCD and PSP imaging technology for small diameter K-file length determination in endodontics. *Clin Oral Investig* 2009 (Epub May 19, in press)
- Vandenberghe B, Corpas L, Bosmans H, Yang J, Jacobs R. A comprehensive in-vitro study of image accuracy and quality for periodontal diagnosis. PART 1: The influence of x-ray generator on periodontal measurements using conventional and digital receptors. *Clin Oral Invest* 2010 (Submitted, 1st revision)
- Vandenberghe B, Bosmans H, Yang J, Jacobs R. A comprehensive in-vitro study of image accuracy and quality for periodontal diagnosis. PART 2: The influence of intraoral image receptor on periodontal measurements. *Clin Oral Invest* 2010 (Submitted, 1st revision)
- Vandenberghe B, Jacobs R. The influence of tube potential on periodontal bone level measurements and subjective image quality using a digital PSP sensor. *J Oral Maxillofac Res* 2010;1:e5

- Vandenberghe B, Jacobs R, Bosmans H. Modern dental imaging: a review of current technology and applications. Eur Radiol 2010 (Submitted)
- Al-Rawi B, Hassan B, Vandenberghe B, Jacobs R. Accuracy assessment of three-dimensional reconstructions of the occlusal tooth surfaces from Cone Beam Computed Tomography scans. J Oral Rehab 2010 (Accepted)

Book Chapters

- Vandenberghe B. Stand van zaken rond digitale beeldvorming. In: Het Tandheelkundig Jaar 2010. p128-141.
- Sarment D, Vandenberghe B. CBCT in Periodontics. In: Cone Beam Computed Tomography in Restorative, Implant, and Surgical Dentistry. (Submitted)
- Vandenberghe B, Nackaerts O. Imaging in Periodontology: 2D versus 3D Visualization Techniques. In: Informatics in Oral Medicine: Advanced Techniques in Clinical and Diagnostic Technologies. Medical Information Science Reference, IGI global, Hershey, pp 204-236.
- Vandenberghe B. Dentale radiografie: tomografische en computer tomografische technieken. In: Techniek in de radiologie. (Submitted)

Other Publications

- Vandenberghe B, Jacobs R. Keulen (en de kaak) in drie dimensies. De Tandarts 2009;385:12-13
- Jacobs R, Vandenberghe B. Professor Reinhilde Jacobs en Bart Vandenberghe: Klinische tips omtrent orale radiologie. De Tandarts 2009;383:10-11

- Vandenberghe B. Evoluties in intra-orale beeldvorming. Eigenschappen en validatie van nieuwe digitale systemen. Dentistnews 2007;March:29-36
- Vandenberghe B. Meer dan afstuderen...Tandheelkundige tijdingen 2007;35:114-119
- Vandenberghe B, Jacobs R. Intra-orale digitale beeldvorming: validatieonderzoek van nieuwe digitale systemen. Contactpunt (VVT) 2006;April:27-30.

Abstracts

- Vandenberghe B, Hassan B, Armellini D, Maes F, Jacobs R. Volumetric quantifications of bone loss for determination of bone grafting accuracy: a pilot study. Programme and abstract book of the 17th International Congress of Dentomaxillofacial Radiology 2009; p59
- Vandenberghe B, Jacobs R, Yang J. Diagnostic validity of 2D digital intra-oral images versus 3D CBCT images in assessment of periodontal breakdown: an in-vitro study. Abstracts and program of the 16th International Congress of Dentomaxillofacial Radiology 2007; p60
- Vandenberghe B, Jacobs R, Yang J. Detection of periodontal bone loss using 2D and 3D Imaging modalities. Report of the 10th European Congress of Dentomaxillofacial Radiology 2006; p115